MOVEMENT QUALITY AND PERFORMANCE ASSESSMENT IN WOMEN'S SOCCER USING DATA-DRIVEN METHODS

by

Xiong Zhao

Thesis submitted to the University of Ottawa
in partial Fulfillment of the requirements for
the degree of Doctor of Philosophy in Human Kinetics

School of Human Kinetics
Faculty of Health Sciences
University of Ottawa
Ottawa, Ontario, Canada

Supervisor:
Ryan B. Graham, PhD

Table of Contents

Acknowledgements

I would like to express my deepest gratitude to all those who supported and encouraged me throughout my doctoral journey.

First and foremost, I am immensely grateful to my supervisor, Dr. Ryan Graham, for your invaluable guidance, patience, and insightful feedback throughout this project. Thank you for supporting my ventures not only in research but also in entrepreneurship. There were many ups and downs, plans interrupted by COVID-19, a leap into founding a company, but your unwavering mentorship provided both stability and inspiration through it all. From the day I landed in Canada to today, nearly seven years later, I have learned and grown tremendously. As challenging as this journey has been, I have cherished every step and would not trade the experience for anything. None of it would have been possible without your support and guidance. Your mentorship shaped not only this thesis, but also my growth as a researcher, innovator, and person.

To my thesis committee members, Dr. Janie Cournoyer and Dr. Pascal Fallavollita, thank you for your thoughtful feedback, encouragement, and guidance throughout this process.

To coaches Steve Johnson, Veronica Mazzella, and Joanna Geck, and to all the players on the University of Ottawa Women's Soccer team, thank you for making this project possible through your time, effort, and enthusiasm. Go Gee-Gees!

To all my colleagues at the Movement Biomechanics and Analytics Laboratory, thank you for making my graduate experience not only intellectually fulfilling but also personally meaningful. You made this journey in Canada truly special for an international student.

To my co-founders at AccMov Health Inc. and project partners at Ex-able, thank you for believing in me and embarking on this uncertain yet rewarding path during such a turbulent time.

To my parents, thank you for your unconditional love and support over the years. You always respected my independence, gave me the freedom to make my own

decisions, and encouraged me to see more of the world and become who I want to be.

Last but certainly not least, to my wife, Dr. Yiyang Chen, you are my best friend, fellow researcher, and travel buddy. Thank you for all the late-night conversations, endless support, and countless coffees. I can't wait to see what the future holds for us. I love you!

General Abstract

Background: Non-contact lower limb injuries are a leading source of loss time and performance impairment in female soccer athletes. Laboratory-based screening methods offer detailed biomechanical insights but lack scalability and field applicability. Recent advances in markerless motion capture and data-driven modeling promise more accessible and interpretable tools for longitudinal athlete monitoring.

Purpose: The overarching goal of this thesis is to develop a comprehensive framework that integrates biomechanical data, machine learning models, and markerless motion capture systems to enhance injury prediction and movement health monitoring in female varsity soccer athletes.

Methods: A single cohort of 25 female varsity soccer players (mean age 20.40 ± 1.98 years) was assessed at pre-, mid-, and post-season during a suite of standardized tasks: countermovement jump, broad jump, lateral hop, Y-Balance, T-Balance, metronome-paced bodyweight squats, reaction time tests, and on-field sprint tests.

Four interrelated studies were conducted: **1)** Seasonal changes in dynamic tasks and sprints assessed via in-lab and field measures to identify performance fluctuations and recovery patterns. **2)** A 3D Goal Equivalent Manifold (GEM) analysis of metronome-paced squats to quantify task-relevant and task-irrelevant motor variability and detect persistent motor control deficits in athletes with concussion history. **3)** An evaluation of four machine learning pipelines, Support Vector Machines (SVM), eXtreme Gradient Boosting (XGBoost), Long Short-Term Memory (LSTM), and a Hybrid Transformer, for interpretable injury prediction in sports. **4)** Validation of 28 two-camera configurations for lower limb joint kinematics accuracy and agreement within configurations and against an 8-camera markerless system (Theia3D).

Results: In **Study 1a**, significant midseason decrements were observed in sprint times (10 m: $\chi^2 = 15.56$, $p < .001$; 20 m: $\chi^2 = 31.21$, $p < .001$; 40 m: $\chi^2 = 7.59$, $p = .023$) and

countermovement jump height (bilateral: $\chi^2 = 18.89$, $p < .001$; unilateral: $\chi^2 = 8.78$, $p = .012$), with partial recovery post-season, while broad jump and L-hop remained stable. Left lower-limb coordination amplitude (MARP, $\chi^2 = 8.09$, $p = .018$) and composite reach score decreased across the season. **Study 1b** revealed that athletes with concussion history had significantly lower 3D GEM performance indices across all timepoints, indicating persistent motor control deficits. In **Study 2**, the Hybrid Transformer outperformed LSTM (AUC = 0.680), XGBoost (AUC = 0.619), and SVM (AUC = 0.342), achieving AUC = 0.740 and 67.6 % accuracy; attention maps highlighted early landing and push-off phases as critical risk periods. **Study 3** demonstrated that two-camera setups (i.e. front-back configurations) estimated sagittal-plane hip and knee flexion/extension with RMSE < 8° and CMC ≈ 1.00, while coronal and transverse planes showed larger errors (RMSE > 10°, CMC < 0.60).

Conclusion: This thesis demonstrates that a unified framework, combining longitudinal biomechanical screening, transformer-based injury prediction, GEM-based motor variability analysis, and field-deployable markerless motion capture, can accurately identify performance decrements and injury risk in female soccer athletes. The findings support scalable, interpretable, and clinically relevant tools for season-long athlete monitoring and targeted injury prevention strategies.

Contributions

Dr. Ryan Graham supervised the project and provided funding, guidance on conceptualization, data analysis, results interpretation, visualization, and writing-review and editing.

Study 1a: This study investigates the biomechanical changes across a competitive season in women's soccer with both laboratory biomechanics testing and on-field sprint tests. X. Zhao designed the protocol, collected, processed, analysed the data, and drafted the manuscript. K. Peng advised on the statistical design, and all co-authors provided critical revisions.

Study 1b: Building on the same dataset, this study introduces a 3D Goal Equivalent Manifold framework to quantify how athletes regulate redundancy during metronome-paced squats. It demonstrates that players with a concussion history display persistently lower performance index throughout the season. X. Zhao implemented the 3D GEM pipeline, performed all analyses, and wrote the manuscript; R. Rahimi collaborated on the mathematical formulation and code verification, and all co-authors offered editorial input.

Study 2: This study compares four machine-learning pipelines, SVM, XGBoost, LSTM, and a Hybrid Transformer, showing that the Transformer achieves the highest accuracy and, through attention maps, localises injury-relevant movement phases. The findings illustrate the clinical value of temporally aware, interpretable models for small, high-dimensional sport datasets. X. Zhao did the data processing, model development, and manuscript preparation. All co-authors reviewed the final manuscript.

Study 3: The final study validates 28 two-camera combinations obtainable from an eight-camera motion capture system, using Pose2Sim pipeline. It identifies Front, Back and Right groups as the optimal low-cost configuration and uses open-source scripts that lower the barrier to field deployment. X. Zhao designed and executed the validation

protocol, processed and analysed the kinematic data, and drafted the manuscript; All co-authors contributed critical feedback.

List of Abbreviations

AAA	Athletic Ability Assessment	**LESS**	Landing Error Scoring System
ACL	Anterior Cruciate Ligament	**LSTM**	Long Short-Term Memory
AI	Artificial Intelligence	**MAE**	Mean Absolute Error
AUC	Area Under the Curve	**MAR**	Missing at Random
BMI	Body Mass Index	**MARP**	Mean Absolute Relative Phase
BJ	Broad Jump	**MKAM**	Maximum Knee Abduction Moment
BPM	Beats Per Minute	**ML**	Machine Learning
CMC	Coefficient of Multiple Correlation	**MoCap**	Motion Capture
CMJ	Countermovement Jump	**MSK**	Musculoskeletal
CNN	Convolutional Neural Network	**MV**	Motor Variability
CNS	Central Nervous System	**PCA**	Principal Component Analysis
COM	Center of Mass	**PI**	Performance Index
CRT	Complex Reaction Time	**RNNs**	Recurrent Neural Networks
CRP	Continuous Relative Phase	**RMSE**	Root Mean Square Error
CV	Computer Vision	**RSI**	Reactive Strength Index
DOF	Degrees of Freedom	**RTMPose**	Real-Time Multi-Person Pose
DP	Deviation Phase	**SHAP**	SHapley Additive exPlanations
EMG	Electromyography	**SIMS**	Soccer Injury Movement Screen
FMS	Functional Movement Screen	**SRT**	Simple Reaction Time
GEE	Generalized Estimating Equations	**SVM**	Support Vector Machine
GEM	Goal-Equivalent Manifold	**TB**	T-Balance
GPU	Graphics Processing Unit	**UCM**	Uncontrolled Manifold
GRF	Ground Reaction Force	**XGBoost**	eXtreme Gradient Boosting
GPS	Global Positioning System	**YB**	Y-Balance
IK	Inverse Kinematics		
IMU	Inertial Measurement Unit		

List of Tables

List of Figures

Chapter 1. General Introduction

Soccer is a high-intensity, multidirectional sport characterized by frequent accelerations, decelerations, rapid changes of direction, jumping, and high-impact physical contact. These biomechanical demands place athletes at substantial risk of both contact and non-contact injuries (López-Valenciano et al., 2020). Epidemiological studies in soccer have revealed that approximately 5.2 injuries occur per 1,000 hours of playing time, which correlates with the level of competition and player age (Allen et al., 2016). Such injuries not only result in significant time lost from training and competition, but also have lasting consequences on physical performance, psychological well-being, and long-term musculoskeletal health.

Understanding the epidemiology and etiology of soccer-related injuries is critical for designing effective and population-specific prevention programs. Notably, while substantial progress has been made in studying injury mechanisms and prevention strategies in male soccer players, female athletes remain underrepresented in the literature (John et al., 2025). This is particularly concerning given that females are disproportionately affected by specific injury types, including anterior cruciate ligament (ACL) tears, hamstring strains, and ankle sprains (Britt et al., 2020; Giza & Micheli, 2005; Renstrom et al., 2008; Xiao et al., 2021). For instance, female players are reported to be four to six times more likely to suffer ACL injuries compared to their male counterparts (Hewett et al., 2005).

This disparity highlights the urgent need for sex-specific injury risk models that account for anatomical, biomechanical, hormonal, and neuromuscular differences between male and female athletes (Hewett et al., 2005; Myer et al., 2008). A systematic review by Fältström et al. (2019) underscores the importance of targeted neuromuscular training programs in mitigating the risk of knee injuries in female players (Fältström et al., 2019), while more recent evidence also points to elevated rates of sports-related concussions in women's soccer (Maemichi & Kumai, 2025; Weber et al., 2020). Female soccer players sustain concussions more often, typically from ball impacts and player collisions, and report more severe or prolonged symptoms than males (Maemichi & Kumai, 2025; Weber et al., 2020).

Despite these trends, injury prevention strategies and rehabilitation protocols are still often developed from male-centric data, which limits their generalizability when applied to female athletes. Without robust, female-focused biomechanical and clinical research, there is a risk of misidentifying injury mechanisms and overlooking modifiable risk factors unique to women's soccer. Thus, developing data-driven, sex-specific screening and assessing frameworks is essential for developing intervention programs, optimizing performance for female athletes (Allen et al., 2016; Weber et al., 2020).

1.1 Sports injury in soccer

1.1.1 Overview of sports injuries in soccer

A sports injury is defined as "a new or recurring musculoskeletal complaint or concussions incurred during competition or training that requires medical attention, regardless of the potential absence from participation" (Engebretsen et al., 2013). These injuries are typically classified into three categories: acute injuries, resulting from a single traumatic event (e.g., sprains, fractures, dislocations, concussions); subacute injuries, which emerge from repetitive microtrauma; and chronic injuries, which develop gradually due to accumulated physiological stress and degenerative changes (Difiori et al., 2014; Paterno et al., 2013; Yang et al., 2012).

Soccer, as one of the most physically demanding and globally played sports, poses a high risk for both contact and non-contact sports injuries. Soccer is characterized by frequent accelerations and decelerations, rapid directional changes, jumping, and repeated physical contacts, all of which contribute to injury risk (López-Valenciano et al., 2020; Roberts et al., 2019). The repetitive nature of running and cutting maneuvers, combined with physical duels, predisposes soccer players to both acute injuries and overuse injuries (Bollars et al., 2014; Yang et al., 2012). Notably, research involving collegiate athletes indicates that acute injuries are more prevalent than overuse injuries in sports like soccer and hockey (Crisco et al., 1994; Garrett, 1996).

A growing body of literature has also emphasized the long-term physical consequences of sports-related concussions, particularly among female soccer players. Although concussions are often perceived as transient neurological events, accumulating evidence emphasizes persistent

impairments in neuromuscular control and movement coordination well after clinical symptom resolution (Howell et al., 2018; Mooney et al., 2020). Female athletes appear to experience prolonged motor recovery trajectories, with some studies reporting slower gait velocities, reduced agility, and greater variability in motor performance long after the initial concussion (Howell et al., 2018; Maemichi & Kumai, 2025).

Moreover, concussion-related impairments are not confined to physical domains alone. The multisystem impact of concussion, encompassing both motor and cognitive systems, may disrupt an athlete's ability to manage dual-task demands, such as executing complex motor tasks while processing tactical information. This interaction between motor and cognitive impairments is especially evident in tasks requiring rapid decision-making under pressure (Caccese et al., 2023; Hassanmirzaei et al., 2021). Dual-task deficits may persist for months or even years, placing athletes at increased risk for re-injury, particularly during high-intensity or unanticipated play scenarios (Weiner et al., 2022).

Importantly, these phenomena may present differently in female athletes compared to their male counterparts. Sex-based differences in neurophysiology, hormone profiles, and motor control strategies contribute to variations in injury mechanism, symptom presentation, and recovery patterns (Hassanmirzaei et al., 2021; Weiner et al., 2022). As such, female-specific injury prevention and return-to-play strategies are warranted.

1.1.2 The underrepresentation of female soccer injury research

Despite the global popularity and rapid growth of women's soccer, research focusing specifically on injury prevention in female athletes remains limited. Historically, sports science literature has been dominated by male-centric studies, resulting in a significant knowledge gap concerning the unique physiological, biomechanical, and hormonal profiles of female soccer players (Randell et al., 2021). This lack of female-specific research is especially concerning given that females are at greater risk of certain injuries, such as ACL tears, hamstring strains, and ankle sprains (Giza & Micheli, 2005; Renstrom et al., 2008). Epidemiological studies report that female athletes sustain ACL injuries at rates two to nine times higher than males (Britt et al., 2020; Hewett

et al., 2005; Xiao et al., 2021).

Several factors contribute to this heightened injury susceptibility. Female soccer players often demonstrate greater knee valgus angles, increased joint laxity, and altered landing mechanics during sport-specific movements (Hewett et al., 2005; Myer et al., 2008). These biomechanical risk factors are further exacerbated by neuromuscular differences and hormonal fluctuations throughout the menstrual cycle. Post-injury, female are more likely to adopt compensatory movement patterns that reduce stability and increase re-injury risk, particularly after ACL tears or concussions (Kakavas et al., 2025).

Concussions represent another critical concern. Female soccer players experience concussions more frequently than their male counterparts, often resulting from player collisions or ball impact (Maemichi & Kumai, 2025; Weber et al., 2020). Evidence suggests that female athletes also report more severe symptoms and exhibit prolonged recovery times (Lynall et al., 2015). One explanation may be that female typically possess lower neck strength and smaller head mass, which reduces their ability to attenuate impact forces during head collisions (Kakavas et al., 2025). Additionally, post-concussion neuromuscular deficits, such as impaired balance, delayed reaction time, and reduced coordination, can persist long after clinical recovery and increase the risk of secondary musculoskeletal injuries (Howell et al., 2018; Kakavas et al., 2025).

Importantly, these impairments are not merely short-term issues. Biomechanical alterations following injury can hinder athletic performance and may contribute to long-term joint degeneration, chronic pain, and early-onset osteoarthritis, emerging public health concerns particularly relevant to female athletes (Lynall et al., 2015). Yet, most existing injury risk models and return-to-play protocols remain generalized and do not account for sex-specific vulnerabilities.

A significant barrier to progress has been the lack of longitudinal, multimodal injury studies that track female athletes over time. As noted by Can et al., (2019), this gap has impeded the development of targeted prevention and rehabilitation strategies. There is a pressing need for data-driven frameworks that integrate biomechanical, neuromuscular, and contextual data, particularly those that leverage artificial intelligence (AI) to extract patterns predictive of injury.

1.1.3 Risk factors for injury in sports

Injury risk in soccer is multifactorial, resulting from a complex interaction of intrinsic and extrinsic factors that influence an athlete's susceptibility to both contact and non-contact injuries (Bahr, 2005). Intrinsic risk factors include neuromuscular imbalances, previous injury history, proprioceptive deficits, reduced range of motion, altered movement patterns, joint laxity, and scar tissue accumulation (Hägglund et al., 2006).

Several studies have emphasized the role of neuromuscular control and anatomical predispositions in injury risk, particularly for female athletes. For instance, hip and knee instability has been closely linked to increased incidence of ACL injuries (Kaneko et al., 2017). Additionally, prior injury history, especially in the lower extremities, has been consistently associated with heightened risk of re-injury (Malone et al., 2017; Niyonsenga & Phillips, 2013). Interestingly, research found that athletes with a history of musculoskeletal injuries can exhibit cognitive and motor control deficits, even in the absence of a diagnosed concussion (Hutchison et al., 2011).

Another crucial, yet often overlooked, intrinsic risk factor is reaction time and cognitive load. The ability to quickly interpret environmental stimuli and execute appropriate motor responses is vital for avoiding collisions, adapting to unpredictable gameplay, and mitigating abnormal loading during high-velocity maneuvers. Delayed reaction time, particularly under fatigue or cognitive overload, has been linked to a greater incidence of injury (Herman et al., 2017). This concern is especially relevant to female soccer players post-concussion, who frequently exhibit persistent deficits in reaction time and motor planning. These impairments can last weeks to months, placing them at continued risk for secondary injuries (Howell et al., 2018; Vedung et al., 2020). Comparative studies indicate that female athletes experience longer recovery durations and report higher symptom burdens than males following concussions, potentially due to sex-based neuroanatomical and hormonal differences (Caccese et al., 2023; Haase et al., 2023; Prien et al., 2020). Moreover, deficits in dual-task performance, where athletes must simultaneously manage cognitive and motor demands, are exacerbated post-concussion. This creates a dangerous vulnerability in soccer, a sport that requires rapid tactical decision-making under physical stress

(Lynall et al., 2015; Maemichi & Kumai, 2025; Vedung et al., 2020). Early concussive events may lead to a compounding effect, increasing the likelihood of future concussions and long-term neuromotor instability.

Environmental factors, such as playing surface type, also influence injury risk. Playing on artificial turf has been associated with increased mechanical stress on knee ligaments, particularly in female athletes, who may be more vulnerable to surface-induced changes in loading mechanics (Alipour Ataabadi et al., 2019; Xiao et al., 2022).

Extrinsic factors, such as training loads, playing intensity, and the frequency of games, also contribute to injury risks. Research highlights that a poor balance between training load and athletes' recovery can lead to greater occurrences of injuries; thus, careful monitoring of training loads is pivotal (Malone et al., 2017; Xiao et al., 2021). Social factors, including team dynamics and coaching strategies, further impact injury susceptibility, reinforcing the need for a holistic injury risk assessment approach in team sport environments (Nawasreh et al., 2022; Niyonsenga & Phillips, 2013).

Many studies indicate that female athletes struggle with delayed reaction times following a concussion, which can persist for extended periods (Howell et al., 2018; Vedung et al., 2020). For instance, Caccese et al. report that females exhibit reduced performance in reaction time tests compared to male athletes, suggesting a greater vulnerability to cognitive deficits post-injury (Caccese et al., 2023). This impairment is troubling as quick decision-making processes are paramount in dynamic sports environments like soccer, influencing on-field effectiveness and awareness of the game (Haase et al., 2023; Vedung et al., 2020). Studies indicate that females may not only experience prolonged recovery periods but also a higher symptom burden compared to males, further contributing to delayed reaction times (Haase et al., 2023; Prien et al., 2020). Notably, the impact of early concussive injuries can result in a compounded risk for future concussions and a persistent struggle with dual-task scenarios, which emphasizes the need for specialized rehabilitation protocols tailored for female athletes (Lynall et al., 2015; Maemichi & Kumai, 2025).

1.1.4 Motor variability and injury risk

Human movement is inherently complex, characterized by an abundance of degrees of freedom (DOFs) and natural variability in movement execution (Scholz & Schöner, 1999). Traditionally, motor variability (MV) was viewed as detrimental to performance, often labeled as "motor noise", and believed to interfere with task consistency and precision (Newell & Slifkin, 1998). However, contemporary perspectives now recognize MV as a functional and adaptive feature of the motor system. Rather than being purely erratic, variability in movement can facilitate the exploration of alternative motor strategies, enhance adaptability to changing environmental or physiological conditions, and reduce the accumulation of localized tissue stress (Bartlett et al., 2007; Dingwell et al., 2010).

While a certain level of variability is considered healthy and even beneficial, excessive or poorly regulated movement variability, particularly when it deviates from task-relevant goals, may reflect neuromuscular instability and impaired motor control. This form of "non-goal-equivalent variability" has been linked to elevated injury risk, as it can signify a breakdown in the coordination strategies needed to stabilize joint mechanics and distribute load efficiently (Cusumano & Dingwell, 2013). Quantifying MV in athletes over the course of a season may be challenging but could provide insights. In the context of female soccer players, assessing MV across a competitive season can offer critical insights into how athletes respond to training load, match exposure, fatigue, and injury history. For instance, deviations from stable motor patterns may signal fatigue accumulation, maladaptive movement compensations post-injury, or insufficient neuromuscular control, factors that can precede injury. Conversely, healthy variability may reflect improved coordination and adaptability (Cowin et al., 2022).

MV can be quantified using a range of approaches, which are broadly categorized into linear and non-linear methods. Linear approaches typically summarize variability using statistical measures such as the cycle-to-cycle mean and standard deviation. These metrics are widely applied in gait and other repetitive movement analyses because they are straightforward to compute and interpret (Stergiou & Decker, 2011). However, they primarily capture the magnitude of variability

and do not account for its temporal structure or underlying control strategies.

In contrast, non-linear methods are increasingly recognized as more suitable for movement quality assessment, as they can describe the structure, organization, and complexity of variability over time (Komar et al., 2015). Non-linear tools can detect subtle changes in motor coordination, adaptability, and stability that linear measures may overlook. Several well-established non-linear frameworks are relevant to the present work, including the Uncontrolled Manifold (UCM), entropy analyses, Continuous Relative Phase (CRP), and the Goal Equivalent Manifold (GEM) approach.

The UCM concept posits that the human motor system possesses more degrees of freedom than strictly necessary for performing a given task, a principle referred to as motor abundance or redundancy (Maldonado et al., 2018; Martin et al., 2019). Rather than viewing this redundancy as problematic, it is considered advantageous, allowing the central nervous system (CNS) to produce flexible and robust movement solutions. The UCM approach assumes that variability is structured to stabilize a specific performance variable. Deviations that interfere with the task goal (orthogonal to the UCM) are minimised, whereas variability in directions that do not affect the goal (along the UCM) is permitted (Cusumano & Dingwell, 2013; Serrien et al., 2018). This organization of variability reflects the presence of motor synergies, where multiple degrees of freedom covary to maintain task performance. UCM analysis has been applied to tasks ranging from walking and kicking to shooting in basketball, archery, and pistol sports, where it has revealed how skilled performers regulate variability to achieve greater accuracy (Komar et al., 2015; Serrien et al., 2018).

Entropy analyses, such as Sample Entropy, are grounded in information theory and evaluate the predictability or regularity of a time series (Alsubaie et al., 2021; Komar et al., 2015). Low entropy values indicate a highly regular, predictable, and less complex signal, whereas higher values indicate greater irregularity and complexity. In the context of motor control, higher entropy may reflect increased adaptability and richer interaction between subsystems. Entropy analysis has been used across various domains, including centre of pressure fluctuations during balance, cardiovascular dynamics, and isometric force production.

Continuous Relative Phase (CRP) quantifies the coordination between two oscillating

segments or joints, providing insight into how body parts move relative to each other over time. By representing the phase relationship continuously across a movement cycle, CRP can reveal differences in coordination strategies across skill levels. For example, CRP analysis of arm-leg coordination in breaststroke swimming has identified distinct patterns in expert versus recreational swimmers, indicating alternative solutions to achieving the same movement outcome (Komar et al., 2015).

The Goal Equivalent Manifold (GEM) framework (Cusumano & Dingwell, 2013) offers a geometric and dynamical perspective on movement control, defining a task through a goal function that specifies the combinations of body states capable of achieving the desired outcome. The GEM represents all possible solutions that meet the goal, for instance, the infinite combinations of movement distance and speed that yield the same movement time (Gates & Dingwell, 2008). Variability can then be decomposed into components perpendicular to the GEM (which affect task success) and tangent to it (which do not). For example, Chehrehrazi et al. (2017) applied the GEM framework to examine variability during lifting tasks and observed significant differences in motor adaptability between healthy individuals and those with non-specific low back pain. These results highlight the potential of GEM-based approaches for detecting subtle motor-control impairments in concussed athletes.

1.2 Movement screening

1.2.1 Traditional movement screening tools

Movement screening is an essential tool for identifying potential injury risks among soccer players. Its focus on biomechanical assessments helps to establish a player's movement competency, pinpointing deficiencies that may lead to injuries (Malone et al., 2017; Ralston et al., 2020). Movement screening is widely employed to assess flexibility, balance, strength, and neuromuscular coordination in athletes (Emery et al., 2015; McCall et al., 2016). Studies have indicated that females often demonstrate less stability and control compared to their male counterparts in certain movement patterns, possibly explaining their higher injury rates (De et al., 2015; Silvers-Granelli et al., 2015).

Widely adopted screening tools include the Functional Movement Screen (FMS), Y-Balance Test, Athletic Ability Assessment (AAA), Landing Error Scoring System (LESS), and the Tuck Jump Assessment (Bulow et al., 2019; McCall et al., 2015). These assessments have been used to detect movement asymmetries, poor landing mechanics, and imbalances that contribute to injury susceptibility (Cook et al., 2006; McKeown et al., 2014).

However, despite their clinical popularity, traditional movement screening tools face several well-documented limitations. First, many of these tools suffer from poor inter- and intra-rater reliability, resulting in inconsistent and subjective scoring (McCunn et al., 2016; Gulgin & Hoogenboom, 2014). Second, most screening systems utilize ordinal scoring scales, which lack sensitivity to subtle differences in motor control and movement variability (Bahr, 2016). Third, athletes can consciously modify their performance once they become familiar with the scoring criteria, reducing the predictive validity of the tests (Frost et al., 2015). Lastly, these tools often lack ecological validity, failing to reflect the complexity of sport-specific movements encountered during real match conditions (Bonazza et al., 2017).

These limitations underscore the need for more objective, scalable, and task-relevant movement assessment tools, especially for use in field settings. Using motion capture (MoCap) system to assess movement quality in different settings (e.g., exercise, rehabilitation and strength and conditioning) has been a research hot spot.

1.2.2 Movement screening using motion capture systems

Popular MoCap systems used in movement screening include optical motion capture, inertial measurement units (IMUs), and RGB-D sensors. Optical motion capture, particularly marker-based optoelectronic systems, remains the reference standard for precise kinematic measurement in controlled laboratory settings (Bernardina et al., 2019; Colyer et al., 2018). By tracking retroreflective markers placed on anatomical landmarks with multiple calibrated cameras, these systems reconstruct three-dimensional marker trajectories from which joint angles and segment kinematics are derived (Clouthier et al., 2020; Mündermann et al., 2006). Their strengths lie in exceptional spatial accuracy (on the order of tenths of millimetres), high temporal resolution, and

suitability for quantifying subtle motion differences relevant to performance or pathology (Zago et al., 2020). However, these benefits come at the cost of high financial and technical demands, substantial setup and preparation times, susceptibility to skin movement artefacts, and restriction to controlled indoor environments (De Brabandere et al., 2020). Such constraints limit their ecological validity for in-field applications.

IMUs, comprising accelerometers, gyroscopes, and often magnetometers, provide an attractive portable alternative for capturing segmental accelerations, angular velocities, and orientations (Ross et al., 2020). Their lower cost, ease of deployment, and suitability for real-world environments have facilitated widespread adoption in sports and clinical monitoring (De Brabandere et al., 2020; McDevitt et al., 2022). IMUs can deliver real-time feedback, support objective movement classification, and enable continuous load and fatigue monitoring (Seshadri et al., 2019). Nonetheless, they are vulnerable to drift, magnetic interference, and reduced spatial interpretability compared to optical systems (Robert-Lachaine et al., 2017). The quality of the device and its algorithms strongly influence measurement accuracy, and the absence of visual data can make qualitative interpretation of movement patterns challenging.

RGB-D cameras, such as Microsoft Kinect, capture both colour (RGB) and depth information, enabling markerless 3D skeleton reconstruction in real time (Colyer et al., 2018; Zago et al., 2020). They offer low-cost, non-invasive motion tracking with minimal participant preparation, making them appealing for interactive rehabilitation systems and preliminary screening. However, their accuracy is generally inferior to high-end motion capture, particularly for subtle kinematic changes or rotations in the transverse plane (Colombel et al., 2020). Performance is further limited by environmental constraints (e.g., sunlight interference), a restricted tracking volume, and occlusion challenges.

1.2.3 Computer vision-based movement analysis

Computer vision and deep learning have revolutionized biomechanical assessment by enabling markerless MoCap systems that extract human movement data from video footage (Mathis et al., 2020; Wei & Kording, 2018). These systems utilize algorithms such as OpenPose

and DeepLabCut to detect key body landmarks in real time, without the need for reflective markers or specialized suits (Cao et al., 2021; Nakano et al., 2020; Slembrouck et al., 2020). This significantly improves usability and accessibility, making biomechanical screening more feasible outside of controlled laboratory environments.

Compared to traditional marker-based systems, markerless solutions offer improved ecological validity, allowing assessments to be performed during natural gameplay or field-based movement screening sessions (Colyer et al., 2018). Combined with AI, extracted kinematic data from video footage can offer insights into movement patterns outside of the laboratory (Di Paolo et al., 2023; Dos et al., 2021; Zago et al., 2020). The portability of these systems, particularly those using single-camera setups, makes them highly appealing in settings where resources are limited. However, single-camera systems often suffer from perspective distortion, occlusion, and difficulty in accurately reconstructing 3D joint positions (Meng et al., 2023; Wade et al., 2022).

To overcome these limitations, multi-camera systems have been developed. These setups triangulate body joint positions in three dimensions, thereby improving the fidelity of movement capture and minimizing errors associated with occlusion or off-axis viewing angles (Xu et al., 2018). For example, Kanko et al. validated a multi-camera markerless system against a gold-standard marker-based setup and found comparable accuracy in estimating lower-limb kinematics in sagittal plane during gait analysis (Kanko et al., 2021). Similarly, Harsted et al. and Song et al. demonstrated that markerless MoCap systems can reliably capture lower extremity joint angles in a variety of populations and tasks (Harsted et al., 2019; Song et al., 2023).

Despite their promise, the accuracy of markerless MoCap systems can be highly dependent on video quality, lighting conditions, and subject positioning. Additionally, real-time applications require significant computational power, which can limit feasibility in some field settings (Janisch et al., 2024). Nevertheless, markerless MoCap can provide more objective and scalable alternatives for injury risk assessment (Mathis et al., 2020; Wei & Kording, 2018).

1.3 Data-driven methods in sports injury prevention

1.3.1 Machine learning for injury prediction

Recent advances in data-driven approaches have transformed the landscape of sports injury prevention, particularly in soccer. The integration of wearable technologies (e.g., GPS units, accelerometers, and inertial sensors) has enabled precise tracking of external load metrics, such as movement intensity, distance covered, and acceleration patterns, across matches and training sessions (Nakahira et al., 2022; Rad et al., 2024). These metrics, when analyzed over time, can provide key indicators of workload fluctuations and potential overtraining, both of which are strongly associated with increased injury risk (Bishop et al., 2022; Díaz-Ochoa et al., 2023).

While wearable sensors have traditionally been used to track external loads, computer vision-based tracking algorithms now offer a non-invasive means of analyzing players' movement patterns during actual matches and training sessions (Joos et al., 2024; Oliveira et al., 2024; Somers et al., 2024). Identifying high-risk movement patterns, such as frequent sudden deceleration or uncontrolled cutting maneuvers, may provide valuable insights for individualized injury prevention programs (D'Onofrio et al., 2024; Kolodziej et al., 2022).

To handle the complexity of these multi-dimensional datasets generated from the sensors, machine learning (ML) has become a central analytical tool. ML models can capture nonlinear relationships between biomechanical, physiological, psychological, and historical injury data, providing more nuanced and individualized injury risk predictions than traditional statistical methods (Claudino et al., 2019; Van Eetvelde et al., 2021).

Several ML algorithms have been adopted in injury prediction. Support Vector Machines (SVM) are a powerful class of algorithms ideal for classification tasks, recognized for their capacity to manage both linear and nonlinear data distributions (Han et al., 2024). The application of SVM in sports has streamlined injury risk assessments by employing various features, such as positional data and performance metrics, to categorize athletes' health statuses.

Similarly, eXtreme Gradient Boosting (XGBoost) has emerged as a favored algorithm due to its high performance and efficiency in predictive accuracy. Research demonstrates that XGBoost's

robustness makes it a solid choice for predictive modeling of injury risk factors across athletes, adapting well to diverse datasets and demonstrating significant performance advantages over traditional statistical methods (Huang et al., 2022). Integrating XGBoost with SHAP (SHapley Additive exPlanations) can further elucidate the contributions of specific variables to predicted injury risks, enhancing interpretability and actionable insights for coaches and medical staff (Ayala et al., 2024).

Long Short-Term Memory (LSTM) Networks, a variant of recurrent neural networks (RNNs), excel in capturing temporal dependencies within sequential data, crucial for analyzing training loads, movement patterns, and performance metrics over time (Han et al., 2024). According to Hong et al., LSTMs have shown promise in predicting athlete injury risk, capable of modeling complex patterns in time-series data that are often linked to injuries (Han et al., 2024). Noteworthy advancements using LSTM include modeling acute and chronic workloads to ascertain their correlation with injury occurrences, ensuring that coaches can modify training regimens proactively. LSTMs are particularly advantageous in dynamic environments where athletes' loads and intensities vary, allowing for timely and context-specific predictions (Hulme et al., 2019; Ullah et al., 2024).

The advent of Transformer models has revolutionized the landscape of ML applications, especially in domains requiring insights from vast and complex datasets (Domaradzki & Kopacka, 2025). Transformers' ability to focus on different aspects of the training process through self-attention mechanisms aligns well with sports injury prevention strategies. They enable practitioners to analyze not only performance metrics but also contextual information regarding movement mechanics, further informing injury risk assessments. Research indicates that hybrid models, which integrate transformers with sequence-based networks like LSTM, could yield improvements in identifying modifiable risk factors for injuries (Domaradzki & Kopacka, 2025). Such capabilities enable a more personalized approach to training and rehabilitation interventions, ultimately fostering better athlete safety and longevity.

Datasets employed for injury prediction often encompass player workload metrics,

biomechanical data, movement screening outcomes, and psychological evaluations (Ayala et al., 2024; Chaaban et al., 2021). A combination of these data points supports comprehensive ML models that can adeptly identify potential injury risks. For instance, Chen et al. demonstrate that integrating wearable technology with Convolutional Neural Network (CNN)-LSTM models enables real-time monitoring and prediction of sports injuries based on physiological parameters, highlighting the continuous evolution of data utilization in injury management (Chen et al., 2025).

Conversely, challenges remain for ML applications in sports injury prediction, particularly concerning the quality and quantity of data necessary for building robust models. As suggested by Huang et al., the accuracy of assessments can be influenced significantly by the selection of features and model architecture used, thereby necessitating careful consideration during model development (Huang et al., 2023; Li et al., 2019).

To address these gaps, this doctoral thesis investigates movement quality and performance changes in a cohort of 25 female varsity soccer athletes monitored across a competitive season using data-driven methods. The dataset includes pre-, mid-, and post-season assessments of biomechanical movement patterns, balance performance, reaction times, and injury records. This design enables the examination of how neuromuscular profiles and injury susceptibility change over time and provides a foundation for developing predictive models tailored to the needs of female athletes.

Taken together, these sex-based disparities in injury epidemiology, biomechanics, and recovery trajectories underscore the importance of developing female-specific injury screening tools, movement monitoring technologies, and interpretable machine learning models that can be translated into real-world applications in sports medicine and coaching environments.

1.4 Objectives and research questions

Global Objective 1: To investigate biomechanical and performance-related changes in varsity women's soccer players throughout the competitive season.

***Study 1a**: Seasonal Variations in Biomechanical Performance Among Female Varsity Soccer Players.*

Research questions:

- How do key movement-performance metrics, sprinting speed, jump capability, balance, reaction time, and inter-joint coordination, change from pre- to mid- to post-season?
- Which stage of the season (pre, mid, post) exhibits the greatest decrements or improvements in each metric?

Global Objective 2: to assess how concussions histories may influence movement quality.

Study 1b*: A 3D Goal Equivalent Manifold Approach to Detecting Season-Long Post-Concussion Motor Deficits in Female Soccer Players.*

Research questions:

- Do athletes with a documented concussion history display lower 3D Performance Index (PI) scores than their non-concussed peers at each seasonal time-point?
- Are temporal-persistence metrics (λ) within the Goal Equivalent Manifold (GEM) framework altered in the concussion group, indicating less effective regulation of task-relevant variability?
- Do between-group differences in PI or λ amplify, diminish, or remain stable from pre- to post-season?

Global Objective 3: To compare different machine learning models in predicting lower limb non-contact injury risk.

Study 2*: From Classical Models to Attention-Based Transformers: A Comparative Study on Injury Prediction Pipelines in Female Varsity Soccer.*

Research questions:

- Which of four pipelines, Support Vector Machine (SVM), XGBoost, Long-Short-Term Memory (LSTM) and Hybrid Transformer, provides the best discrimination between injured and non-injured athletes?
- Does including time-series kinematic data (LSTM, Transformer) yield higher predictive performance than models using only engineered summary features (SVM, XGBoost)?

- Can attention weights (Transformer) and SHAP values (XGBoost) reveal the specific movement phases and features most closely associated with elevated injury risk?

Global Objective 4: To validate the effect of two-camera placement on the accuracy of 3-D lower-limb joint-kinematic estimates.

Study 3*: Evaluating the Influence of Two-Camera View Configurations on Markerless 3D Joint Angle Estimation Across Athletic Movements.*

Research questions:

- How does 3D joint-angle error (RMSE, MAE, bias) vary across the 28 two-camera combinations derived from an eight-camera motion capture system configuration?
- Do sagittal-plane angles show systematically lower errors than coronal or transverse-plane angles across configurations?
- Which broad placement categories (Front/Back, Left/Right, Diagonal, Same-quadrant) provide acceptable accuracy for field screening of lower-limb kinematics?

Chapter 2. General Methodology

Twenty-five athletes from the University of Ottawa's varsity women's soccer team were recruited. Data collection included in-lab testing at pre-season, mid-season, and post-season to assess biomechanical changes, and in-field testing during regular training, with data collected by coaches and shared for analysis. This dual approach, combined with the injury records provided by the team's athletic therapists at the end of the season, ensures a comprehensive evaluation of controlled and real-world performance for injury prevention and performance optimization.

2.1 Participants

Twenty-five athletes from the University of Ottawa's women's soccer team participated in the study. Demographic characteristics (mean ± SD) were: age = 20.40 ± 1.98 years; height = 1.66 ± 0.06 m; weight = 63.31 ± 7.94 kg; BMI = 22.9 ± 2.30 kg/m²; left leg length = 86.64 ± 5.63 cm; and right leg length = 86.44 ± 5.41 cm. Player positions included eight defenders, seven forwards, six midfielders, and four goalkeepers. One defender was left-handed, and two defenders were left-foot dominant.

Participants met the following inclusion criteria: (1) ≥18 years of age; (2) able to understand English instructions; (3) fully cleared for athletic participation with no current musculoskeletal injury or concussion; (4) able to complete 40 bilateral bodyweight squats; and (5) not color-blind, as reaction time tasks involved color-based visual stimuli. This study was approved by the Research Ethics Board at University of Ottawa (file #: H-07-24-10628). Participants were informed of their right to withdraw at any time without consequence, and all data were anonymized prior to analysis to ensure confidentiality.

2.2 Movement selection rationale

A battery of functional movement tasks was selected to comprehensively evaluate lower-limb power, neuromuscular control, balance, and motor coordination in female varsity soccer players across the competitive season. The standing broad jump was included to assess horizontal

explosive power, which is essential for sprinting and cutting performance (Markovic et al., 2004; Wisløff et al., 2004). The countermovement jump (bilateral and single-leg) was used to evaluate vertical power and inter-limb asymmetries, which are commonly monitored in fatigue and injury risk assessment (Bishop et al., 2018; Gathercole et al., 2015). To assess dynamic balance and postural control, the Y-Balance test was employed due to its sensitivity in identifying deficits associated with injury risk (Butler et al., 2013; Plisky et al., 2006). Similarly, single-leg hop for distance (L-hop) tests were used to evaluate unilateral power and functional symmetry. This task is more directly sport-specific, reflecting the repeated unilateral loading and rapid direction changes inherent to soccer match play. The L-hop has also been widely used to assess return-to-sport readiness and inter-limb asymmetry following lower-limb injury (Gustavsson et al., 2006; Noyes et al., 1991). The T-Balance test, performed under eyes-open and eyes-closed conditions, was included to probe postural control under varying sensory input, which may be influenced by fatigue or concussion history (Guskiewicz et al., 2001; Paillard & Noé, 2006). The task also mirrors sport-specific demands in soccer, where players frequently stabilize on a single leg to execute technical skills such as passing, trapping, or shooting while maintaining balance against external perturbations. Additionally, simple and complex reaction time tests for both upper and lower limbs were used to evaluate neuromotor response speed and decision-making under time constraints (Nakamoto & Mori, 2008; Spierer et al., 2010). Finally, participants completed a repetitive body-weight squat task (35 repetitions at 40 beat per minute) to facilitate the analysis of intra-individual movement variability under controlled fatigue, supporting advanced variability-based assessments such as the Goal Equivalent Manifold (GEM) and Continuous Relative Phase (CRP) (Dingwell & Marin, 2006; Stergiou & Decker, 2011). This moderate speed (40 beat per minute) was selected based on a pilot study and logistical constraints related to athlete availability. This integrated selection was designed to balance ecological validity with sensitivity to neuromechanical performance and injury-relevant metrics.

2.3 Protocol

Data collection was conducted at pre-season (week 1), mid-season (week 9), and post-season (week 15) to assess both biomechanical changes in the laboratory and sprint performance.

Upon arrival for in-lab testing, participants provided informed consent, completed a questionnaire on their training and injury history (Appendix B), and had their leg length, height, and weight measured. After familiarization, they performed a 5-second static trial in anatomical pose (A-pose) for model scaling, one trial each of T-balance (eyes open and closed), Y-balance and L-hop on both legs, three single-leg (left and right) and bilateral countermovement jumps, three broad jumps, and two reaction time tests for both upper and lower limbs using four FitLights (FITLIGHT Sports Corp., Ontario, Canada) in randomized order. After a minimum 5-minute rest, participants performed 35 bodyweight squats to a metronome at 40 beat per minute (BPM). See detailed movement description in Appendix A. Whole-body kinematics and kinetics were synchronously captured using eight Vicon Vue cameras (Vicon, Oxford, UK) and two force plates (Bertec Corp., Columbus, OH, USA), sampled at 60 Hz and 1000 Hz, respectively, with video data processed using Theia3D v2024 Apollo (Theia Markerless Inc., Kingston, ON, Canada). Neither the kinematics nor the kinetics were captured during the reaction time tests, and except for the consent form, the same protocol was repeated at mid- and post-season sessions. The camera configuration did not change across all testing sessions throughout the season, but the system was recalibrated prior to each data collection session.

For in-field testing, coaches conducted sprinting tests (10, 20, 40, and 60 meters) using timing gates (Brower Timing Systems, Utah, USA) at the same three time points as in-lab testing. The Veo Cam 3 (Veo Technologies, NY, USA) recorded games and training sessions throughout the season, with playing minutes tracked by the coaches. Injury records were provided by the team's athletic therapists at the end of the season.

2.4 General data pre-processing

After in-lab data collection, videos from all eight cameras were transferred and analyzed using

Theia3D (Theia Markerless Inc., Kingston, ON, Canada) and Visual3D (C-Motion Inc., Germantown, MD) to extract 3D kinematics of the center of mass (COM), joint angles and joint moments. Ground reaction forces were obtained from force plates. Final joint kinematics and kinetic data were exported to MATLAB R2019b (The MathWorks Inc., Natick, MA, USA). Data were then filtered and further processed for use in the analyses described within each study (see individual study sections). Sprint test data collected by coaches were analyzed for performance outcomes. Reaction time (s) captured using FitLights (FITLIGHT Sports Corp., Ontario, Canada), and sprint time (s) were used directly in the statistical analysis.

Data preprocessing and analysis for deep learning and computer vision tasks was performed using Python on a high-performance server running Ubuntu 22.04, equipped with three NVIDIA TITAN RTX GPUs and an Intel® Xeon® Gold 6248 CPU @ 2.50 GHz.

Chapter 3. Study 1a: Seasonal Variations in Biomechanical Performance Among Female Varsity Soccer Players

*Submitted to *BMC Sports Science, Medicine and Rehabilitation* *

Xiong Zhao[1], Kangyi Peng[2], Janie Cournoyer[1], Ryan B. Graham[1]

[1]*School of Human Kinetics, Faculty of Health Sciences, University of Ottawa, Ottawa, Ontario, Canada*

[2]*Department of Statistics and Actuarial Science, Faculty of Science, Simon Fraser University, Burnaby, BC, Canada*

Abstract

Objectives: This study aimed to investigate changes in movement performance across a competitive season in female varsity soccer players, integrating in-lab biomechanical assessments with field-based performance measures.

Methods: Twenty-five female varsity soccer players (age 20.40 ± 1.98 years) were tested at pre-, mid-, and post-season stages. Laboratory measures included countermovement jump (CMJ), broad jump, bilateral bodyweight squats, reaction time, Y-balance, T-balance, and L-hop. Field-based tests assessed sprint performance (10 m, 20 m, 40 m, and 60 m).

Results: Sprint times significantly increased mid-season at 10 m ($\chi^2 = 15.56$, $p < .001$), 20 m ($\chi^2 = 31.21$, $p < .001$), and 40 m ($\chi^2 = 7.59$, $p = .023$), with partial recovery post-season. Lower-limb complex reaction time worsened significantly from pre- to post-season ($\chi^2 = 10.45$, $p = .005$), while left upper-limb simple reaction time improved significantly across the season ($\chi^2 = 10.57$, $p = .005$). CMJ heights declined significantly, particularly bilaterally ($\chi^2 = 18.89$, $p < .001$) and in the left leg ($\chi^2 = 8.78$, $p = .012$). Broad jump and L-hop measures remained stable across the season, with no significant main effects observed for jump distance, peak power ($\chi^2=2.22$, $p=.330$), or maximum knee abduction moments (MKAM_L: $\chi^2 = 0.67$, $p = .715$; MKAM_R: $\chi^2 = 1.48$, $p = .477$). Y-balance performance improved post-season, notably in right medial-posterior reach ($\chi^2 = 9.05$, $p = .011$) and left medial-posterior foot acceleration ($\chi^2 = 8.05$, $p = .018$). Knee-ankle coordination amplitude

and variability increased significantly mid-season (MARP: $\chi^2 = 8.09$, $p = .018$; DP: $\chi^2 = 6.39$, $p = .041$).

Conclusion: Female varsity soccer players exhibited significant fluctuations in biomechanical assessments and sprinting, highlighting critical periods of reduced performance and recovery. These findings emphasize the importance of targeted monitoring and tailored training interventions at different stages of a season for injury prevention and performance optimization in female soccer athletes.

3.1 Introduction

Female soccer has experienced significant growth globally, reflected by increasing participation rates, enhanced media visibility, and rising investment at both professional and collegiate levels (Fédération Internationale de Football Association, 2018). This heightened popularity underscores the critical need to improve our understanding of athletic performance and injury risk factors specific to female soccer players. Despite this necessity, research in sport science continues to predominantly focus on male athletes, leaving gaps in knowledge concerning the unique physiological and biomechanical demands female athletes face (Emmonds et al., 2020).

Female soccer players cover 4 to 13 km per game, including 0.2-1.7 km at high speeds, with a high number of rapid accelerations and changes of direction (Bradley & Vescovi, 2015; Mohr et al., 2008). High-intensity actions, although comprising only 8-12% of the total distance, are critical for performance and often coincide with injury mechanisms, such as non-contact anterior cruciate ligament (ACL) injuries, and concussions. Female soccer players also often experience a higher incidence of ACL injuries and patellofemoral pain syndrome, compared to their male counterparts (Sanchez-Sanchez et al., 2025). These increased injury risks have been associated with anatomical differences, such as a wider pelvis and greater quadriceps angle (Q-angle), hormonal fluctuations influencing ligament laxity, and distinct neuromuscular control mechanisms (Silvers-Granelli et al., 2015). Additionally, differences in muscle recruitment patterns and strength contribute significantly to the susceptibility of female athletes to injuries.

Athletic performance in soccer is a complex interplay of physiological, biomechanical, and neuromuscular factors, all subject to fluctuation throughout a competitive season (Bishop et al., 2022; Díaz-Ochoa et al., 2023; Emmonds et al., 2020; Meckel et al., 2018). Changes in movement performance can stem from accumulated fatigue, varying training loads, adaptation to competition demands, and inherent injury risk (Díaz-Ochoa et al., 2023; Raeder et al., 2024). Understanding these changes and managing training regimes are crucial to sustain optimal athletic performance and reduce injury risk, especially in female athletes whose physiological recovery profiles may differ from their male counterparts (Nyby et al., 2024). Comprehensive biomechanical monitoring of performance across an entire competitive season remains relatively rare, particularly for female soccer players. Typically, studies rely on isolated, strength-based tests, such as one-repetition maximum squats, or sport-specific conditioning tests (e.g., Yo-Yo Intermittent Recovery Test) (Impellizzeri et al., 2008; Silva et al., 2013). In contrast, the present study adopts a biomechanical perspective, incorporating a broader set of screening tasks including jump, sprinting, change of direction, balance, reaction assessments, and inter-joint coordination tests. These assessments allow for a more comprehensive examination of neuromuscular control and motor strategies beyond raw strength or endurance (Bishop et al., 2022; González-Fernández et al., 2022; Kirishima & Anan, 2024).

The aim of this study was to investigate how a range of movement performance indicators, spanning sprinting, jumping, balance, coordination, and reaction time, change across a competitive season in female varsity soccer players. Based on previous literature, it is hypothesized that sprint, jump, and reaction performance would improve from preseason to midseason, followed by declines post-season due to fatigue. We also expected changes in coordination variability and balance to reflect midseason neuromuscular stress with potential recovery or adaptation by the end of the season (Emmonds et al., 2020; Kirishima & Anan, 2024; Meckel et al., 2018; Pau et al., 2014).

3.2 Methods

3.2.1 Participants

Twenty-five athletes from the University of Ottawa's women's soccer team participated in the study. Demographic characteristics (mean ± SD) were: age = 20.40 ± 1.98 years; height = 1.66 ± 0.06 m; weight = 63.31 ± 7.94 kg; BMI = 22.9 ± 2.30 kg/m²; left leg length = 86.64 ± 5.63 cm; and right leg length = 86.44 ± 5.41 cm. Player positions included eight defenders, seven forwards, six midfielders, and four goalkeepers. One defender was left-handed, and two defenders were left-foot dominant.

Participants met the following inclusion criteria: (1) ≥ 18 years of age; (2) able to understand English instructions; (3) fully cleared for athletic participation with no current musculoskeletal injury or concussion; (4) able to complete 40 bilateral bodyweight squats; and (5) not color-blind, as reaction time tasks involved color-based visual stimuli. This study was approved by the Research Ethics Board at University of Ottawa (file #: H-07-24-10628). Participants were informed of their right to withdraw at any time without consequence, and all data were anonymized prior to analysis to ensure confidentiality.

3.2.2 Protocol

Data collection was conducted at pre-season (week 1), mid-season (week 9), and post-season (week 15) to assess both biomechanical changes in the laboratory and sprint performance. In-field sprint tests (10, 20, 40, and 60 meters) were administered during regular training by coaches using timing gates (Brower Timing Systems, Utah, USA) as shown in Figure 3.1, and data were shared for analysis.

Upon arrival for in-lab testing, participants provided informed consent, and had their leg length, height, and weight measured. After familiarization, they completed one trial each of T-balance (eyes open and closed), Y-balance and L-hop on both legs, three single-leg (left and right) and bilateral countermovement jumps, three broad jumps, and two reaction time tests for both upper and lower limbs using four FitLights (FITLIGHT Sports Corp., Ontario, Canada) in

randomized order. After a minimum 5-minute rest, participants performed 35 bodyweight squats to a metronome at 40 beat per minute (BPM). See detailed movement description in Appendix A. Whole-body kinematics and kinetics were recorded in synchronization using an 8-camera markerless motion capture system (Theia Markerless Inc., Kingston, ON, Canada) and two force plates (Bertec Inc., Ohio, USA), sampled at 60 Hz and 1000 Hz, respectively. Neither the kinematics nor the kinetics were captured during the reaction time tests, and except for the consent form, the same protocol was repeated at mid- and post-season sessions.

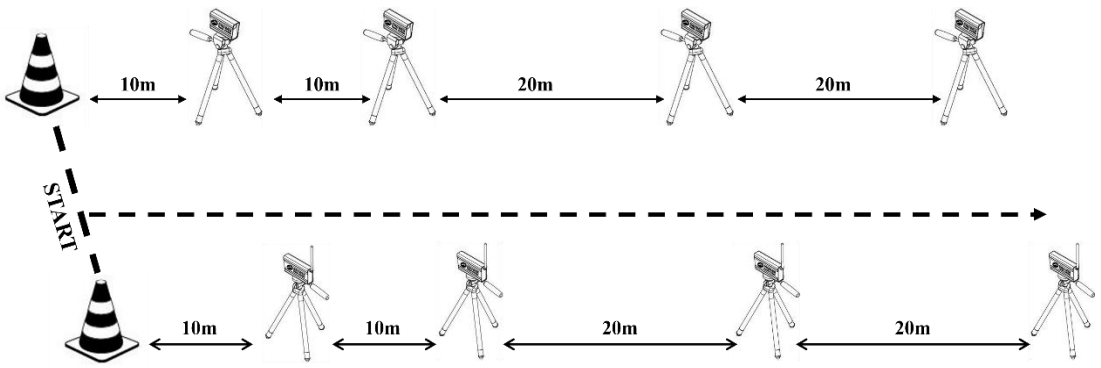

Figure 3.1: Sprint test setup: start line between two cones and timing gates on tripods at 10 m, 20 m, 40 m, and 60 m.

3.2.3 Data processing

After in-lab data collection, videos were processed using Theia3D (Theia Markerless Inc., Kingston, ON, Canada) and analyzed in Visual3D (C-Motion Inc., Germantown, MD) to extract 3D kinematics of the center of mass (COM), joint angles and joint moments. Ground reaction forces were obtained from force plates. To ensure consistency of the squat, only the final 30 repetitions were retained for analysis. Each repetition was segmented based on the COM vertical trajectory. For each screening movement, linear metrics were computed using custom scripts in MATLAB R2019b (The MathWorks Inc., Natick, MA, USA). Kinematic and kinetic data were low-pass filtered using a fourth-order Butterworth filter with 6 Hz and 10 Hz cutoff frequencies, respectively.

Sprint test data collected by coaches were analyzed for performance outcomes. Reaction time (s) captured using FitLights (FITLIGHT Sports Corp., Ontario, Canada) (Myers et al., 2023), and

sprint time (s) were used directly in the statistical analysis.

For the countermovement jump (CMJ), jump height (m) and reactive strength index (RSI) were calculated from vertical COM displacement and kinetic data, respectively (Markwick et al., 2015). Similarly, for the broad jump, average horizontal displacement (m) and takeoff peak power normalized to body mass (W/kg) were computed (Anicic et al., 2023; Boone et al., 2021; Sha et al., 2021).

During the T-balance test, COM sway area was extracted from the whole-body model adopted from (Prieto et al., 1996), and a performance index was calculated as the ratio of sway area with eyes closed to eyes open (Figure 3.2). For the Y-balance test, reach score (normalized to % leg length) and average acceleration (m/s²) of the reaching foot were calculated for each direction. Composite reach scores (average of the three directions) were also computed for each leg (González-Fernández et al., 2022; Plisky et al., 2009).

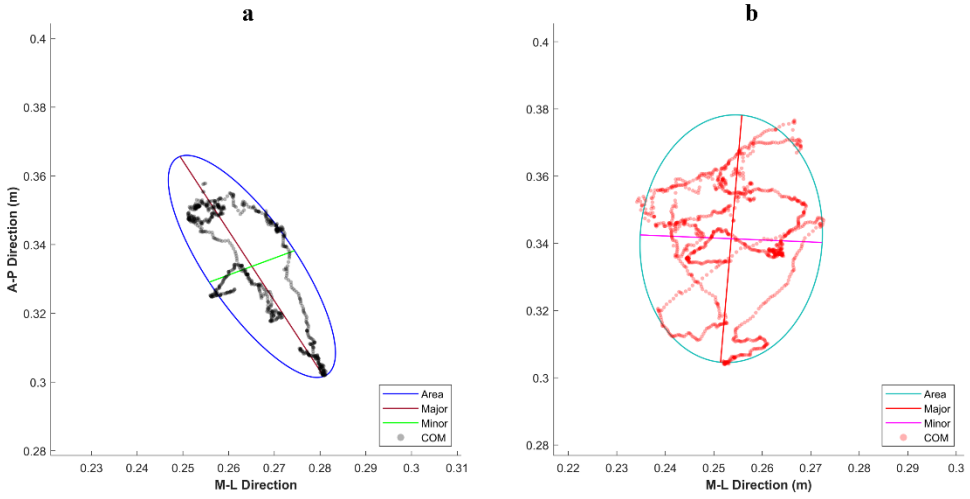

Figure 3.2: COM sway during a right-leg T-balance for the same participant: (a) eyes closed, (b) eyes open. Each panel plots mediolateral (M-L, x-axis) versus anteroposterior (A-P, y-axis, forward-facing) COM trajectories (dots), with a 95% confidence ellipse (colored) enclosing the sway area. The ellipse's major axis represents the principal (largest) sway direction and the minor axis the secondary sway.

Continuous relative phase (CRP) provides a way to describe inter-joint coordination and is frequently applied in clinical settings. By mapping joint angles across the entire movement cycle

onto a phase plane, CRP captures spatiotemporal dynamics (Kirishima & Anan, 2024). At each time point, the phase angle of one joint is subtracted from that of another to derive the CRP angle, which reflects their relative in-phase (close to 0°) or anti-phase (approaching 180°) relationship (Figure 3.3). MARP (Mean Absolute Relative Phase) and DP (Deviation Phase) from each joint pair were calculated to assess how consistently the two joints were coordinated (Kirishima & Anan, 2024). MARP quantifies the amplitude of intersegmental coordination, indicating whether segments or joints move in-phase or out-of-phase, whereas DP reflects the variability of this coordination pattern. Specifically, mean values of the MARP and DP of hip-knee and knee-ankle joint pairs on both sides were assessed during the squat task in this study.

Before statistical analysis, data were adjusted for limb dominance, where applicable, with the right leg designated as dominant and the left as non-dominant.

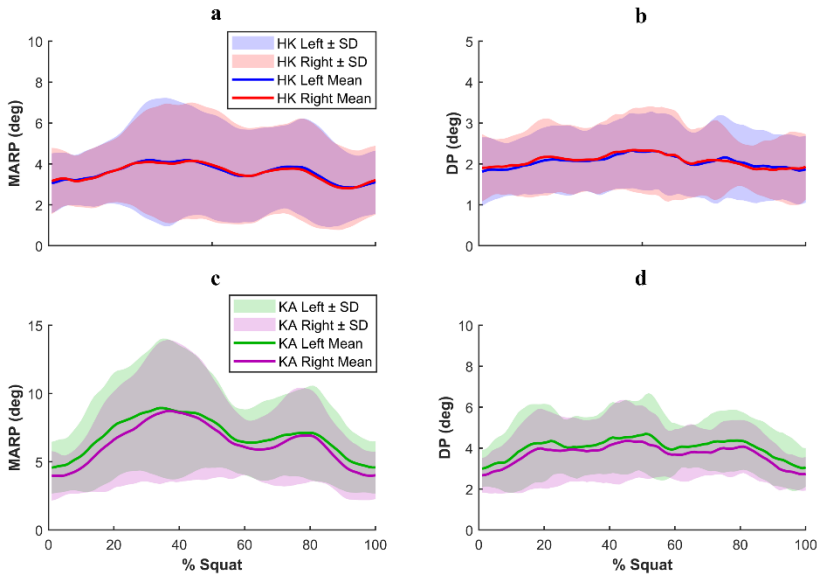

Figure 3.3: Group mean ± SD curves of MARP and DP for pre-season squats. (a) Hip-Knee MARP; (b) Hip-Knee DP; (c) Knee-Ankle MARP; (d) Knee-Ankle DP. The x-axis for all panels represents % of the squat cycle, y-axis represents the magnitude in degrees.

3.2.4 Statistical analysis

All statistical analyses were performed using IBM SPSS Statistics, Version 25.0 (IBM Corp., Armonk, NY, USA). Prior to modeling, the distribution of each continuous outcome variable

was assessed using Shapiro-Wilk tests. To assess changes in movement performance across the season, a generalized linear model for repeated measures was estimated using generalized estimating equations (GEE). GEEs were used to account for within-subject correlations and allowed the inclusion of participants with partially missing data (Ballinger, 2004). Cases with incomplete timepoints were retained in the analysis under the assumption that data were missing at random (MAR). Stage (pre-, mid-, post-season) was modeled as a categorical predictor with pre-season as the reference. Parameter estimates from the generalized linear model with GEE estimation were used to assess changes over time, with pre-season set as the reference category. Estimated coefficients (*B*) reflect the mean difference (M) in the outcome at each stage relative to pre-season, along with standard errors (SE) and associated Wald χ^2 tests. Where applicable, pairwise comparisons were performed using Sequential Bonferroni adjustment. Significance was set at $p < 0.05$.

To test robustness of this method, GEE was rerun including only the participants who completed pre-, mid-, and post-season assessments. Group mean difference was compared at each stage between completers and full-sample data before rerunning the generalized linear model with GEE. A significant difference would suggest informative dropout, because injuries accounted for most post-season missingness.

3.3 Results

At pre-season (week 1), 23 participants completed the in-lab and 20 the sprint test. At mid-season (week 9), 24 participants completed the in-lab and 19 the sprint test. At post-season (week 15), 20 participants completed the in-lab and 13 the sprint test. Missing participants varied by position (defenders, midfielders, forwards, and goalkeepers).

When the model was limited to participants with complete data, several metrics, specifically the MARP of the right Knee-Ankle pair, the complex reaction time test for lower limbs, and the Y-balance reach score of the right leg in the medial-posterior direction, became only marginally significant compared to the full-sample dataset. In every case, the effect sizes and directions

remained similar to the full-sample GEE, but the *p*-values exceeded 0.05, and no additional metrics reached significance.

Significant seasonal changes were observed across several movement tasks. Sprint times over 10 m, 20 m, and 40 m increased at mid-season, with only partial recovery by post-season. Lower-limb complex reaction time slowed by post-season, while left upper-limb simple reaction time improved across the season. Bilateral and left-leg countermovement jump heights declined significantly from pre-season. In the Y-Balance task, right posteromedial reach distance and foot acceleration increased from mid- to post-season. Finally, right Knee-Ankle coordination during squats showed significant changes, with increased coordination amplitude (anti-phase) mid-season.

3.3.1 Sprint

Descriptive statistics (Table 3.1) showed that sprint times generally increased from pre- to mid-season, with partial recovery at post-season. The greatest slowdown was observed at 10 m and 20 m sprints during mid-season.

Table 3.1: Descriptive statistics of sprint times (s) of 10 m, 20 m, 40 m, and 60 m at pre-, mid-, and post-season.

Stage	10m (s)*	20m (s)*	40m (s)*	60m (s)
pre	1.90 ± 0.10	3.26 ± 0.11	5.88 ± 0.21	8.51 ± 0.31
mid	2.08 ± 0.22	3.43 ± 0.14	6.02 ± 0.30	8.64 ± 0.45
post	1.94 ± 0.11	3.33 ± 0.17	5.94 ± 0.28	8.67 ± 0.45

Note: Values are presented as mean ± standard deviation. * = statistical significance was found in the task.

A significant main effect of stage was found for sprint times at 10 m (χ^2 (2) = 15.56, $p < .001$), 20 m (χ^2 (2) = 31.21, $p < .001$), and 40 m (χ^2 (2) = 7.59, $p = .023$) (Figure 3.4a-c). Pairwise comparisons revealed slower sprint times at mid-season compared to both pre- and post-season at all three distances (all $p < .05$). Sprint time at post-season remained elevated compared to pre-season at 10 m ($p = .014$) and 20 m ($p = .010$). No significant stage effect was found for the 60 m sprint (χ^2 (2) = 2.91, $p = .233$), indicating long-distance sprint performance remained stable across the season at team level.

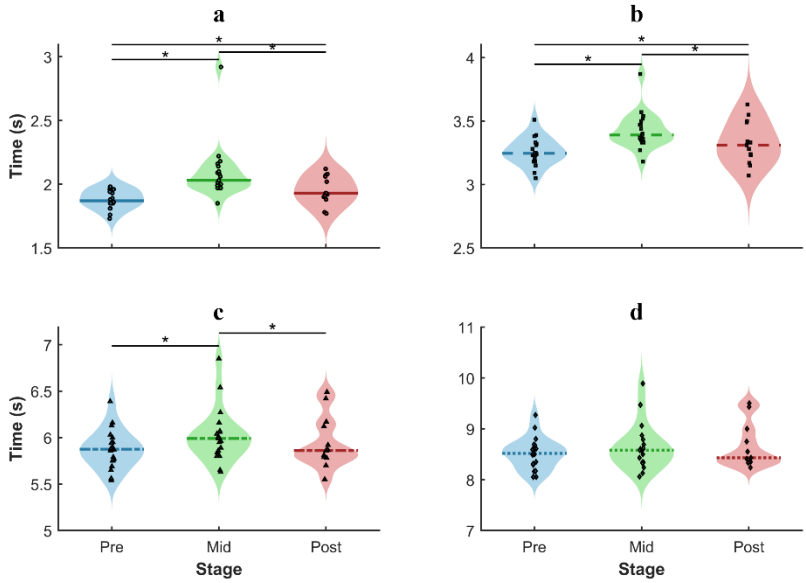

Figure 3.4: Violin plots of sprint times at (a) 10 m, (b) 20 m, (c) 40 m, and (d) 60 m for Pre, Mid, and Post seasons. Each violin shows the full distribution (dots) and mean (dashed line). Asterisks mark significant differences ($p < .05$).

3.3.2 Reaction time

As shown in Table 3.2, complex reaction time of the lower limb (CRT_Lower) showed a progressive increase from pre- to post-season (0.65 ± 0.08 s to 0.71 ± 0.06 s), while simple reaction time of the left upper limb (SRT_LU) decreased from 0.52 ± 0.07 s to 0.48 ± 0.05 s. Reaction times for other limbs and tasks remained relatively stable across stages, with minimal changes in mean values and standard deviations.

Table 3.2: Descriptive statistics of reaction times (in seconds) across season stages.

Stage	SRT_LU*	SRT_RU	SRT_LL	SRT_RL	CRT_Upper	CRT_Lower*
pre	0.52 ± 0.07	0.49 ± 0.06	0.58 ± 0.05	0.56 ± 0.05	0.60 ± 0.07	0.65 ± 0.08
mid	0.48 ± 0.06	0.47 ± 0.05	0.60 ± 0.05	0.56 ± 0.06	0.58 ± 0.05	0.68 ± 0.07
post	0.48 ± 0.05	0.49 ± 0.07	0.59 ± 0.05	0.57 ± 0.03	0.61 ± 0.05	0.71 ± 0.06

Note: Values are presented as mean ± standard deviation. * = statistical significance was found in the task; SRT = Simple Reaction Time; CRT = Complex Reaction Time; LU = Left Upper limb, RU = Right Upper limb, LL = Left Lower limb, RL = Right Lower limb.

A significant main effect of stage was found for lower-limb complex reaction time

(CRT_Lower), (χ^2 (2) = 10.45, p = .005) (Figure 3.5a), with slower response times at post-season compared to pre-season (p = .006) and mid-season (p = .026). For simple reaction time tasks (SRT), only the left upper limb showed a significant effect of stage, (χ^2 (2) = 10.57, p = .005) (Figure 3.5c), with faster reaction at both mid-season (p = .004) and post-season (p = .008) compared to pre-season. When the model was rerun on participants with complete data, the main effect of stage became marginal (χ^2 (2) = 5.78, p = .060), but no mean difference was observed between completers and full-sample dataset.

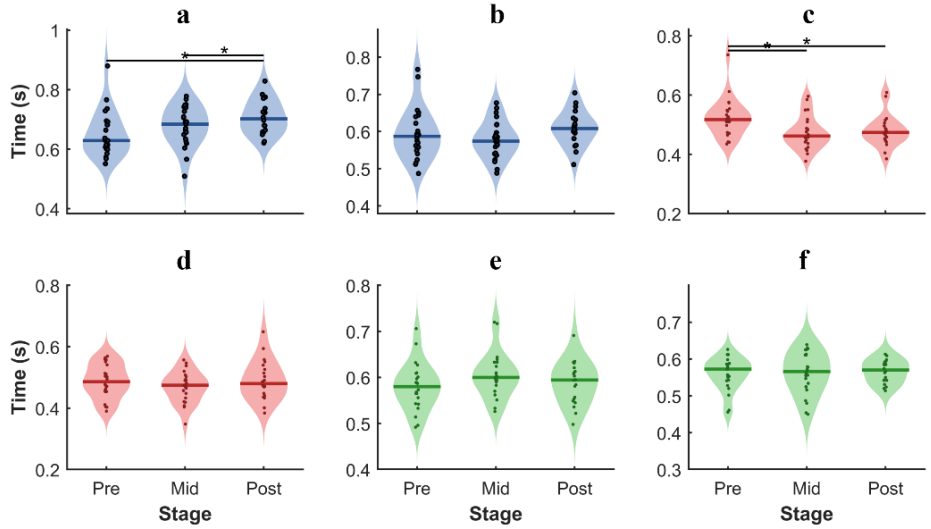

Figure 3.5: Violin plots of reaction time tests across Pre, Mid, and Post seasons for: (a) CRT_LL, (b) CRT_UL, (c) SRT_UL, (d) SRT_UR, (e) SRT_LL, (f) SRT_LR. Dots represent individual values; solid horizontal lines within each plot denote means; asterisks indicate significant pairwise differences.

3.3.3 Countermovement jump

A general decrease in CMJ height was observed over the season, particularly in the bilateral and left single-leg conditions. In contrast, RSI values remained relatively stable across stages as shown in Table 3.3.

Table 3.3: Descriptive statistics of jump height (m) and reactive strength index (RSI) of countermovement jumps across the season.

Stage	Height_L*	RSI_L	Height_R	RSI_R	Height_Bi*	RSI_Bi
pre	0.30 ± 0.05	0.74 ± 0.28	0.29 ± 0.05	0.75 ± 0.30	0.37 ± 0.06	0.93 ± 0.26

mid	0.28 ± 0.06	0.80 ± 0.30	0.26 ± 0.06	0.71 ± 0.27	0.33 ± 0.06	0.90 ± 0.30
post	0.27 ± 0.05	0.81 ± 0.27	0.26 ± 0.05	0.77 ± 0.30	0.30 ± 0.05	0.80 ± 0.34

Note: Values are presented as mean ± standard deviation. * = statistical significance was found; Height = Jump height; RSI = Reactive Strength Index; L = Left leg; R = Right leg; Bi = Bilateral.

Statistical analysis revealed a significant main effect of stage on left-leg jump height (χ^2 (2) = 8.78, p = .012) (Figure 3.6d), with a significant decline from pre- to post-season (p = .010). The bilateral jump height also showed a strong effect of stage (χ^2 (2) = 18.89, p < .001) (Figure 3.6e), with significantly lower values at both mid- (p = .005) and post-season (p < .001) compared to pre-season. Right-leg jump height showed a marginal effect (χ^2 (2) = 4.91, p = .086), with a significant decrease at mid-season compared to pre-season (p = .039). In contrast, no significant stage effects were found for RSI.

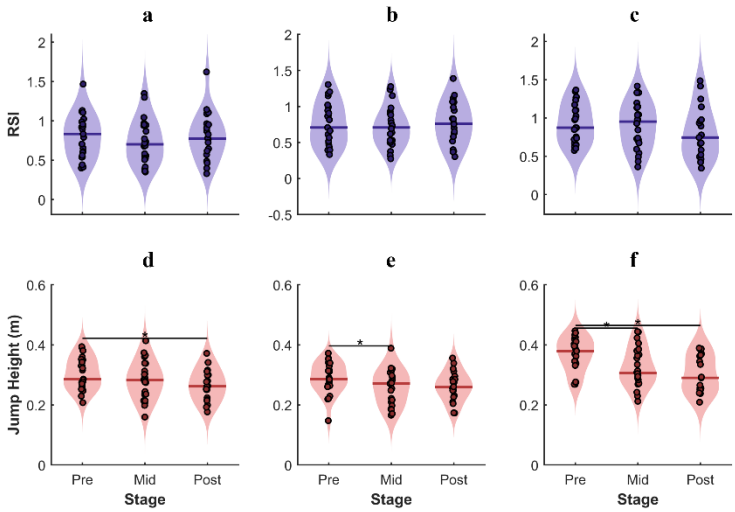

Figure 3.6: Violin plots showing reactive strength index (RSI) and jump height during CMJ tasks at Pre, Mid, and Post seasons: (a) RSI_Left, (b) RSI_Right, (c) RSI_Bilateral, (d) Jump Height_Left, (e) Jump Height_Right, (f) Jump Height_Bilateral. Each violin displays individual data points (dots) and group means (solid horizontal lines within each plot), with horizontal black lines and asterisks indicating significant pairwise differences.

3.3.4 Broad jump

A decrease in broad jump distance was observed from pre-season to mid- and post-season, accompanied by minor fluctuations in peak power output across stages (Table 3.4). However, no

significant main effect of stage was found for broad jump distance (χ^2 (2) = 2.22, p = .330) or normalized peak power (χ^2 (2) = 1.18, p = .555).

Table 3.4: Average distance and peak power normalized to body mass of broad jump across season stages.

Stage	Distance (m)	Peak Power (W/kg)
pre	2.10 ± 0.15	19.36 ± 3.15
mid	2.05 ± 0.19	18.59 ± 2.48
post	2.05 ± 0.18	19.04 ± 2.95

Note: Values are presented as mean ± standard deviation.

3.3.5 L-hop

Results (Table 3.5) showed relatively stable maximum knee abduction moments (MKAM) across all three time points, with minor fluctuations. Specifically, MKAM values for both left and right limb landings showed modest increases at mid-season, more pronounced on the left (non-dominant) side, before returning to baseline levels by post-season. Statistical analysis confirmed no significant main effect of stage on MKAM for either the left limb (χ^2 (2) = 0.67, p = .715) or right limb (χ^2 (2) = 1.48, p = .477).

Table 3.5: Normalized maximum knee abduction moments of peak knee abduction moment during L-Hop task.

Stage	MKAM_L (Nm/kg)	MKAM_R (Nm/kg)
pre	0.23 ± 0.10	0.21 ± 0.05
mid	0.25 ± 0.09	0.22 ± 0.08
post	0.23 ± 0.05	0.22 ± 0.05

Note: Values are presented as mean ± standard deviation. MKAM = Peak knee abduction moment normalized to body mass; L = Left limb landing; R = Right limb landing.

3.3.6 Y-balance

Reach scores were relatively consistent as shown in Table 3.6a and Figure 3.7. Only a significant effect of stage was observed for the right medial-posterior score (χ^2 (2) = 9.05, p = .011)

(Figure 3.7e). Pairwise comparisons revealed a significant increase from mid- to post-season (p = .009). However, the significance reduced when the model was rerun on participants who completed all three sessions with no mean difference (χ^2 (2) = 5.50, p = .064).

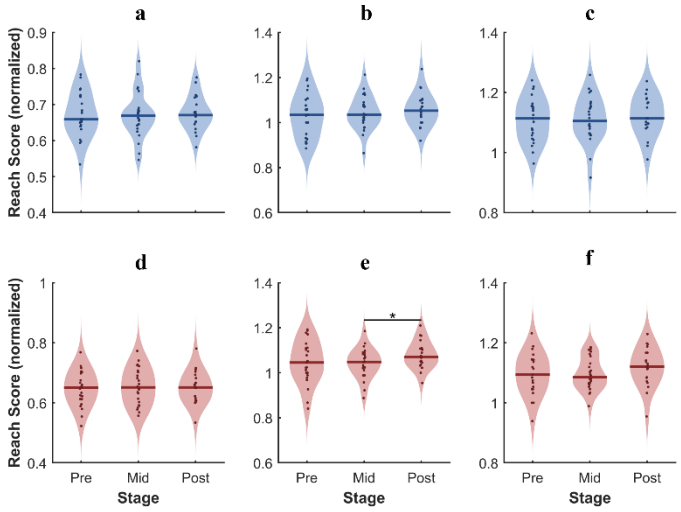

Figure 3.7: Violin plots of normalized Y-balance reach scores at Pre, Mid, and Post seasons for: (a) Left Anterior, (b) Left Posteromedial, (c) Left Posterolateral, (d) Right Anterior, (e) Right Posteromedial, and (f) Right Posterolateral directions. Each violin shows individual data points (dots) and group means (solid lines within each plot), with horizontal black lines and asterisks indicating significant pairwise differences.

Composite reach scores, the average of the reach scores in three directions, (Table 3.6b) did not show any significant change across the season.

For the accelerations of the reaching foot (Table 3.6c and Figure 3.8), a significant main effect of stage was found for left medial-posterior acceleration (χ^2 (2) = 8.05, p = .018). Pairwise comparisons indicated a significant increase in acceleration from mid- to post-season (p = .047) (Figure 3.8b).

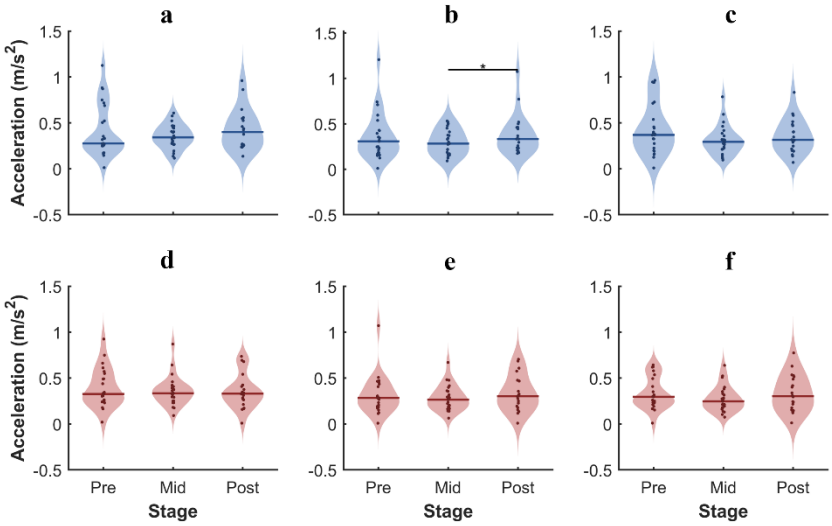

Figure 3.8: Violin plots of reaching-foot acceleration (m/s^2) during the Y-balance test at Pre, Mid, and Post seasons for (a) Left Anterior, (b) Left Posteromedial, (c) Left Posterolateral, (d) Right Anterior, (e) Right Posteromedial, and (f) Right Posterolateral directions. Dots represent individual trials, solid horizontal lines denote group means, and the asterisk in indicates a significant difference.

Table 3.6a: Reach score in three directions of both legs (% leg length).

Stage	Left			Right		
	ANT	MP	LP	ANT	MP*	LP
pre	67 ± 6	103 ± 9	111 ± 7	65 ± 6	105 ± 10	110 ± 7
mid	67 ± 6	104 ± 7	111 ± 8	65 ± 6	104 ± 7	110 ± 5
post	68 ± 5	106 ± 7	112 ± 7	65 ± 5	108 ± 6	112 ± 7

Table 3.6b: Composite scores: (ANT+MP+LP)/3.

Stage	Composite Left	Composite Right
pre	93.53 ± 6.46	93.22 ± 5.76
mid	94.57 ± 5.86	92.63 ± 5.40
post	95.11 ± 5.27	95.08 ± 5.10

Table 3.6c: Reaching foot's acceleration (m/s^2) during Y-Balance.

Stage	Left			Right		
	ANT	MP*	LP	ANT	MP	LP
pre	0.42 ± 0.29	0.36 ± 0.26	0.42 ± 0.27	0.39 ± 0.21	0.31 ± 0.21	0.33 ± 0.17
mid	0.35 ± 0.13	0.29 ± 0.14	0.31 ± 0.16	0.36 ± 0.16	0.28 ± 0.14	0.27 ± 0.14

post	0.42 ± 0.22	0.38 ± 0.22	0.35 ± 0.19	0.35 ± 0.19	0.33 ± 0.20	0.33 ± 0.20

Note: Values are presented as mean ± standard deviation. * = statistical significance was found; ANT = Anterior; MP = Medial-posterior; LP = Lateral-posterior; Composite scores reflect the average normalized reach score across directions for each limb.

3.3.7 T-balance

The sway area ratios of the non-dominant leg (left) were greater than the dominant (right) leg across the season (Table 3.7). Although the dominant leg exhibited a higher sway area ratio than the non-dominant leg at mid-season, no significant main effect of stage was observed for sway area ratios (eyes closed over eyes open) in either leg (Left: χ^2 (2) = 0.44, p = .802; Right: χ^2 (2) = 0.90, p = .639). Mean sway area ratios on the non-dominant side dipped at mid-season, while the dominant side showed a gradual increasing trend toward the end of the season; however, neither change reached statistical significance.

Table 3.7: Sway area ratios of eyes closed over open during T-Balance tasks.

Stage	SA_Ratio Left	SA_Ratio Right
pre	6.19 ± 9.07	4.39 ± 4.32
mid	5.13 ± 4.51	5.50 ± 7.45
post	6.71 ± 11.76	6.00 ± 5.44

Note: Values are presented as mean ± standard deviation. SA_Ratio = Sway area ratio, calculated as sway area during eyes closed divided by sway area during eyes open. Left = Left leg stance; Right = Right leg stance.

3.3.8 Squat

MARP and DP values increased slightly from pre- to post-season, particularly in the Knee-Ankle couplings as shown in Table 3.8 and Figure 3.9. Statistical results showed no significant stage effect for Hip-Knee MARP or DP in either limb.

Table 3.8: Descriptive statistics of Continuous Relative Phase (CRP) results during squats.

Stage	Left				Right			
	Hip-Knee		Knee-Ankle		Hip-Knee		Knee-Ankle	
	MARP	DP	MARP	DP	MARP	DP	MARP*	DP*

pre	3.55 ± 1.68	2.06 ± 0.66	6.81 ± 2.38	4.02 ± 1.19	3.53 ± 1.79	2.06 ± 0.68	6.27 ± 2.33	3.67 ± 1.15
mid	3.65 ± 1.81	2.10 ± 0.87	8.20 ± 3.58	4.70 ± 1.94	3.90 ± 2.04	2.15 ± 0.87	8.01 ± 3.15	4.70 ± 2.13
post	4.30 ± 2.53	2.27 ± 1.09	7.63 ± 4.02	4.39 ± 1.72	4.55 ± 2.84	2.34 ± 1.19	7.13 ± 2.72	4.32 ± 1.57

Note: Values are presented as mean ± standard deviation. * = statistical significance was found; MARP = Mean Absolute Relative Phase; DP = Deviation Phase; MARP reflects the average phase lag between joints, while DP reflects the variability in coordination patterns during bodyweight squats.

For the Knee-Ankle coupling, the stage effect was statistically significant for right-limb MARP (χ^2 (2) = 8.09, p = .018), and DP (χ^2 (2) = 6.39, p = .041), with post hoc comparisons indicating a significant increase in right-limb MARP from pre- to mid-season (p = .025) (Figure 3.9d). No other pairwise comparisons reached significance after adjustment.

The main stage effect for the right Knee-Ankle MARP became marginal (χ^2 (2) = 4.05, p = .132) when reran the model on only completers after no mean difference was confirmed.

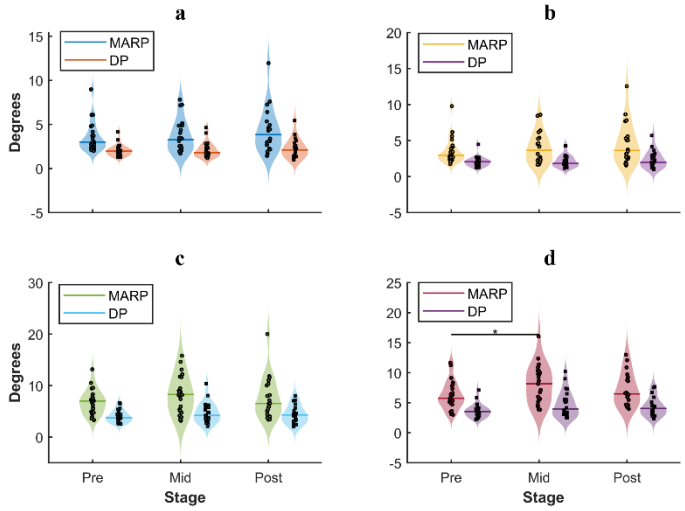

Figure 3.9: Violin plots of continuous relative phase (CRP) metrics during squats across Pre, Mid, and Post seasons. In each panel, the left violin represents MARP, and the right violin represents DP. (a) depicts left Hip-Knee; (b) left Knee-Ankle; (c) right Hip-Knee; (d) right Knee-Ankle. Individual participant values are overlaid as dots, and solid horizontal lines within each plot indicate group means. A horizontal black line and asterisk mark a significant difference.

3.4 Discussion

This study aimed to investigate seasonal changes in movement performance among female varsity soccer players by integrating laboratory-based biomechanical assessments with field-based

performance measures. The results indicate that while performance remained stable in certain tasks, such as the L-Hop and broad jump, notable fluctuations were observed in sprinting, CMJ, reaction time, and inter-joint coordination. These changes likely reflect the dynamic interplay of cumulative fatigue, physiological adaptation, and recovery throughout the competitive season. The partial recovery observed at the post-season stage may be attributed to a reduction in overall training load during the latter part of the season (Savolainen et al., 2024).

3.4.1 Physical performance

The significant mid-season decline observed in sprint performance, particularly at short distances, aligns with previous research identifying cumulative fatigue from increased training and match demands during this period (Bishop et al., 2022; Meckel et al., 2018). This decline may also reflect inadequate recovery strategies during intense competition phases, potentially predisposing athletes to injuries (Emmonds et al., 2020). Partial recovery noted post-season suggests that the reduction in training volume or intensity typically implemented towards the end of the season may partially alleviate accumulated fatigue (Raeder et al., 2024).

Jump performance, particularly CMJ, is recognized as an indicator of lower-limb power and neuromuscular readiness in soccer (Markovic, 2007). In our study, CMJ height decreased significantly mid-season and remained depressed at post-season in both bilateral and left single-leg conditions. This decline may reflect accumulated fatigue and neuromuscular strain across the competitive schedule, which aligns with earlier work reporting seasonal reductions in jump performance in female and male footballers (Meckel et al., 2018; Silva et al., 2013). Interestingly, reactive strength index (RSI) remained stable throughout the season, suggesting that while maximal power output diminished, stretch-shortening cycle efficiency may have been preserved (Gathercole et al., 2015).

Broad jump distance and peak power output remained stable across all three testing time points, suggesting that horizontal force production capacity was not significantly affected over the course of the season. This contrasts with the more fatigue-sensitive CMJ height, possibly due to differing neuromechanical demands between vertical and horizontal tasks (Boone et al., 2021).

While less frequently used as a diagnostic tool in soccer compared to CMJ, broad jump performance provides valuable information on horizontal explosiveness, which is critical for acceleration and first-step quickness.

3.4.2 Change of direction biomechanics

Unlike traditional change of direction (COD) tests such as the T-test or 505 agility tests, which measure task completion time (Sun et al., 2025), our study examined biomechanical responses during the L-Hop, focusing on maximum knee abduction moments (MKAM) at landing. This approach allows a more direct assessment of joint loading and ACL injury risk, particularly in females who are more susceptible to valgus collapse during lateral movements (Hewett et al., 2005; Silvers-Granelli et al., 2015). While we found no significant changes in MKAM across the season, a subtle mid-season increase, particularly in the non-dominant limb, suggests the potential for transient changes in landing mechanics related to fatigue. These findings emphasize the importance of biomechanical evaluations that go beyond time-based agility metrics, offering deeper insight into neuromuscular control and joint health.

3.4.3 Balance

Improvements in Y-balance post-season, particularly in the right medial-posterior reach and left medial-posterior foot acceleration, suggest favorable neuromuscular adaptations or enhanced proprioceptive and balance control capabilities toward the end of the competitive season (Nyby et al., 2024). Y-balance lower composite scores or asymmetries in reach distance have been associated with increased risk of non-contact injuries, including ankle sprains and ACL tears (Butler et al., 2013; Plisky et al., 2009). Additionally, foot acceleration during the reaching movement may reflect dynamic control and reactive capacity, both critical for injury prevention during cutting or single-leg stance tasks (Gidu et al., 2022; Gonell et al., 2015).

Although no statistically significant changes were observed in T-balance performance across the season, the mid-season dip in sway area ratios on the non-dominant side and the gradual increase on the dominant side were notable. This directional trend may suggest asymmetrical

neuromuscular adaptations or compensation patterns related to fatigue, workload distribution, or limb dominance during the competitive season (Nyby et al., 2024; Pau et al., 2014). The T-balance test may have been subject to ceiling effects, where the sensitivity of the measure was insufficient to detect subtle within-season changes in postural control among high-functioning athletes (Chinsongkram et al., 2016; Guskiewicz et al., 2001).

3.4.4 Reaction time and coordination

Reaction time, particularly lower-limb complex reaction time (CRT), worsened significantly from pre- to post-season, suggesting degradation of neuromuscular responsiveness and central processing speed with accumulated fatigue (Rentz et al., 2021). Conversely, simple reaction time in the left upper limb improved over time, possibly reflecting repeated exposure and limb dominance effects. These results align with mixed literature on fatigue and reaction time, where task complexity and modality (upper vs. lower limb) may influence fatigue sensitivity (Wilkerson et al., 2017). Given the importance of reaction speed in game decision-making and injury prevention, especially during unanticipated movements, tailored neuromotor training may be beneficial.

The findings revealed a mid-season increase in both MARP and DP values for knee-ankle coordination, suggesting a shift in inter-joint coordination and an increase in movement variability. While increased variability is often interpreted as a sign of neuromuscular fatigue or instability, it is important to note that not all variability is detrimental. In fact, a certain level of movement variability is considered beneficial, as it may reflect flexible motor strategies that help distribute mechanical loads more evenly across joints and tissues (Harbourne & Stergiou, 2009). Conversely, excessively rigid coordination patterns, with reduced variability, have been associated with increased joint stress and overuse injuries due to repetitive loading on the same structures (Hamill et al., 1999; Stergiou & Decker, 2011). Therefore, the mid-season increase in variability observed in our study may reflect an adaptive response to manage cumulative mechanical demands rather than a negative sign of fatigue.

Overall, our findings highlight that key biomechanical and neuromuscular variables fluctuate

across the competitive season in female soccer players. Sprint and vertical jump performance declined mid-season and failed to fully recover post-season, indicating the need for in-season maintenance of explosive strength. At the same time, subtle changes in balance, coordination, and joint loading suggest underlying neuromuscular fatigue that may increase injury risk if left unaddressed. Strength and conditioning staff should incorporate both time-based and biomechanical screening tools throughout the season to tailor training loads, monitor fatigue, and reduce the likelihood of overuse injuries in female soccer athletes.

3.4.5 Limitations

This study was limited by a relatively small sample size and some missing data, largely due to injury-related attrition. Rerunning the GEE on complete cases produced effect estimates similar in direction and magnitude to the full-sample analysis, though *p*-values shifted into the marginal range, likely due to reduced statistical power. As no statistically significant differences were found in group means or standard deviations between completers and the full sample, we interpret the full-sample GEE under the assumption that data were missing at random. Nonetheless, future studies with larger cohorts and more complete follow-up are needed to validate these findings. Given that most missingness was injury-related, results should be interpreted with appropriate caution.

Additionally, training load and playing time data were lacking in this study. These variables are known to influence both performance and injury risk and may serve as important covariates in future models (Bowen et al., 2017; Malone et al., 2017). Furthermore, the impact of accumulated load versus training progression on various aspects of movement performance needs further clarification (Bishop et al., 2022; Díaz-Ochoa et al., 2023).

3.5 Conclusion

Seasonal variations in movement performance among female varsity soccer players reflect dynamic changes in physical readiness and neuromuscular function across the competitive season. These findings emphasize the need for continuous performance monitoring, along with

individualized training and recovery strategies that align with each phase of the season. Integrating biomechanical assessments and responsive load management protocols may enhance athletic performance and reduce injury risk, ultimately promoting safer and more effective development in female soccer players.

3.6 Acknowledgements

The authors would like to sincerely thank all the athletes from the University of Ottawa's women's soccer team for their time, effort, and commitment throughout the study. We are also grateful to the coaching staff for their invaluable support, coordination, and facilitation of data collection during the competitive season. This study would not have been possible without their collaboration.

3.7 References

Anicic, Z., Janicijevic, D., Knezevic, O. M., Garcia-Ramos, A., Petrovic, M. R., Cabarkapa, D., & Mirkov, D. M. (2023). Assessment of Countermovement Jump: What Should We Report? *Life*, *13*(1), 190.

Ballinger, G. A. (2004). Using Generalized Estimating Equations for Longitudinal Data Analysis. *Organizational Research Methods*, *7*(2), 127-150.

Bishop, C., Abbott, W., Brashill, C., Loturco, I., Beato, M., & Turner, A. (2022). Seasonal Variation of Physical Performance, Bilateral Deficit, and Interlimb Asymmetry in Elite Academy Soccer Players: Which Metrics Are Sensitive to Change? *Journal of Strength and Conditioning Research*, *37*, 358-365.

Boone, J. B., Vandusseldorp, T. A., Feito, Y., & Mangine, G. T. (2021). Relationships Between Sprinting, Broad Jump, and Vertical Jump Kinetics Are Limited in Elite, Collegiate Football Athletes. *Journal of Strength and Conditioning Research*, *35*(5), 1306-1316.

Bowen, L., Gross, A. S., Gimpel, M., & Li, F. X. (2017). Accumulated workloads and the acute: Chronic workload ratio relate to injury risk in elite youth football players. *British Journal of Sports Medicine*, *51*(5), 452-459.

Bradley, P. S., & Vescovi, J. D. (2015). Velocity Thresholds for Women's Soccer Matches: Sex Specificity Dictates High-Speed-Running and Sprinting Thresholds - Female Athletes in Motion (FAiM). *International Journal of Sports Physiology and Performance*, *10*(1), 112-116.

Butler, R. J., Lehr, M. E., Fink, M. L., Kiesel, K. B., & Plisky, P. J. (2013). Dynamic Balance

Performance and Noncontact Lower Extremity Injury in College Football Players: An Initial Study. *Sports Health*, *5*(5), 417-422.

Chinsongkram, B., Chaikeeree, N., Saengsirisuwan, V., Horak, F. B., & Boonsinsukh, R. (2016). Responsiveness of the Balance Evaluation Systems Test (BESTest) in People with Subacute Stroke. *Physical Therapy*, *96*(10), 1638.

Díaz-Ochoa, A., Gómez-Renaud, M., Hoyos-Flores, J. R., Hernández-Cruz, G., (FEADEF), F. E. de A. de D. de E. F. (F E. F. E. de A. de D. de E. F. sica, & (México), A. U. of N. L. (México) A. U. of N. L. (2023). *Variations in physical performance during a competitive season in Mexican female varsity soccer players by playing position*.

Emmonds, S., Sawczuk, T., Scantlebury, S., Till, K., & Jones, B. (2020). Seasonal Changes in the Physical Performance of Elite Youth Female Soccer Players. *Journal of Strength and Conditioning Research*, *34*(9), 2636-2643.

Fédération Internationale de Football Association. (2018). *Women's Football Strategy*.

Gathercole, R., Sporer, B., Stellingwerff, T., & Sleivert, G. (2015). Alternative Countermovement-Jump Analysis to Quantify Acute Neuromuscular Fatigue. *International Journal of Sports Physiology and Performance*, *10*(1), 84-92.

Gidu, D. V., Badau, D., Stoica, M., Aron, A., Focan, G., Monea, D., Stoica, A. M., & Calota, N. D. (2022). The Effects of Proprioceptive Training on Balance, Strength, Agility and Dribbling in Adolescent Male Soccer Players. *International Journal of Environmental Research and Public Health*, *19*(4), 2028.

Gonell, A. C., Romero, J. A. P., & Soler, L. M. (2015). Relationship Between the Y-Balance Test Scores and Soft Tissue Injury Incidence in A Soccer Team. *International Journal of Sports Physical Therapy*, *10*(7), 955.

González-Fernández, F. T., Martínez-Aranda, L. M., Falces-Prieto, M., Nobari, H., & Clemente, F. M. (2022). Exploring the Y-Balance Test Scores and Inter-limb Asymmetry in Soccer Players: Differences Between Competitive Level and Field Positions. *BMC Sports Science, Medicine and Rehabilitation*, *14*(1), 1-13.

Guskiewicz, K. M., Ross, S. E., & Marshall, S. W. (2001). Postural Stability and Neuropsychological Deficits After Concussion in Collegiate Athletes. *Journal of Athletic Training*, *36*(3), 263.

Hamill, J., Van Emmerik, R. E. A., Heiderscheit, B. C., & Li, L. (1999). A Dynamical Systems Approach to Lower Extremity Running Injuries. *Clinical Biomechanics*, *14*(5), 297-308.

Harbourne, R. T., & Stergiou, N. (2009). Movement Variability and the Use of Nonlinear Tools: Principles to Guide Physical Therapist Practice. *Physical Therapy*, *89*(3), 267-282.

Hewett, T. E., Myer, G. D., Ford, K. R., Heidt, R. S., Colosimo, A. J., McLean, S. G., Van Den Bogert, A. J., Paterno, M. V., & Succop, P. (2005). Biomechanical Measures of

Neuromuscular Control and Valgus Loading of The Knee Predict Anterior Cruciate Ligament Injury Risk in Female Athletes: A Prospective Study. *American Journal of Sports Medicine*, *33*(4), 492-501.

Impellizzeri, F. M., Rampinini, E., Castagna, C., Bishop, D., Ferrari Bravo, D., Tibaudi, A., & Wisloff, U. (2008). Validity of A Repeated-sprint Test for Football. *International Journal of Sports Medicine*, *29*(11), 899-905.

Kirishima, A., & Anan, M. (2024). Interjoint Coordination at Different Squatting Speeds in Healthy Adults. *Cureus*, *16*(8), e67620.

Malone, J. J., Lovell, R., Varley, M. C., & Coutts, A. J. (2017). Unpacking the Black Box: Applications and Considerations for Using GPS Devices in Sport. *International Journal of Sports Physiology and Performance*, *12*(s2), S2-18.

Markovic, G. (2007). Does Plyometric Training Improve Vertical Jump Height? A meta-analytical Review. *British Journal of Sports Medicine*, *41*(6), 349-355.

Markwick, W. J., Bird, S. P., Tufano, J. J., Seitz, L. B., & Haff, G. G. (2015). The Intraday Reliability of the Reactive Strength Index Calculated from a Drop Jump in Professional Men's Basketball. *International Journal of Sports Physiology and Performance*, *10*(4), 482-488.

Meckel, Y., Doron, O., Eliakim, E., & Eliakim, A. (2018). Seasonal Variations in Physical Fitness and Performance Indices of Elite Soccer Players. *Sports*, *6*(1), 14.

Mohr, M., Krustrup, P., Andersson, H., Kirkendal, D., & Bangsbo, J. (2008). Match Activities of Elite Women Soccer Players at Different Performance Levels. *Journal of Strength and Conditioning Research*, *22*(2), 341-349.

Myers, L. R., Toonstra, J. L., & Cripps, A. E. (2023). The Test-Retest Reliability and Minimal Detectable Change of the FitLight Trainer™. *International Journal of Athletic Therapy and Training*, *28*(2), 84-88.

Nyby, J. M., Martinez, R. L., Holmgren, N. J., Bruneau, M. L., Roque, A. F., Cunha, J. M., & Jensen, C. D. (2024). Female Soccer Players Experience Faster Recovery Following Practices and Games Later in The Competitive Season. *Medicine & Science in Sports & Exercise*.

Pau, M., Ibba, G., & Attene, G. (2014). Fatigue-Induced Balance Impairment in Young Soccer Players. *Journal of Athletic Training*, *49*(4), 454.

Plisky, P. J., Gorman, P. P., Butler, R. J., Kiesel, K. B., Underwood, F. B., & Elkins, B. (2009). The Reliability of an Instrumented Device for Measuring Components of the Star Excursion Balance Test. *North American Journal of Sports Physical Therapy: NAJSPT*, *4*(2), 92.

Prieto, T. E., Myklebust, J. B., Hoffmann, R. G., Lovett, E. G., & Myklebust, B. M. (1996). Measures of Postural Steadiness: Differences Between Healthy Young and Elderly Adults. *IEEE Transactions on Biomedical Engineering*, *43*(9), 956-966.

Raeder, C., Kämper, M., Praetorius, A., Tennler, J.-S., & Schoepp, C. (2024). Metabolic, Cognitive and Neuromuscular Responses to Different Multidirectional Agility-like Sprint Protocols in Elite Female Soccer Players - A Randomised Crossover Study. *BMC Sports Science, Medicine and Rehabilitation*, *16*(1).

Rentz, L. E., Brandmeir, C. L., Rawls, B. G., & Galster, S. M. (2021). Reactive Task Performance Under Varying Loads in Division I Collegiate Soccer Athletes. *Frontiers in Sports and Active Living*, *3*, 707910.

Sanchez-Sanchez, J., Raya-González, J., Martín, V., & Rodríguez Fernández, A. (2025). Understanding Injuries in Young Female Soccer Players: A Narrative Review on Incidence, Mechanism, Location Risk Factors, and Preventive Strategies. *Applied Sciences 2025, Vol. 15, Page 1612*, *15*(3), 1612.

Savolainen, E. H. J., Ihalainen, J. K., Vänttinen, T., & Walker, S. (2024). Changes in Female Football Players' In-Season Training Load, Intensity and Physical Performance: Training Progression Matters More Than Accumulated Load. *Frontiers in Sports and Active Living*, *6*.

Sha, Z., Zhou, Z., & Dai, B. (2021). Analyses of Countermovement Jump Performance in Time and Frequency Domains. *Journal of Human Kinetics*, *78*(1), 41.

Silva, J. R., Magalhaes, J., AscensaO, A., Seabra, A. F., & Rebelo, A. N. N. (2013). Training Status and Match Activity of Professional Soccer Players Throughout a Season. *Journal of Strength and Conditioning Research*, *27*(1), 20-30.

Silvers-Granelli, H., Mandelbaum, B., Adeniji, O., Insler, S., Bizzini, M., Pohlig, R., Junge, A., Snyder-Mackler, L., & Dvorak, J. (2015). Efficacy of the FIFA 11+ Injury Prevention Program in The Collegiate Male Soccer Player. *American Journal of Sports Medicine*, *43*(11), 2628-2637.

Stergiou, N., & Decker, L. M. (2011). Human Movement Variability, Nonlinear Dynamics, And Pathology: Is There a Connection? *Human Movement Science*, *30*(5), 869-888.

Sun, M., Soh, K. G., Ma, S., Wang, X., Zhang, J., & Yaacob, A. Bin. (2025). Effects of Speed, Agility, and Quickness (SAQ) Training on Soccer Player Performance - A Systematic Review and Meta-Analysis. *PLOS ONE*, *20*(2), e0316846.

Wilkerson, G. B., Simpson, K. A., & Clark, R. A. (2017). Assessment and Training of Visuomotor Reaction Time for Football Injury Prevention. *Journal of Sport Rehabilitation*, *26*(1), 26-34.

Chapter 4. Study 1b: A 3D Goal Equivalent Manifold Approach to Detecting Season-Long Post-Concussion Motor Deficits in Female Soccer Players

*Submitted to *Scientific Reports**

Xiong Zhao[1], Reza Rahimi[1], Allison Clouthier[1], Janie Cournoyer[1], Ryan B. Graham[1]

[1]*School of Human Kinetics, Faculty of Health Sciences, University of Ottawa, Ottawa, Ontario, Canada*

Abstract

Objectives: This study aims to investigate whether a 3D Goal Equivalent Manifold (GEM) analysis could detect persistent motor control deficits across a competitive season in female soccer players with a history of concussion.

Methods: Twenty-five female varsity soccer players (11 with concussion history, 14 without) completed bilateral bodyweight squats synchronized with a metronome (40 bpm) at pre-, mid-, and post-season. Whole-body kinematics were captured using a markerless motion capture system. GEM analysis decomposed variability into task-relevant and task-irrelevant components, producing a 3D performance index (PI) and temporal persistence metrics (λ).

Results: Players with concussion history exhibited significantly lower PI scores (M = 9.48 ± 1.60) compared to those without (M = 16.26 ± 2.45; p = .017), with no significant seasonal changes or interactions. No significant differences emerged for temporal persistence metrics, although the concussion group consistently showed trends toward less effective regulation in task-relevant dimensions.

Conclusion: The 3D GEM approach effectively identified persistent motor control deficits in female soccer players with concussion histories, underscoring its potential in clinical assessments and monitoring throughout rehabilitation and return-to-play programs.

4.1 Introduction

Sports-related concussions are prevalent in soccer, particularly among female athletes with

incidence estimates ranging from 0.27 to 0.35 concussions per 1,000 athlete-exposures in matches, and even higher during competitive matches (Gessel et al., 2007; Zuckerman et al., 2015). Notably, females are more likely to have prolonged recovery times and exhibit greater neurocognitive deficits post-concussion compared to males (Broshek et al., 2005; Covassin et al., 2013). Beyond acute symptoms, growing evidence suggests that concussion can result in persistent impairments in cognitive, neuromuscular, and motor control, which may remain even after clinical symptom resolution (Gaudet et al., 2022, 2024; Thériault et al., 2011). These lingering deficits are of particular concern in high-level athletes, where performance demands require both fine-tuned coordination, dynamic stability and decision making.

Persistent neuromuscular control deficits can influence injury risk and performance efficiency, especially in tasks that demand rapid decision-making, balance, and inter-limb coordination (Fino et al., 2019; Iverson et al., 2006, 2012; Lynall et al., 2015). Female athletes with a history of concussion often demonstrate reduced balance and altered coordination under cognitively demanding or dual-task conditions, scenarios more reflective of in-game performance (Kieffer et al., 2022; Monoli et al., 2024). Recent research has identified persistent alterations in joint coordination patterns among varsity athletes more than a year after their most recent concussion, indicating enduring deficits in inter-segmental motor control that continue to affect performance during functional tasks (Liu et al., 2024). Another study also suggests that concussion may increase the risk of anterior cruciate ligament (ACL) injuries, particularly among female athletes (Kakavas et al., 2025). These findings highlight the interconnected nature of concussion-related motor deficits and musculoskeletal injury susceptibility, reinforcing the need for comprehensive movement screening tools in this population.

Several studies have documented long-lasting impairments in gait and dynamic postural control among female athletes with concussion histories. Martini et al. reported sustained deficits in gait stability under dual-task conditions, highlighting the persistent nature of concussion-induced motor dysfunction (Martini et al., 2011). Similarly, concussed athletes exhibited increased gait variability and reduced biomechanical control when performing tasks simultaneously with

cognitive demands (Kakavas et al., 2025). These deficits may increase susceptibility to future injuries, particularly lower extremity musculoskeletal injuries, which have been frequently associated with previous concussion events (Fino et al., 2019; Lynall et al., 2015).

Recent research emphasizes the need for dynamic, dual-task paradigms that more closely mimic sport-specific demands. Tasks that concurrently engage cognitive and motor systems, such as walking while solving arithmetic or timed movements synchronized to external cues, have proven more sensitive in revealing lingering impairments post-concussion (Fino et al., 2016a; Kakavas et al., 2025; Martini et al., 2011). The inclusion of dual-task paradigms is particularly relevant for female athletes, who may experience greater cognitive-motor interference compared to their male counterparts following concussion (Catena et al., 2007).

Traditional post-concussion assessments often rely on static balance tests (e.g., The Balance Error Scoring System (BESS)) or isolated cognitive measures (e.g., reaction time), which may fail to detect subtle but functionally relevant deficits (Barnes et al., 2024; Dunne et al., 2023; Johnston et al., 2017). To address this gap, researchers have advocated for more ecologically valid assessments that simultaneously challenge neuromuscular and cognitive systems. Dual-task paradigms, such as walking while responding to auditory stimuli, impose concurrent cognitive loads that tax attentional resources and reveal impairments in motor control not observable under single-task conditions (Fino et al., 2016b; Howell et al., 2013). The squat is a fundamental movement pattern that challenges multiple lower extremity joints and muscle groups simultaneously, providing an integrated assessment of neuromuscular control and inter-segmental coordination (Kritz et al., 2009). In athletic populations, it is a universal whole-body task foundational to both training and rehabilitation. Compared to gait-based dual-task paradigms, the squat imposes greater postural and mechanical demands. When synchronized to a metronome, it introduces a temporal constraint that requires athletes to continuously integrate sensory input and motor output, thus functioning as a cognitively demanding, dual-task movement. Chehrehrazi et al., (2017) showed that such temporal constraints during lifting tasks can uncover meaningful differences in motor variability. Therefore, the bilateral bodyweight squat synchronized to a

metronome (40 BPM) was selected in the present study as a sport-relevant, cognitively and physically demanding task that may be especially sensitive to subtle, persistent motor control deficits in athletes with a concussion history (Chehrehrazi et al., 2017; Sedighi & Nussbaum, 2019).

The human neuromusculoskeletal system exhibits inherent redundancy, meaning that multiple biomechanical strategies can be employed to accomplish the same motor task. This flexibility allows for successful performance even in the presence of impairments such as those resulting from concussion, by redistributing control across joints and muscles to maintain functional output. This redundancy, also known as movement variability (MV), is reflected in the concept of equifinality; multiple optimal solutions for the same outcome, bounded by limits of adaptability and sensitivity to perturbation (Bernstein, 1967; Stergiou et al., 2006). MV within this space can be informative; excessive variability suggests instability or exploring, while overly rigid patterns may indicate reduced adaptability (Stergiou, 2018). Quantifying and interpreting this variability are central to understanding post-concussion motor control.

The Goal Equivalent Manifold (GEM) framework offers a powerful means of evaluating MV by partitioning it into goal-relevant and goal-equivalent components (Cusumano & Dingwell, 2013). Unlike traditional variability metrics, GEM provides insight into how movement deviations align or conflict with task demands. Recent studies have demonstrated the effectiveness of GEM analyses in capturing subtle, persistent motor control impairments that conventional assessments might overlook. For instance, Chehrehrazi et al. utilized GEM to analyze lifting variability and found significant differences in motor adaptability between healthy controls and populations with non-specific lower back pain (Chehrehrazi et al., 2017). These findings underscore the potential of GEM-based methodologies for identifying nuanced impairments in concussed athletes.

Traditional GEM analyses have predominantly employed two-dimensional models, such as, displacement and velocity. However, for rhythmically constrained movements, timing precision is an equally important component of successful task execution. Therefore, this study introduces an enhanced three-dimensional GEM model by explicitly incorporating timing error as a third execution variable. Timing error quantifies deviations from the ideal cycle time, capturing subtle

temporal regulation impairments otherwise obscured in conventional 2D analyses. Comparing the results from both the traditional 2D GEM and the proposed 3D GEM will further clarify the added value and sensitivity of integrating temporal variability into the GEM framework.

Thus, the objective of this study was to apply a three-dimensional GEM framework to quantify motor control deficits associated with concussion history in female soccer players. To evaluate the temporal sensitivity of these deficits, assessments were conducted at three distinct time points across the competitive season: pre-season, mid-season, and post-season. Assessing multiple time points allowed for the examination of both the persistence and evolution of neuromuscular control over time, beyond the limitations of single-time-point screening approaches. It was hypothesized that athletes with a history of concussion would demonstrate consistently lower performance indices and increased temporal variability across all testing sessions, relative to non-concussed athletes. These differences were expected to reflect persistent disruptions in neuromuscular regulation associated with prior brain injury.

4.2 Methods

4.2.1 Participants

Twenty-five female varsity soccer players from the University of Ottawa were recruited, including 11 with a history of concussion (7 within one-year) and 14 without. Participants were grouped based on self-reported, medically diagnosed concussions within the past three years. For simplicity, participants with a history of concussion are referred to as the "concussion" group, and those with no history of concussion as the "non-concussion" group throughout the manuscript. Demographics (mean ± SD) for the non-concussion group were: age = 20.36 ± 2.17 years, height = 1.64 ± 0.07 m, weight = 61.15 ± 5.38 kg, and BMI = 22.72 ± 1.81 kg/m². For the concussion group: age = 20.45 ± 1.81 years, height = 1.69 ± 0.05 m, weight = 66.06 ± 9.94 kg, and BMI = 23.13 ± 2.89 kg/m².

Inclusion criteria were: (1) age ≥ 18 years old; (2) full medical clearance for athletic participation; and (3) ability to complete 40 repetitions of a bilateral bodyweight squat to a

metronome, used as a measure of coordination and neuromuscular control. This study was approved by the Research Ethics Board at University of Ottawa (file #: H-07-24-10628). Participants were informed of their right to withdraw at any time without consequence, and all data were anonymized prior to analysis to ensure confidentiality.

4.2.2 Protocol

Testing was conducted at three time points: pre-season (week 1), mid-season (week 9), and post-season (week 15). Upon arrival, participants provided informed consent, completed an injury history questionnaire, and had their height and weight measured (pre-season only).

After familiarization, participants performed 35 bodyweight squats to a metronome (Figure 4.1 bottom) at 40 BPM. Participants began each squat from an upright position with fully extended hips and knees. A full repetition involved descending until both thighs dropped below or parallel to the ground, keeping the heels on the floor, and returning to the upright position. Participants were instructed to squat down and stand up in sync with the metronome beat to the best of their ability (Figure 4.1). No additional constraints were imposed to allow natural movement variability. Whole-body kinematics were captured using an 8-camera markerless motion capture system (Theia Markerless Inc., Kingston, ON, Canada) at 60 Hz. During the same data collection session, participants completed a series of additional movement screening tasks, a single bilateral trial of T-Balance and Y-Balance, one bilateral L-Hop trial, three repetitions of bilateral countermovement jumps, three broad jumps, and two reaction time tasks presented in randomized order. These assessments were part of a broader testing battery but are beyond the scope of the present analysis. The full testing protocol, excluding consent form and questionnaire, was repeated at mid- and post-season.

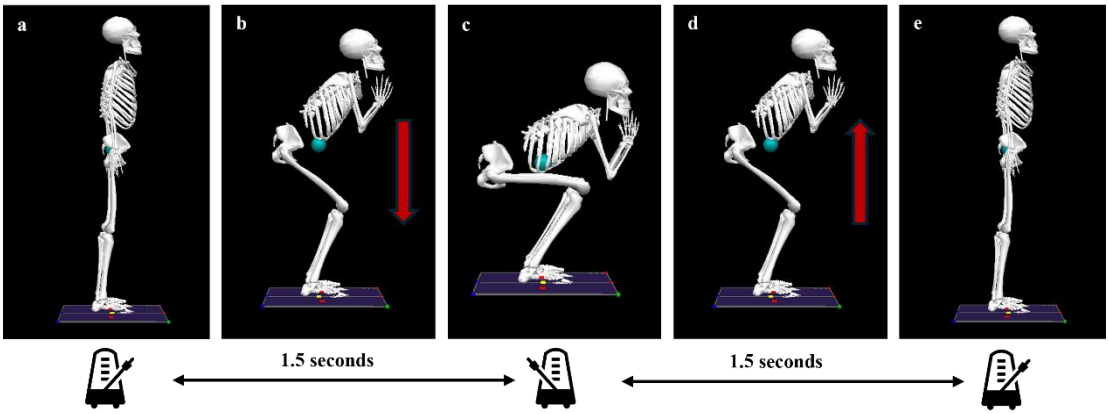

Figure 4.1: Demonstration of the bilateral body-weight squat to a metronome: (a) start upright with hips and knees fully extended; (b) descent toward thighs at least parallel to the floor; (c) bottom position; (d) ascent from the bottom; (e) return to full extension.

4.2.3 Data analysis

After data collection, videos were processed using Theia3D (Theia Markerless Inc., Kingston, ON, Canada) and analyzed in Visual3D (C-Motion Inc., Germantown, MD, USA) to extract each participant's center of mass (COM) kinematics. The kinematic data were exported to Matlab R2019b (The MathWorks Inc., MA, USA) for processing. Custom scripts were used to apply a fourth-order zero-lag Butterworth filter with a 6 Hz cutoff frequency. To ensure consistency and that they reached steady-stage motion, only the final 30 repetitions were retained for analysis. Each repetition was segmented based on the COM vertical trajectory. For each rep, displacement and velocity of the COM were computed using Euclidean distance and first-derivative of displacement, respectively. Timing error was calculated as the deviation (in seconds) between the actual start and end of each repetition and the ideal timing based on the 40-bpm metronome cue (3 seconds per repetition: 1.5 seconds down and 1.5 seconds up).

The motion of the body's COM in the sagittal plane was used to represent the primary control variable for this movement (Sedighi & Nussbaum, 2017, 2019). With the body-level variables being the displacement (D) and the velocity (V) of the COM, the goal is maintaining constant time (T) through all trials, and the goal is defined as Equation (4.1):

$$T = D_n/V_n \quad (4.1)$$

where D_n is the displacement of the COM for cycle n, and V_n is the linear velocity of the COM for that cycle. This relationship was set equal to a target movement time T_{target} (i.e., 3 seconds), leading to a scalar goal function Equation (4.2) that applies to each observed pair (D_n, V_n):

$$f(D,V) = D/V - T_{target} = 0 \quad (4.2)$$

However, because the task (squatting to a metronome) demands precise temporal control, a timing error term T_{err} that explicitly captures deviations from the target timing was introduced, acting as a dimension of execution variability. In other words, the timing error, T_{err}, was modeled as a third execution (body-level) variable that directly parameterizes the global timing constraint, thereby linking body-level control to the task-level goal mathematically. This expands the manifold to represent spatio-temporal solutions rather than purely spatial (2D GEM) solutions and addresses a limitation of the 2D GEM, in which any cycle-time deviation is implicitly treated as goal-relevant error even when D and V covary in a coordinated way. The revised goal function, defined for each trial-specific set of values $(D_n, V_n, T_{err,n})$, is given in Equation (4.3):

$$f(D,V,T_{err}) = D/V - T_{target} - T_{err} = 0 \quad (4.3)$$

This formulation implies that for a given execution triple $(D_n, V_n, T_{err,n})$, the task goal is perfectly achieved when the measured ratio D_n/V_n is exactly equal to the sum of the target time T_{target} and the observed timing deviation $T_{err,n}$. A nonzero $T_{err,n}$ thus reflects the extent to which a trial deviates temporally from the ideal execution, and by integrating this component into the GEM framework, both kinematic and temporal aspects of the performance can be assessed.

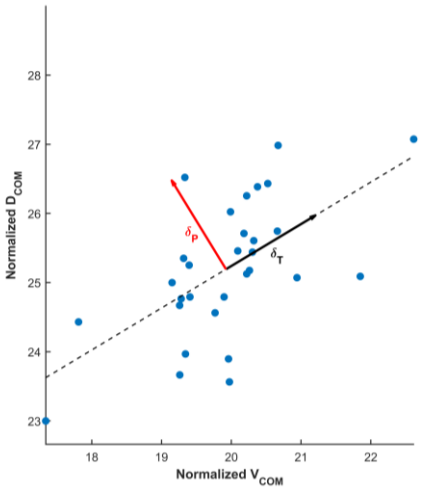

Figure 4.2: Visualization of the two-dimensional goal equivalent manifold (GEM) analysis of the squat. Individual dots represent individual repetitions. The diagonal dash line stands for the GEM, δ_T and δ_P are unit vectors for variations along the GEM and deviations perpendicular to the GEM.

To compare MV between participants in the proposed analysis, D and V were normalized to each participant's standard deviations across cycles (Dingwell et al., 2010). The two-dimensional approach was extended by incorporating timing error (T_{err}) as a third dimension, reflecting the temporal demands of the task. Any combination of normalized values ($D_n\ V_n\ , T_{err,n}$) that satisfies this equation lies on the goal-equivalent manifold (GEM) (see Figure 4.2, black dash line). A perfect task execution, T_{target}, in this case should equal to three seconds. To define the task-consistent operating point (D^*, V^*, T^*_{err}), we computed the point on the GEM that minimized the Euclidean distance to the mean of execution vector, defined by the average displacement, velocity, and timing error, across all repetitions. Specifically, this operating point was obtained by solving a constrained optimization problem where the objective was to minimize Equation (4.4):

$$\min_{(D,V,T_{err})\in GEM} (D-\bar{D})^2 + (V-\bar{V})^2 + (T_{err}-\bar{T}_{err})^2 \qquad (4.4)$$

subject to the nonlinear constraint $\frac{D}{V} - T_{err} = T_{target}$, ensuring the operating point satisfied the task timing requirement. The resulting operating point (D^*, V^*, T^*_{err}) was then normalized using the standard deviation of displacement and velocity across trials to align with the normalized 3D

execution space used in subsequent GEM decomposition. Variability relative to the operating point is computed as Equations (4.5):

$$\begin{aligned} \Delta D_n &= D_{n,nor} - D^* \\ \Delta V_n &= V_{n,nor} - V^* \\ \Delta T_n &= T_{err,n} - T^*_{err} \end{aligned} \tag{4.5}$$

To capture the structure of motor variability, the deviation vector for each cycle was given by $\Delta X_n = [\Delta D_n,\ \Delta V_n,\ \Delta T_n]$. This decomposition was obtained by first calculating the gradient (or Jacobian) of the goal function at the operating point (D^*, V^*, T^*_{err}) (Equation 4.6):

$$J = \left[\frac{\partial f}{\partial D}, \frac{\partial f}{\partial V}, \frac{\partial f}{\partial T_{err}}\right]\Big|_{(D^*,V^*,T^*_{err})} = \left[\frac{1}{V^*}, -\frac{D^*}{(V^*)^2}, -1\right] \tag{4.6}$$

After normalizing, $\hat{J} = \frac{J}{\|J\|}$, the null space of J defines the directions in the 3D execution space along which variability does not affect the task outcome (i.e., the goal-equivalent manifold or GEM). Let $E = null(J)$ denote a 3×2 matrix, where each column corresponds to an orthonormal tangent vector to the GEM manifold. The variability vector ΔX_n was then decomposed into goal-equivalent variability ($\delta_{T1}\ and\ \delta_{T2}$), i.e. variability along the GEM, which does not affect task performance and goal-relevant variability (δ_P), i.e. variability perpendicular to the GEM, which directly influences performance. Mathematically, this is expressed as Equations (4.7):

$$\begin{aligned} \delta_{T1}(n) &= \Delta \mathrm{X}_n \cdot E(:,1) \\ \delta_{T2}(n) &= \Delta \mathrm{X}_n \cdot \mathrm{E}(:,2) \\ \delta_P(n) &= \Delta \mathrm{X}_n \cdot \hat{J}^T \end{aligned} \tag{4.7}$$

To quantify performance, the overall Performance Index (PI) is defined as the ratio of the standard deviation of the goal-equivalent variability to that of the goal-relevant variability Equation (4.8):

$$PI_{3D} = \frac{\sqrt{std(\delta_{T1})^2 + std(\delta_{T2})^2}}{std(\delta_P)} \quad (4.8)$$

A greater 3D performance index (PI_{3D}) indicates that a larger proportion of the variability is directed along the GEM (i.e., "good" variability that does not negatively impact task performance), reflecting superior task performance (Chehrehrazi et al., 2017; Sedighi & Nussbaum, 2019). An example of the 3D GEM plot is shown in Figure 4.4.

To further assess the temporal persistence of trial-to-trial variability, the lag-1 autocorrelation coefficients (λ_{T1}, λ_{T2}, and λ_P) for each of the goal-equivalent directions (δ_{T1}, δ_{T2}) and the goal-relevant direction (δ_P) were computed using Pearson correlation between its value in trial n and trial n+1 across the 30 repetitions. This reflects the degree of temporal dependence in the respective variability dimensions. Higher λ values indicate greater persistence in the corresponding dimension, whereas values near zero suggest more random or adaptive behavior across repetitions (Sedighi & Nussbaum, 2017, 2019).

2D GEM analyses were conducted to provide a direct comparison with our proposed 3D GEM framework. The calculations followed the same procedure described above, except that timing error, T_{err}, was excluded. As a result, only two execution variables, displacement and velocity, were used to compute the goal-equivalent variability δ_T, goal-relevant variability δ_P, and their corresponding lag-1 autocorrelation metrics (λ_T and λ_P). The 2D performance index (PI_{2D}) was also calculated as defined in Equation (8) with only δ_T and δ_P. To evaluate the added variance of incorporating timing error into the GEM framework, the total variability in both the $[D \quad V]$ and $[D \quad V \quad T_{err}]$ execution spaces was computed. For each time point, the variance of T_{err} was calculated, and its proportion relative to the total 3D execution variance was computed using the Equation (4.9):

$$Proportion_{var} = \frac{Variance(T_{err})}{Total\ Variance[D \quad V \quad T_{err}]} \times 100\% \qquad (4.9)$$

This analysis provided an estimate of how much temporal variability contributed to the overall execution variability in the metronome-paced squat task.

4.2.4 Statistical analysis

All statistical analyses were performed using IBM SPSS Statistics, Version 25.0 (IBM Corp., Armonk, NY, USA). Prior to modeling, the distribution of each continuous outcome variable was assessed using Shapiro-Wilk tests. A generalized linear model with generalized estimating equations (GEE) for repeated measures was used to examine the effects of stage, concussion history, and their interaction on 2D/3D performance index. GEE estimation was used to account for within-subject correlations and allowed the inclusion of participants with partially missing data (Ballinger, 2004). Stage was modeled as a categorical predictor with pre-season as the reference. Parameter estimates from the generalized linear model with GEE estimation were used to assess changes over time, with pre-season set as the reference category. Estimated coefficients (*B*) reflect the mean difference (M) in the outcome at each stage relative to pre-season, along with standard errors (SE) and associated Wald χ^2 tests. Where applicable, pairwise comparisons used Sequential Bonferroni adjustment. Significance was set at $p < .05$.

To assess the impact of missing data, a sensitivity analysis was conducted by only including participants who completed all pre-, mid- and post-season sessions. Group mean difference was compared at each stage between completers and all data available before rerunning the generalized linear model with GEE.

To assess whether participant evaluations on 2D PI and 3D PI were consistent, monotonic (Spearman's ρ) and rank (Kendall's τ) correlations between 2D PI and 3D PI were computed at each time-point. Nonparametric measures and exact *p*-values were reported when distributions were skewed. To evaluate the influence of extreme observations, Spearman's ρ was repeated after 5% symmetric winsorization of both 2D and 3D PIs, and a leave-one-out analysis was conducted (recomputing ρ after removing each participant in turn). Potential outliers in PI were identified by

group using the Tukey quartile rule. For a simple between-group snapshot, 2D PI and 3D PI were compared between non-concussion and concussion groups using the Mann-Whitney U test (two-sided $\alpha = .05$).

4.3 Results

In the pre-season (week 1), 23 participants completed the in-lab session, with one defender (concussion) and one midfielder (non-concussion) absent (non-concussion: concussion = 13:10). In the mid-season (week 9), 24 participants completed the session, with one non-concussed midfielder missing (13:11). In the post-season (week 15), 20 participants completed the session, with five players absent: two forwards (one concussion, one non-concussion), one non-concussed midfielder, and two defenders (one concussion, one non-concussion) (11:10). When the model was limited to participants with complete data, no mean difference was found, and the previously observed significant effects persisted in both the 2D and 3D analyses.

At pre-season, timing error contributed approximately 14.74% (0.35 / 2.35) of the total variability. This contribution was lower at mid-season at 6.34% (0.14 / 2.14) and rose again post-season to 15.64% (0.37 / 2.37). On average across the season, timing error explained 12.24% of the total movement variability. Group means for 2D and 3D performance index and their temporal persistence metrics across all three time points are summarized in Table 4.1 and Table 4.2, respectively.

Table 4.1: Summary statistics of 2D performance index and temporal persistence metrics (λ_T, λ_{P_2D}) by group and season stage.

Stage	Group	PI_{2D}	λ_T	λ_{P_2D}
pre	concussion	1.08 ± 0.16	0.56 ± 0.23	-0.40 ± 0.20
	non-concussion	1.15 ± 0.31	0.41 ± 0.20	-0.41 ± 0.16
mid	concussion	1.07 ± 0.22	0.46 ± 0.19	-0.44 ± 0.12
	non-concussion	1.28 ± 0.65	0.36 ± 0.23	-0.43 ± 0.16
post	concussion	1.11 ± 0.21	0.41 ± 0.30	-0.42 ± 0.19
	non-concussion	1.27 ± 0.54	0.40 ± 0.24	-0.22 ± 0.28

Note: Values are presented as mean ± standard deviation; * = statistical significance was found; PI_{2D} = 2D Performance

Index; λ_T, = lag-1 autocorrelation of task-irrelevant components; λ_{P_2D} = temporal persistence within the task-relevant space in 2D GEM.

2D PI values ranged from 1.07 to 1.28 across all groups and time points, with generally lower values in the group with concussion history at all time points, though not statistically significant. The GEE results indicated no significant main effect of concussion history on 2D PI, χ^2 (1) = 1.57, p = .21, nor for stage, χ^2 (1) = 1.54, p = .46, or their interaction, χ^2 (1) = 1.42, p = .49. For λ_T, values ranged from 0.36 to 0.56, and for λ_{P_2D}, values remained consistently negative (-0.44 to -0.22) across all time points. Similarly, no significant effects were observed for λ_T (concussion: $\chi^2(1) = 2.11$, p = .15; stage: χ^2 (1) = 1.30, p = .52; stage × concussion interaction: χ^2 (1) = 0.59, p = .75) or λ_{P_2D} (concussion: $\chi^2(1) = 1.89$, p = .17; stage: $\chi^2(1) = 2.83$, p = .24; stage × concussion interaction: χ^2 (1) = 3.09, p = .21).

Table 4.2: Summary statistics of performance index and temporal persistence metrics (λ_{T1}, λ_{T2}, λ_P) by group and season stage.

Stage	Group	PI_{3D}*	λ_{T1}	λ_{T2}	λ_P
pre	concussion	7.17 ± 4.25	0.14 ± 0.27	0.00 ± 0.34	-0.24 ± 0.25
	non-concussion	16.40 ± 16.88	0.05 ± 0.30	0.08 ± 0.34	-0.16 ± 0.29
mid	concussion	9.28 ± 5.31	-0.01 ± 0.19	0.00 ± 0.37	-0.27 ± 0.24
	non-concussion	13.59 ± 9.66	-0.05 ± 0.22	0.04 ± 0.37	-0.26 ± 0.21
post	concussion	12.44 ± 12.82	0.05 ± 0.25	0.00 ± 0.42	-0.25 ± 0.31
	non-concussion	19.60 ± 16.70	0.03 ± 0.25	0.17 ± 0.33	-0.13 ± 0.28

Note: Values are presented as mean ± standard deviation; * = statistical significance was found; PI_{3D} = 3D Performance Index; λ_{T1}, λ_{T2} = lag-1 autocorrelation of task-irrelevant components; λ_P = temporal persistence within the task-relevant space.

At each stage of the season, players with a history of concussion exhibited significantly lower 3D PI scores compared to those without a concussion history (Table 4.2). The largest discrepancy was seen at the pre-season stage (7.17 vs. 16.40), and although the concussion group improved over time and the non-concussion group dipped at mid-season, the non-concussion group consistently maintained significantly higher 3D PI values (Figure 4.3). Players in the both groups tended to show random or adaptive behavior in task-relevant space (λ_{T1}, λ_{T2}). However, the

concussion group exhibited consistently lower values in λ_P.

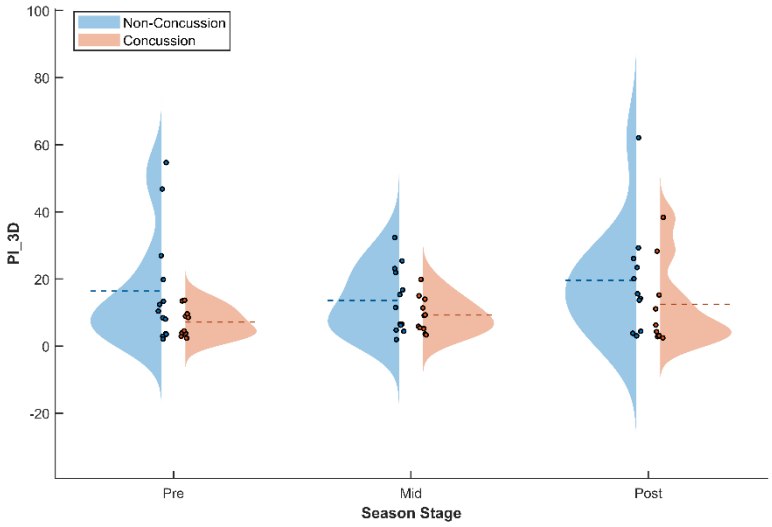

Figure 4.3: Raincloud plot of 3D PI for Non-Concussion (blue) and Concussion (orange) groups across Pre, Mid, and Post season stages. Each half-violin displays the full distribution of individual PI values (dots), while the dashed horizontal lines denote group mean.

The main effect of concussion history on 3D PI was significant, χ^2 (1) = 5.74, p = .017, with players without a history of concussion (M = 16.26, SE = 2.59) exhibiting higher 3D PI values than those with a concussion history (M = 9.34, SE = 1.57). Neither the main effect of stage, χ^2 (2) = 2.79, p = .248, nor the Stage × Concussion interaction, χ^2 (2) = 1.69, p = .428, were statistically significant.

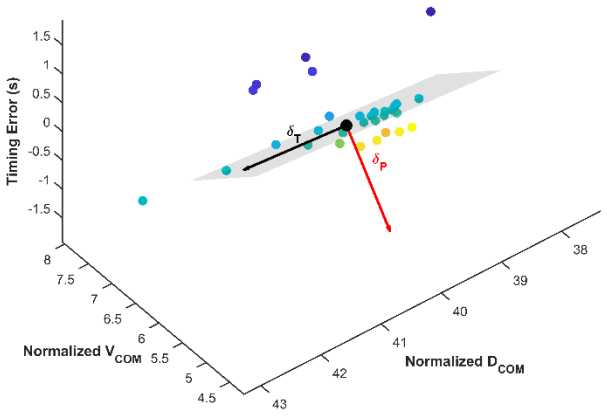

Figure 4.4: 3D GEM visualization of one participant. Each point shows a repetition in normalized COM displacement, velocity, and timing error space. Colors also indicate timing error for better visualization in 3D space, with darker ones lagging the beat and lighter ones leading. The grey

plane represents the GEM plane; δ_T and $\delta_P$represent variability along and perpendicular to the GEM, respectively.

No significant effects of Stage, Concussion or Stage × Concussion interaction were observed for λ_{T1} and λ_{T2} as shown in Figure 4.5 below.

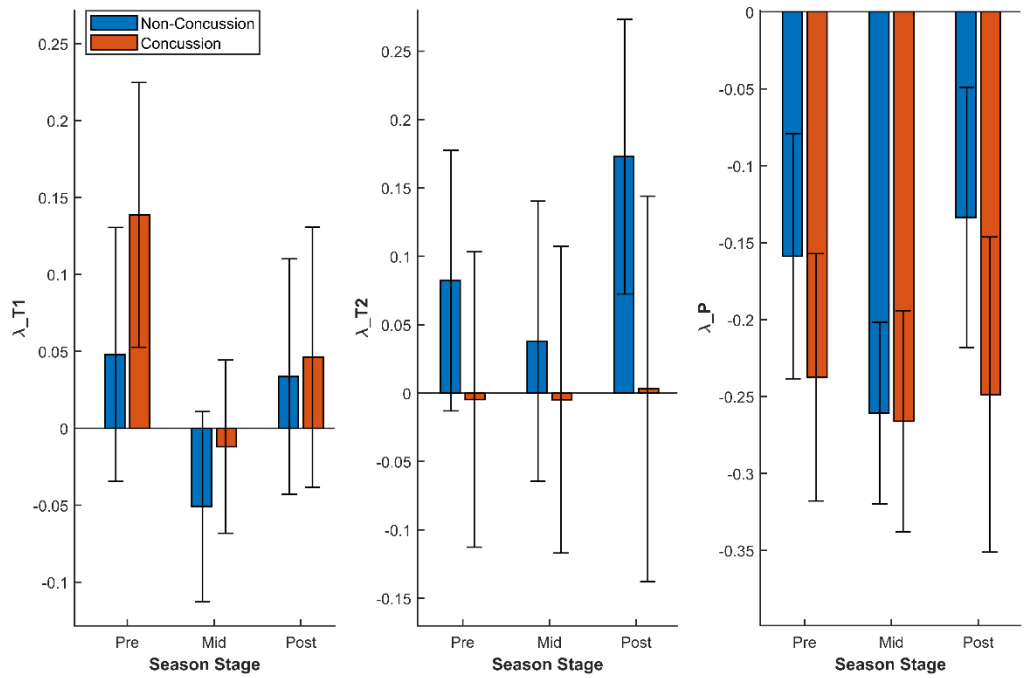

Figure 4.5: Bar plots of λ_{T1}, λ_{T2}, and λ_P values for Non-Concussion (blue) and Concussion (orange) groups at Pre, Mid, and Post seasons. Each bar shows the group mean and error bars represent ±1 SD.

Similarly, no significant effects emerged for λ_P in 3D analysis, which reflects trial-to-trial regulation in task-relevant performance space. Estimated marginal means indicated that players with concussion history consistently exhibited lower λ_P values across all stages (pre: M = -0.24, SE = 0.08; mid: M = -0.27, SE = 0.07; post: M = -0.25, SE = 0.10) than players without concussion history (pre: M = -0.16, SE = 0.08; mid: M = -0.26, SE = 0.06; post: M = -0.13, SE = 0.08).

Table 4.3: Summary of concordance between 2D and 3D PIs at pre-, mid-, and post-season, with within-group correlations and robustness checks.

Stage	Overall ρ (*p*)	Overall τ (*p*)	NC ρ (*p*)	C ρ (*p*)	Winsorized ρ (*p*)	Leave-one-out ρ range
pre	0.676 (.001)	0.478 (.001)	0.659 (.017)	0.721 (.024)	0.676 (.001)	0.630-0.729
mid	0.640 (.001)	0.471 (.001)	0.676 (.014)	0.673 (.028)	0.640 (.001)	0.598-0.748
post	0.657 (.002)	0.453 (.005)	0.827 (.003)	0.650 (.067)	0.657 (.002)	0.625-0.718

Note: ρ = Spearman rank-order correlation; τ = Kendall's tau. NC = non-concussion; C = concussion. Values are correlations with two-sided exact *p*-values in parentheses; complete-case analyses only. Winsorized ρ was computed after 5% symmetric winsorization of both performance indices. The leave-one-out range is the minimum-maximum Spearman ρ obtained when iteratively removing each participant once.

As shown in Table 4.3, across pre-, mid-, and post-season sessions, 2D and 3D PIs were consistently and positively associated (overall Spearman $\rho \approx 0.64$-0.68; Kendall $\tau \approx 0.45$-0.48). Within-group associations were positive at each stage, with the strongest correlation in the non-concussion group at post ($\rho = 0.827$). Robustness checks (5% winsorization and leave-one-out) yielded nearly identical estimates and narrow ranges, indicating the findings were not driven by single observations; occasional 3D PI Tukey outliers were flagged (pre: one non-concussion; post: one non-concussion) and one potentially influential case at mid (non-concussion), but inferences were unchanged. Single-timepoint rank-sum tests detected no significant non-concussion vs. concussion differences for either 2D or 3D PI at any stage (pre: 3D $p = .369$, 2D $p = .556$; mid: 3D $p = .271$, 2D $p = .817$; post: 3D $p = .224$, 2D $p = .879$).

4.4 Discussion

This study examined the impact of concussion history on motor control deficits in female soccer players using GEM analysis in both 2D and 3D. We hypothesized that players with a history of concussion would exhibit persistently lower motor control performance indices (PI) and altered temporal persistence in motor variability across a competitive season compared to players without concussion histories. Additionally, we anticipated these deficits would remain stable over the

season, highlighting lasting neuromuscular impairment despite medical clearance.

By treating timing error as a body-level variable tied to the global constraint, the 3D GEM separates temporal regulation from spatial coordination, classifies coordinated spatio-temporal trade-offs as goal-equivalent, and isolates only goal-relevant error, thereby increasing sensitivity to post-concussion deficits in a rhythm-constrained task. The inclusion of timing error as an additional execution dimension in the GEM framework was shown to meaningfully contribute to the total variability captured in the task. Specifically, timing error accounted, on average, for approximately 12% of the overall execution variability across the competitive season. Although no universal threshold exists for interpreting additional variance, literature suggests that modest increases in explained variance (5-15%) can provide meaningful insights (Cohen, 1988). Given the inherent rhythmic demands of this task, explicitly modeling temporal variability enhances the ecological validity of the GEM approach, capturing nuances of neuromuscular control that a spatial-only (2D) analysis might overlook. Both 2D and 3D GEM analyses revealed that female soccer players with a history of concussion consistently demonstrated lower PI across the season. However, only the 3D GEM, which incorporated timing error as a third execution variable, captured statistically significant group differences across the season, highlighting the added value of accounting for temporal variability when assessing task-relevant motor control.

Further, as shown in Table 4.3, 2D and 3D PIs exhibited consistent, moderate–strong positive concordance overall and within both groups, indicating that the spatio-temporal index (3D PI) largely preserves the athlete ranking captured by the spatial-only index (2D PI) while extending it to include timing regulation. Robustness checks (identical 5% winsorized ρ and narrow leave-one-out ranges) show that these associations are not driven by single observations; the few flagged 3D PI outliers (non-concussion at pre and post) did not change the inferences. Coupled with non-significant single-timepoint group comparisons, this pattern supports the utility of the 3D GEM, by explicitly incorporating timing error, to detect season-long, concussion-related decrements in performance regulation. Notably, according to Equation 4.8, a high 3D PI does not necessarily reflect an outlier: when an athlete keeps timing errors small and coordinates displacement and

velocity so that deviations project mostly along the manifold, the 3D PI increases even without extreme values.

The finding aligns with previous literature highlighting persistent deficits in neuromuscular function, including reduced coordination, impaired balance, and altered dynamic stability, well beyond clinical recovery and symptom resolution (Covassin et al., 2013; Kieffer et al., 2022; Iverson et al., 2012). Studies have reported persistent motor deficits in athletes post-concussion, emphasizing the need for extended assessment periods to capture subtle, ongoing impairments. For instance, Gaudet et al. documented persistent postural control deficits in female athletes during dual-task scenarios, highlighting the potential influence of cognitive load on post-concussion balance recovery (Gaudet et al., 2024). Similarly, Monoli et al. observed sustained impairments in motor and cognitive dual-task performance, suggesting long-term disruptions to cognitive-motor integration following concussion (Monoli et al., 2024).

Interestingly, no significant seasonal variations or interaction effects between concussion history and stage of the season were observed, suggesting that these motor control impairments are stable rather than transient or context-dependent (e.g., training load). Such consistency underscores the long-lasting impact of concussions on neuromuscular control systems, potentially heightening vulnerability to recurrent injuries or reduced performance quality over prolonged periods (Monoli et al., 2024). Chen et al. similarly reported stable inter-joint coordination deficits in concussed individuals, suggesting these impairments are robust and enduring (Chen et al., 2015). These stable motor control deficits might not be evident through traditional clinical assessments, emphasizing the importance of employing sensitive analytical methods like GEM to detect subtle yet clinically relevant impairments.

Temporal persistence metrics (λ values) exhibited non-significant yet consistent trends toward less effective trial-to-trial motor regulation in players with concussion histories. Previous studies suggest such subtle trends might be linked to impaired neural processing and diminished cognitive-motor integration post-concussion (Fino et al., 2019; Lynall et al., 2015; Thériault et al., 2011). This diminished motor regulation capacity could reflect an ongoing disruption in neural

mechanisms responsible for motor planning and adaptation, further highlighting the complexity of complete functional recovery after concussion. For example, Chen et al. reported increased variability in hip-knee coordination during gait, hypothesizing a reduced cognitive processing capacity as a contributing factor (Chen et al., 2015). This is consistent with broader evidence indicating persistent deficits in attention, cognitive flexibility, and executive function post-concussion (Parker et al., 2006).

Additionally, Fino et al. demonstrated increased lower extremity injury rates post-concussion, suggesting impaired motor planning and adaptive responses could significantly elevate subsequent injury risks (Fino et al., 2019). Lynall et al. found similar heightened risks of musculoskeletal injury in athletes who recently recovered from concussion, emphasizing the clinical importance of identifying persistent motor control impairments early and accurately (Lynall et al., 2015).

Clinically, these findings carry substantial implications. They emphasize the necessity for ongoing and detailed neuromuscular monitoring beyond traditional symptom management. Given GEM's sensitivity in detecting subtle deficits, it presents a valuable tool for clinicians to objectively assess and tailor rehabilitation strategies. Integrating GEM analysis into routine clinical practice can provide quantitative insights that help refine individualized rehabilitation protocols, monitor athlete progress more effectively, and support informed return-to-play decisions, ultimately enhancing athlete safety and performance resilience (Nordström et al., 2014; Patricios et al., 2023).

Several studies have recommended targeted neuromuscular interventions aimed explicitly at improving coordination, stability, and adaptive motor control post-concussion. For instance, targeted neuromuscular training has been shown to effectively reduce injury risk and enhance motor performance in post-concussion recovery phases (Dubose et al., 2017; Ippersiel et al., 2018). However, specific rehabilitation programs addressing altered inter-segmental coordination post-concussion remain underexplored, highlighting an important area for future investigation. Ippersiel et al., speculated similar altered coordination patterns might represent adaptive strategies to compromised proprioception in low back pain populations, a hypothesis applicable to concussion

populations as well (Ippersiel et al., 2018).

One of the most notable strengths of this study is the integration of a metronome-paced bilateral squat task, which represents a dual-task paradigm requiring both postural control and temporal synchronization. Unlike traditional balance or reaction time tasks, this design imposes heightened cognitive-motor demands, thereby serving as a more ecologically valid and challenging evaluation of motor performance. Dual-task paradigms have been shown to be particularly sensitive in revealing lingering motor and cognitive deficits post-concussion that may otherwise go unnoticed (Catena et al., 2007; Howell et al., 2013; Parker et al., 2006). Prior research demonstrates that these tasks, combining motor and cognitive elements, can unmask subtle impairments in gait, balance, and inter-limb coordination (Fino et al., 2016; Martini et al., 2011). For example, Fino et al. found that dual-task gait assessments revealed persistent dynamic balance deficits even after symptom resolution, while Kakavas et al. observed altered biomechanics and variability during walking under dual-task conditions, supporting their use in post-concussion assessments (Fino et al., 2016; Kakavas et al., 2025).

Further strengthening the study is the methodological innovation in GEM analysis. By incorporating timing error as a third dimension into the execution space, this modified GEM framework advances beyond conventional two-dimensional applications. It enables a more holistic analysis of motor control by capturing spatial variability and temporal precision, critical in tasks demanding rhythmic coordination. Unlike the Uncontrolled Manifold (UCM) framework, which evaluates how athletes manage variability to achieve consistent outcomes without requiring an explicit goal function, the GEM approach is especially valuable in sports assessments because it incorporates a clearly defined goal function. This allows for detailed analysis of how athletes regulate performance by coordinating both body-level and task-level variables to achieve task-specific goals (Cusumano & Dingwell, 2013).

Collectively, the combination of a dual-task paradigm and a refined 3D GEM method offer a valid framework for evaluating post-concussion motor control. It facilitates the identification of persistent deficits that may not be captured through conventional assessments, supporting a more

nuanced understanding of functional recovery.

4.4.1 Limitations

This study has its limitations. First, although the generalized linear model with GEE is well-suited to handle missing data, the relatively small sample size constrained the statistical power and limited the generalizability of the findings. While consistent trends were observed, a larger sample would increase confidence in the robustness of observed group differences. Second, participants with a concussion history varied in terms of the time elapsed since their most recent concussion. The heterogeneity in injury recency likely introduced variability in the extent of motor control impairment, potentially masking time-dependent recovery patterns. Third, the bodyweight squat was performed at a fixed pace synchronized to a 40 BPM metronome. Although this moderate speed was selected based on a pilot study and logistical constraints related to athlete availability, using a single preset tempo may not have accurately captured each athlete's natural movement rhythm or their maximal motor control capacity.

Future research should continue exploring GEM's utility across diverse athletic populations and tasks, including assessments at varying movement speeds to better reflect individual control capacities. Investigations should also compare acute versus chronic stages post-concussion and examine how motor control deficits evolve over time and relate to subsequent injury risk. Longitudinal research employing advanced biomechanical and electrophysiological methods could provide deeper insight into the mechanisms underlying persistent motor impairments post-concussion. Further studies should also investigate the effectiveness of neuromuscular training interventions specifically designed to improve motor coordination deficits identified through 3D GEM analysis, thus offering direct, evidence-based recommendations for clinical rehabilitation practices.

4.5 Conclusion

This study demonstrated the utility of 3D GEM analysis in identifying persistent motor control deficits in female soccer players with concussion histories. These deficits remained stable

throughout the season, highlighting a gap between clinical recovery and functional neuromuscular recovery. From a practical standpoint, clinicians may consider integrating GEM assessments into preseason screenings to establish individual motor control baselines and identify athletes at elevated risk. Additionally, GEM-derived metrics can help determine readiness for return-to-play by assessing dynamic control in functional tasks, rather than relying solely on symptom reports. Rehabilitation specialists should also use GEM analysis to evaluate the effectiveness of neuromuscular training interventions over time, adapting programs in real time to the athlete's performance trajectory. This approach supports a shift toward function-based, personalized rehabilitation models, ensuring that athletes regain not only symptom-free status, but also optimal biomechanical resilience needed for sport-specific demands. and highlights the clinical value of advanced analytical tools such as GEM.

These findings advocate for refined rehabilitation protocols and comprehensive management strategies designed explicitly to address persistent neuromuscular impairments in concussed athletes, facilitating safer and more effective returns to competitive play.

4.6 References

Ballinger, G. A. (2004). Using Generalized Estimating Equations for Longitudinal Data Analysis. *Organizational Research Methods*, *7*(2), 127-150.

Barnes, A., Smulligan, K., Wingerson, M. J., Little, C., Lugade, V., Wilson, J. C., & Howell, D. R. (2024). A Multifaceted Approach to Interpreting Reaction Time Deficits After Adolescent Concussion. *Journal of Athletic Training*, *59*(2), 145-152.

Bernstein, N. (1967). *The Co-ordination and Regulation of Movements*. Pergamon Press.

Broshek, D. K., Kaushik, T., Freeman, J. R., Erlanger, D., Webbe, F., & Barth, J. T. (2005). Sex differences in outcome following sports-related concussion. *Journal of Neurosurgery*, *102*(5), 856-863.

Catena, R. D., van Donkelaar, P., & Chou, L. S. (2007). Altered Balance Control Following Concussion Is Better Detected with an Attention Test During Gait. *Gait & Posture*, *25*(3), 406-411.

Chehrehrazi, M., Sanjari, M. A., Mokhtarinia, H. R., Jamshidi, A. A., Maroufi, N., & Parnianpour, M. (2017). Goal Equivalent Manifold Analysis of Task Performance in Non-specific LBP and Healthy Subjects during Repetitive Trunk Movement: Effect of Load, Velocity, Symmetry.

Human Movement Science, *51*, 72-81.

Chen, H. L., Lu, T. W., & Chou, L. S. (2015). Effect of Concussion on Inter-Joint Coordination During Divided-Attention Gait. *Journal of Medical and Biological Engineering*, *35*(1), 28-33.

Cohen, J. (1988). *Statistical Power Analysis for the Behavioral Sciences Second Edition*.

Covassin, T., Moran, R., & Wilhelm, K. (2013). Concussion Symptoms and Neurocognitive Performance of High School and College Athletes Who Incur Multiple Concussions. *The American Journal of Sports Medicine*, *41*(12), 2885-2889.

Cusumano, J. P., & Dingwell, J. B. (2013). Movement Variability Near Goal Equivalent Manifolds: Fluctuations, Control, and Model-based Analysis. *Human Movement Science*, *32*(5), 899-923.

Dingwell, J. B., John, J., & Cusumano, J. P. (2010). Do Humans Optimally Exploit Redundancy to Control Step Variability in Walking? *PLoS Computational Biology*, *6*(7), e1000856.

Dubose, D. F., Herman, D. C., Jones, D. L., Tillman, S. M., Clugston, J. R., Pass, A., Hernandez, J. A., Vasilopoulos, T., Horodyski, M., & Chmielewski, T. L. (2017). Lower Extremity Stiffness Changes after Concussion in Collegiate Football Players. *Medicine and Science in Sports and Exercise*, *49*(1), 167-172.

Dunne, L. A. M., Cole, M. H., Cormack, S. J., Howell, D. R., & Johnston, R. D. (2023). Validity and Reliability of Methods to Assess Movement Deficiencies Following Concussion: A COSMIN Systematic Review. *Sports Medicine - Open*, *9*(1), 1-25.

Fino, P. C., Becker, L. N., Fino, N. F., Griesemer, B., Goforth, M., & Brolinson, P. G. (2019). Effects of Recent Concussion and Injury History on Instantaneous Relative Risk of Lower Extremity Injury in Division I Collegiate Athletes. *Clinical Journal of Sport Medicine*, *29*(3), 218-223.

Fino, P. C., Nussbaum, M. A., & Brolinson, P. G. (2016). Locomotor Deficits in Recently Concussed Athletes and Matched Controls During Single and Dual-Task Turning Gait: Preliminary Results. *Journal of NeuroEngineering and Rehabilitation*, *13*(1), 65.

Gaudet, C. E., Iverson, G. L., Kissinger-Knox, A., Van Patten, R., & Cook, N. E. (2022). Clinical Outcome Following Concussion Among College Athletes with A History of Prior Concussion: A Systematic Review. *Sports Medicine - Open*, *8*(1), 1-16.

Gessel, L. M., Fields, S. K., Collins, C. L., Dick, R. W., & Comstock, R. D. (2007). Concussions Among United States High School and Collegiate Athletes. *Journal of Athletic Training*, *42*(4), 495.

Howell, D. R., Osternig, L. R., & Chou, L. S. (2013). Dual-Task Effect on Gait Balance Control in Adolescents with Concussion. *Archives of Physical Medicine and Rehabilitation*, *94*(8), 1513-1520.

Ippersiel, P., Robbins, S., & Preuss, R. (2018). Movement Variability in Adults with Low Back

Pain During Sit-to-Stand-to-Sit. *Clinical Biomechanics*, *58*, 90-95.

Iverson, G. L., Brooks, B. L., Collins, M. W., & Lovell, M. R. (2006). Tracking Neuropsychological Recovery Following Concussion in Sport. *Brain Injury*, *20*(3), 245-252.

Iverson, G. L., Echemendia, R. J., LaMarre, A. K., Brooks, B. L., & Gaetz, M. B. (2012). Possible Lingering Effects of Multiple Past Concussions. *Rehabilitation Research and Practice*, *2012*(1), 316575.

Johnston, W., Coughlan, G. F., & Caulfield, B. (2017). Challenging Concussed Athletes: The Future of Balance Assessment in Concussion. *QJM: An International Journal of Medicine*, *110*(12), 779-783.

Kakavas, G., Malliaropoulos, N., Skarpas, G., & Forelli, F. (2025). The Impact of Concussions on Neuromuscular Control and Anterior Cruciate Ligament Injury Risk in Female Soccer Players: Mechanisms and Prevention - A Narrative Review. *Journal of Clinical Medicine*, *14*(9), 3199.

Kieffer, E., Brolinson, P., & Rowson, S. (2022). Dual-Task Gait Performance Following Head Impact Exposure in Male and Female Collegiate Rugby Players. *International Journal of Sports Physical Therapy, 17(3).*

Kritz, M., Cronin, J., & Hume, P. (2009). The bodyweight squat: a movement screen for the squat pattern. *Strength and Conditioning Journal*, *31*(1), 76-85.

Liu, K., Chan, T. C. Y., Burkhart, T. A., & Hutchison, M. G. (2024). Altered Inter-Segmental Coordination in Athletes with A History of Concussion. *Journal of Sports Sciences*.

Lynall, R. C., Mauntel, T. C., Padua, D. A., & Mihalik, J. P. (2015). Acute Lower Extremity Injury Rates Increase after Concussion in College Athletes. *Medicine and Science in Sports and Exercise*, *47*(12), 2487-2492.

Martini, D. N., Sabin, M. J., Depesa, S. A., Leal, E. W., Negrete, T. N., Sosnoff, J. J., & Broglio, S. P. (2011). The Chronic Effects of Concussion on Gait. *Archives of Physical Medicine and Rehabilitation*, *92*(4), 585-589.

Monoli, C., Morris, A., Crofts, R., Fino, N. F., Petersell, T. L., Jameson, T., Dibble, L. E., & Fino, P. C. (2024). Acute and Longitudinal Effects of Sport-related Concussion on Reactive Balance. *MedRxiv*, 2024.03.28.24305029.

Nordström, A., Nordström, P., & Ekstrand, J. (2014). Sports-Related Concussion Increases the Risk of Subsequent Injury by About 50% in Elite Male Football Players. *British Journal of Sports Medicine*, *48*(19), 1447-1450.

Parker, T. M., Osternig, L. R., Van Donkelaar, P., & Chou, L. S. (2006). Gait Stability Following Concussion. *Medicine and Science in Sports and Exercise*, *38*(6), 1032-1040.

Patricios, J. S., Schneider, K. J., Dvorak, J., Ahmed, O. H., Blauwet, C., Cantu, R. C., Davis, G. A., Echemendia, R. J., Makdissi, M., McNamee, M., Broglio, S., Emery, C. A., Feddermann-Demont, N., Fuller, G. W., Giza, C. C., Guskiewicz, K. M., Hainline, B., Iverson, G. L.,

Kutcher, J. S., … Meeuwisse, W. (2023). Consensus Statement on Concussion in Sport: The 6th International Conference on Concussion in Sport-Amsterdam, October 2022. *British Journal of Sports Medicine*, *57*(11), 695-711.

Sedighi, A., & Nussbaum, M. A. (2017). Temporal Changes in Motor Variability during Prolonged Lifting/Lowering and the Influence of Work Experience. *Journal of Electromyography and Kinesiology*, *37*, 61-67.

Sedighi, A., & Nussbaum, M. A. (2019). Exploration of Different Classes of Metrics to Characterize Motor Variability during Repetitive Symmetric and Asymmetric Lifting Tasks. *Scientific Reports*, *9*(1), 9821.

Stergiou, N. (2018). *Nonlinear Analysis for Human Movement Variability* (N. Stergiou, Ed.1st). CRC Press.

Stergiou, N., Harbourne, R. T., & Cavanaugh, J. T. (2006). Optimal Movement Variability: A New Theoretical Perspective for Neurologic Physical Therapy. *Journal of Neurologic Physical Therapy*, *30*(3), 120-129.

Thériault, M., De Beaumont, L., Tremblay, S., Lassonde, M., & Jolicoeur, P. (2011). Cumulative Effects of Concussions in Athletes Revealed by Electrophysiological Abnormalities on Visual Working Memory. *Journal of Clinical and Experimental Neuropsychology*, *33*(1), 30-41.

Zuckerman, S. L., Kerr, Z. Y., Yengo-Kahn, A., Wasserman, E., Covassin, T., & Solomon, G. S. (2015). Epidemiology of Sports-related Concussion in NCAA Athletes from 2009-2010 to 2013-2014. *American Journal of Sports Medicine*, *43*(11), 2654-2662.

Chapter 5. Study 2: From Classical Models to Attention-Based Transformers: A Comparative Study on Injury Prediction Pipelines in Female Varsity Soccer

*Submitted to *Journal of Biomechanics**

Xiong Zhao[1], Victor Chan[1], Ryan B. Graham[1]

[1]*School of Human Kinetics, Faculty of Health Sciences, University of Ottawa, Ottawa, Ontario, Canada*

Abstract

Objectives: This study aimed to compare four commonly used machine learning pipelines, Support Vector Machine (SVM), eXtreme Gradient Boosting (XGBoost), Long Short-Term Memory (LSTM), and a Hybrid Transformer, for predicting non-contact lower limb and lower back injuries in female varsity soccer players. Special emphasis was placed on evaluating model performance, interpretability, and applicability in sports settings.

Methods: Twenty-five female soccer athletes completed preseason and midseason biomechanical assessments involving anthropometrics, performance and functional tasks (e.g., T-balance, Y-balance, L-hop), broad jump (BJ), countermovement jumps (CMJ), and squats captured via markerless 3D motion analysis. Each model was trained using five-fold Group K-Fold cross-validation on structured and/or time-series inputs, depending on its architecture. Performance was evaluated using ROC-AUC, accuracy, precision, recall, F1-score, and confusion matrices and interpretability was assessed using SHAP and attention scores for XGBoost and Hybrid Transformer, respectively.

Results: The Hybrid Transformer model demonstrated the highest performance (AUC = 0.740, accuracy = 67.6%), followed by LSTM (AUC = 0.660), XGBoost (AUC = 0.619), and SVM (AUC = 0.342). Attention weight analysis revealed that the Transformer model emphasized early landing and push-off phases during high-demand tasks in injured athletes. Traditional models exhibited lower discriminative performance and lacked temporal interpretability.

Conclusion: Comparing structured and temporal modeling pipelines revealed that the Hybrid

Transformer, leveraging native attention mechanisms, is particularly well-suited to biomechanical injury prediction tasks due to its balance of accuracy and interpretability. By identifying vulnerable movement phases associated with elevated injury risk, this modeling approach offers actionable insights for personalized athlete training, rehabilitation, and proactive injury prevention strategies in female soccer.

5.1 Introduction

Soccer is the most widely played sport globally, with a growing participation rate among female athletes (Randell et al., 2021). However, increased participation has also led to an increased rate of sport-related injuries, particularly non-contact lower limb injuries, among female players compared to their male counterparts (Enright et al., 2020; Gebert et al., 2018). Lower limb injuries, especially anterior cruciate ligament (ACL) ruptures, can be career-threatening and have long-term consequences on physical function and quality of life (Anicic et al., 2023; Kotsifaki et al., 2023).

The increased susceptibility of female soccer players to such injuries is multifactorial, encompassing anatomical, hormonal, biomechanical, and neuromuscular risk factors (Alentorn-Geli et al., 2009; Bahr, 2003). While it is unlikely that a single variable can directly predict injury, statistical models like logistic regression have identified numerous contributing factors (Bittencourt et al., 2016). These risk factors are commonly classified as intrinsic, such as sex, age, prior injury history, strength, balance, coordination, training load, and psychological state (de la Motte et al., 2019; McCall et al., 2015; Smith et al., 2012); and extrinsic, including field conditions, surface type, match congestion, and equipment (Lawrence et al., 2016; Robotti et al., 2020).

While some extrinsic factors can only be controlled through rule changes, environmental adaptations, and the design of sport-specific equipment, modifiable intrinsic factors offer a more proactive target for personalized injury prevention. These include strength, flexibility, balance, and neuromuscular control, components often assessed through functional movement screens (Bennett et al., 2017; Emery & Pasanen, 2019). In other words, modifiable risk factors can offer more actionable insights for injury prevention, whereas unmodifiable factors such as previous injury

history primarily serve as indicators of risk rather than direct intervention targets. For instance, biomechanical patterns such as excessive knee valgus during landing and inadequate trunk stability have been repeatedly associated with increased injury risk (Kotsifaki et al., 2023; Siesmaa et al., 2022). Thus, targeted neuromuscular training to correct landing mechanics and enhance knee and trunk stability could reduce an athlete's risk of injury.

A wide array of screening tools has been developed to evaluate these modifiable factors, including the Functional Movement Screen (FMS), Y-Balance Test, Landing Error Scoring System (LESS), and sport-specific assessments like the Soccer Injury Movement Screen (SIMS) and the Athletic Ability Assessment (AAA) (Bulow et al., 2019; Clagg et al., 2015; McKeown et al., 2014). However, many of these rely on subjective visual scoring, which has been criticized for poor inter- and intra-rater reliability (Gulgin & Hoogenboom, 2014; Onate et al., 2012). This subjectivity limits their predictive validity and scalability. Moreover, because these tests typically assess one or a few biomechanical factors in isolation, they may fail to capture the multifactorial nature of injury risk. In contrast, machine learning (ML) models can simultaneously integrate and analyze numerous interacting variables, offering a more holistic and scalable approach to injury prediction.

To improve objectivity and predictive power, ML approaches have increasingly been applied in sports injury prediction. Algorithms such as Support Vector Machines (SVMs) and gradient-boosted decision trees (e.g., XGBoost) have shown promise in classifying injury risk based on movement screening or sensor-derived data (Ghasemzadeh et al., 2015; Nassis et al., 2023). More recently, recurrent neural networks (RNNs) and their variants like Long Short-Term Memory (LSTM) networks have been used to capture temporal dependencies in biomechanical signals and gait cycles (Dorschky et al., 2020; Mavor et al., 2023). LSTM models have demonstrated strong performance in strictly time-series biomechanical data applications, such as in single-IMU soldier survivability analysis and instrumented insole-based gait monitoring in both healthy and clinical populations (Mavor et al., 2023, 2025).

However, these models vary considerably in interpretability, which is essential in injury prevention contexts where clinical decision-making demands not only high performance but also

insights into which features contribute to a prediction (Murdoch et al., 2019). While XGBoost models offer relatively high accuracy, they typically require manual feature engineering, and interpretability must be enhanced post hoc using methods such as SHAP (SHapley Additive exPlanations) to identify influential predictors (Lundberg & Lee, 2017). SVMs, while robust in high-dimensional spaces, offer limited transparency, when particularly using non-linear kernels, and often act as "black boxes" in clinical settings (Ribeiro et al., 2016). LSTM models capture sequential dynamics effectively, but their internal representations are difficult to interpret without specialized techniques, and they offer limited insight into which time windows or features drive classification (Che et al., 2018). Given these limitations, there is a growing interest in models that combine high performance with built-in interpretability, a niche where Transformer-based architectures are increasingly recognized as promising alternatives, offering both parallel temporal modeling and attention-based explanations.

Transformers, originally developed for natural language processing (Vaswani et al., 2017), address these limitations by leveraging self-attention mechanisms to model temporal dependencies in a fully parallelized manner. This allows the model to weigh the relative importance of different time points or features simultaneously, without relying on recurrent structures. Transformers have since been adapted for a range of time-series applications, including human activity recognition, gait analysis, and, more recently, sports science applications like ACL injury prediction and rehabilitation monitoring (Bai et al., 2025; Schilling et al., 2024).

In the context of movement screening for injury prediction, transformer models are particularly well-suited because movement features are inherently interdependent; errors in hip mechanics may co-occur with compensations at the knee or ankle, forming complex, multi-joint patterns that evolve over time (Kotsifaki et al., 2023; Myer et al., 2010). Traditional models may struggle to capture these nonlinear and temporally distributed patterns. In contrast, Transformers use self-attention mechanisms to learn contextual relationships across time by simultaneously evaluating all positions in a sequence. Through multi-head self-attention, the model can capture diverse dependencies at multiple temporal scales in parallel, allowing it to attend to critical phases

of movement or joint interactions that contribute most to injury risk (Vaswani et al., 2017; Zeng et al., 2022). Just as large language models like ChatGPT leverage this same mechanism to identify relevant words and phrases across long textual sequences to generate coherent responses, transformer-based models in biomechanics can weigh temporally distant but biomechanically meaningful signals, enhancing both predictive accuracy and interpretability. Prior studies have demonstrated their superior performance in pose estimation and human activity recognition tasks (Schilling et al., 2024), and recent work has highlighted their potential in biomechanical and clinical modeling (Jauhiainen et al., 2022). Furthermore, the interpretability afforded by attention maps allows practitioners to identify which movement phases are driving predictions, providing actionable insights for targeted interventions (Vaswani et al., 2017).

This study aims to address the methodological gap in injury prediction by comparing four common ML pipelines, Support Vector Machine (SVM), XGBoost, Long Short-Term Memory (LSTM), and a Hybrid Transformer, using multimodal data collected from female varsity soccer players. Each model was evaluated based on its ability to predict non-contact lower limb injury risk using a combination of static (e.g., injury history, anthropometrics) and dynamic (e.g., jump and balance kinematics) features. By contrasting structured-data models with time-series models, this study explores not only predictive accuracy but also model interpretability and practical utility. Special attention is given to attention-weight analysis in the Hybrid Transformer to illustrate how temporal patterns may be linked to injury risk.

It is hypothesized that time-series models (LSTM and Hybrid Transformer) will outperform structured-data models (SVM and XGBoost) due to their ability to capture temporal patterns in movement, and that the Hybrid Transformer will additionally offer interpretable insights through its built-in attention mechanism.

5.2 Methods

5.2.1 Data collection

5.2.1.1 Participant

Twenty-five athletes from the University of Ottawa's women's varsity soccer team participated in the study. Demographic characteristics (mean ± SD) were: age = 20.40 ± 1.98 years; height = 1.66 ± 0.06 m; weight = 63.31 ± 7.94 kg; BMI = 22.90 ± 2.30 kg/m².

5.2.1.2 Protocol

Data collection was conducted at two time points: pre-season (week 1) and mid-season (week 9), to assess changes in both laboratory-based biomechanics and sprint performance. In-field sprint tests over 10, 20, 40, and 60 meters were administered during regular training sessions by coaches using electronic timing gates (Brower Timing Systems, Utah, USA). Sprint performance data were subsequently shared for analysis. Total play time (in minutes) was manually tracked by the coaching staff. Additionally, *player moments*, a feature of the Veo Cam 3 (Veo Technologies, NY, USA), were used to capture periods of close ball-player interaction during 19 recorded matches. These moments (in minutes) were treated as proxies for high-intensity play, as the auto-detection algorithm flags segments involving direct engagement with the ball.

Upon arrival for laboratory testing, participants provided written informed consent. Anthropometric measurements, including leg length, height, and weight, were recorded. Following a familiarization period, participants completed a randomized battery of functional movement tasks: one trial each of the T-balance test (eyes open and eyes closed), Y-balance test, and L-hop on each leg; three single-leg (left and right) and three bilateral countermovement jumps (CMJs); three standing broad jumps; and two reaction time tasks for both upper and lower limbs using four FitLights (FITLIGHT Sports Corp., Ontario, Canada). A detailed description of each task is provided in Appendix A.

After a minimum five-minute rest period, participants performed 35 consecutive bodyweight squats to a metronome set at 40 beats per minute (BPM). Whole-body kinematics during the tasks were captured using an eight-camera markerless motion capture system (Theia Markerless Inc.,

Kingston, ON, Canada), sampled at 60 Hz. No kinematic or kinetic data were recorded during the reaction time tests. Aside from the initial consent process, the same protocol was repeated during the mid-season session.

This study was approved by the Research Ethics Board at University of Ottawa (file #: H-07-24-10628). Participants were informed of their right to withdraw at any time without consequence, and all data were anonymized prior to analysis to ensure confidentiality.

5.2.2 Data preparation

Data from both the pre-season (week 1) and mid-season (week 9) sessions were included, resulting in a dataset of 50 observations (25 participants × 2 time points). Each entry was labeled based on injury status at the end of the season. Since the movement tasks involved whole-body movements, non-contact lower back injuries sustained during the season were also considered relevant and, for simplification, grouped together with non-contact lower limb injuries.

Table 5.1: Injury classification and breakdown of injury types among participants.

Group	Number	Injury Types (n)
No injury	24	–
Injured group	26	Ankle sprain (8)
		Muscle strains (14): hip adductors (4), hip flexors (2), quadriceps (4), hamstrings (3), calves (1)
		MCL sprain (1), ACL injury (1)
		Low back pain (2)

Note: Participants were grouped as no injury (n = 24) or non-contact lower limb/lower back injury (n = 26). Injury types included ankle sprains (n = 8), muscle strains (n = 14), MCL sprain (n = 1), ACL injury (n = 1), and low back pain (n = 2).

Participants were categorized into two groups according to whether they sustained an injury during the season: no injury (n = 24) and those with a non-contact lower limb or lower back injury (n = 26). The injured group included primarily ankle sprains and muscle strains, alongside isolated cases of ACL injury, MCL sprain, and lower back pain (see Table 5.1 for breakdown). The dataset incorporated four main modalities: anthropometric and injury history data (see Table 5.2),

performance metrics (Table 5.3), time-series kinematic data, and injury labels.

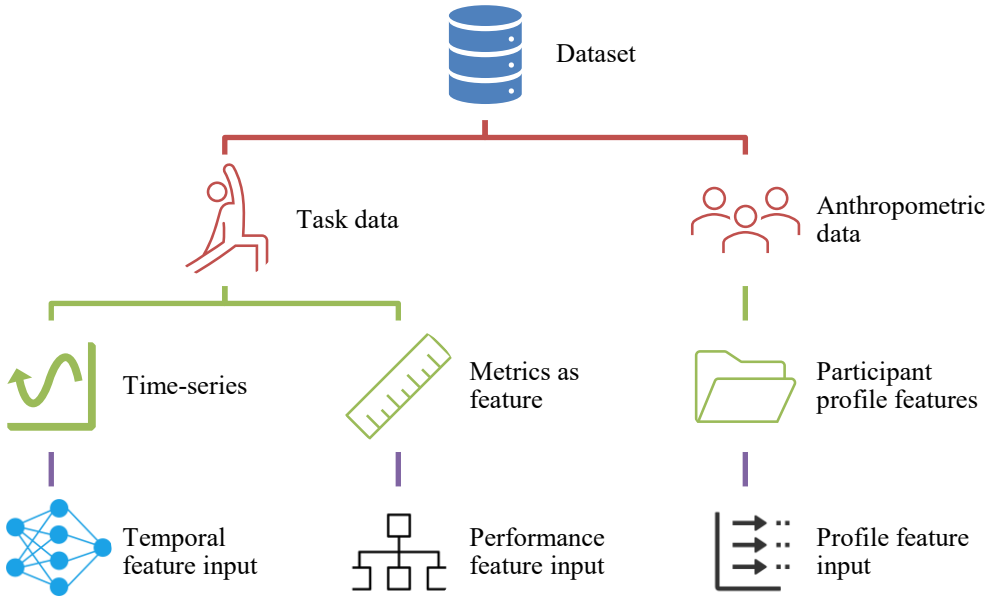

Figure 5.1: The workflow of data preparation. Anthropometric and injury-related variables were compiled into profile feature inputs. Task data were either processed as time-series for temporal feature inputs or summarized into discrete performance metrics for performance feature inputs.

After data collection, video recordings were processed using Theia3D (Theia Markerless Inc., Kingston, ON, Canada) and analyzed in Visual3D (C-Motion Inc., Germantown, MD) to extract 3D kinematic data. Ground reaction forces were acquired via force plates (Bertec Inc., Ohio, USA). Custom MATLAB scripts (R2019b; The MathWorks Inc., Natick, MA, USA) were used to compute metrics for each movement. Kinematic and kinetic data were low-pass filtered using a fourth-order Butterworth filter with cutoff frequencies of 6 Hz and 10 Hz, respectively.

Table 5.2: Anthropometric, training, and injury history variables included in the dataset.

Variable name	Description	Note
Age, Height and Body mass	Units: years, meters and kilograms, respectively	
BMI	Body mass/(height)^2	
Position	Forward, midfield, defense, or	One-hot encoded

	goalkeeper	
Dominant Hand and Foot	Right:1; Left: 0	
Training Starting Age	e.g., 12 years old	Self-reported
Weekly Training Hours	e.g., 4 hours/week	Self-reported
Additional Weekly Training Hours	e.g., 2 hours beyond regular sessions	Self-reported
Number of Concussions	e.g., 2	Past 10 years, self-reported
Number of Musculoskeletal Injuries	e.g., 5	Self-reported
Total Time Missed Due to Previous Musculoskeletal Injuries	e.g., 50 days	Self-reported
Match Play Time per Season Phase	Tracked in minutes by coaching staff	
Intense Moments During Match Play	Captured using Veo Cam auto-detection algorithm	

Note: BMI = body mass index. Intense Moments During Match Play refer to periods of close interaction between the player and the ball, automatically detected by the Veo Cam 3 using its built-in algorithm. These moments were used as a proxy for high-intensity game play.

Two types of input features were created depending on the modeling approach (Figure 5.1). For traditional models (e.g., SVM, XGBoost), a static feature set was constructed by extracting biomechanical metrics from each movement (Figure 5.1: *Performance feature input*) and combining them with anthropometric and injury history data (Figure 5.1: *Profile feature input*). For deep learning models (e.g., LSTM, hybrid Transformer), a temporal feature (Figure 5.1: *Temporal feature input*) set was used by time-normalizing and filtering the full 3D kinematic time-series to 300 frames per trial without metric extraction. These time-series inputs were then combined with the same anthropometric and injury history data (Figure 5.1: *Profile feature input*) to form the model input.

The extracted biomechanical features are summarized in Table 5.2. For example, countermovement jump (CMJ) metrics included jump height, reactive strength index (RSI) (Markwick et al., 2015) and normalized peak power; broad jump metrics included horizontal distance and normalized power (Anicic et al., 2023; Boone et al., 2021; Sha et al., 2021). Y-balance

tests produced reach scores (normalized to leg length) and average acceleration (m/s^2) of the reaching foot. Composite reach scores (the average across the three directions) were also calculated for each leg (González-Fernández et al., 2022; Plisky et al., 2009).

For the T-balance test, sway area (eyes closed/open) were calculated for each leg. Squat task performance was evaluated using a goal equivalent manifold (GEM)-based performance index (PI), which captures movement variability, with higher values indicating better performance (Chehrehrazi et al., 2017; Cusumano & Dingwell, 2013; Furuki & Takiyama, 2018). During L-hop tests, the maximum knee abduction moment (MKAM) was extracted. Reaction time tests yielded simple and complex reaction times for both upper and lower limbs using FitLights (FITLIGHT Sports Corp., Ontario, Canada).

The final label used for all classification models was non-contact lower-limb injury, given its prevalence among female soccer players and its relevance to movement-based injury prediction.

Table 5.3: Screening movements and corresponding biomechanical metrics.

Movement	Metrics	Note
Broad Jump (BJ)	Distance, normalized peak power (W/kg)	
Countermovement Jump (CMJ)	Height, RSI, normalized peak power (W/kg)	Left, right and bilateral
L-hop	Maximum Knee Abduction Moment (MKAM)	Left and right
T-balance	Composite score, average acceleration of reaching foot	Left and right
Y-balance	Sway area with eyes open/closed	Left and right
Bilateral squat	Performance Index (GEM-based)	
Sprint	10m, 20m, 40m and 60m times	Measured in seconds
Reaction Tasks	CRT_Low, CRT_Up, SRT_UL/R and SRT_LL/R	Measured in seconds

Note: RSI = Reactive Strength Index; MKAM = Maximum Knee Abduction Moment; Performance Index = movement variability calculated using the Goal Equivalent Manifold (GEM) method (see Study 1b); CRT = Complex Reaction Time; SRT = Simple Reaction Time; UL/R = Upper-limb Left/Right; LL/R = Lower-limb Left/Right.

5.2.3 Model selection and training

5.2.3.1 Environment setup

All experiments were conducted on a Linux server (Ubuntu 20.04 LTS) equipped with three NVIDIA TITAN RTX GPUs and an Intel® Xeon® Gold 6248 CPU @ 2.50 GHz. Model training and inference were implemented in Python 3.9, using PyTorch 2.6.0 and XGBoost 2.1.4.

5.2.3.2 Classification task

Four popular classification models were trained and evaluated to predict non-contact lower limb injuries: SVM, XGBoost, LSTM and a Hybrid Transformer model. As illustrated in Figure 5.1, static features included performance metrics and profile data, while temporal features contained trunk and lower limb time-series kinematics of broad jump, countermovement jump, L-hop, T-balance and Y-balance (Trunk flexion/extension and rotation; hip flexion/extension, abduction/adduction and rotation; knee flexion/extension; and ankle inversion/eversion).

5.2.3.3 Training and parameters

When static data were partially missing, imputation was performed using group means. Participants with missing temporal features were excluded entirely. All static input features were z-score standardized before training. Table 5.4 summarizes the final hyperparameter configurations for all four models. For SVM and XGBoost, optimal parameters were determined via grid search. For LSTM and the Hybrid Transformer, parameters were manually tuned based on pilot experiments and guidance from prior studies.

Since both pre- and mid-season assessments were included for each participant, the design leveraged within-subject longitudinal data. To avoid data leakage, where data from the same participant appears in both training and validation sets, Group K-Fold cross-validation was applied so that all data from each participant remained within a single fold. This strategy prevented leakage between train and test sets and allowed for a more realistic evaluation on unseen individuals (Dehghani et al., 2019).

Table 5.4: Final hyperparameter configurations used in each classification model.

Hyperparameter	SVM	XGBoost	LSTM	Hybrid Transformer
Batch size	—	—	8	8
Learning rate	—	0.1	1e-3	3e-4
Epochs	—	—	30	30
Early stopping patience	—	—	5	5
Optimizer	—	—	Adam	Adam
Loss function	—	Logloss	BCEWithLogits	BCEWithLogits (weighted)
Regularization	C:10; gamma:scale; kernel:RBF	max_depth: 5	L2: 1e-5	Weight decay: 1e-4
Number of estimators	—	50	—	—
Class imbalance strategy	class_weight=balanced	scale_pos_weight=1.5	pos_weight per fold	pos_weight per fold
Dropout	—	—	0.3	0.3
Architecture specifics	—	—	hidden_size: 64	d_model: 64, 2 layers, 4 heads

Note: This table presents the final hyperparameters used for each model, either selected via grid search (SVM and XGBoost) or manually tuned based on pilot testing and prior literature (LSTM and Hybrid Transformer). Dashes (—) indicate parameters not applicable to the respective model.

5.2.3.3.1 SVM

SVM is a classical supervised learning algorithm grounded in the concept of finding an optimal hyperplane that maximizes the margin between classes in a high-dimensional feature space (Cortes et al., 1995). The margin-based formulation makes SVM particularly effective in handling smaller datasets with clear class boundaries. Prior work has shown that SVM can perform competitively on injury prediction tasks when applied to biomechanical datasets (Huang et al., 2022), though their performance often declines when feature interactions become highly non-linear or when time series data are involved. The SVM model in this work was implemented using both radial basis function (RBF) and linear kernels. The linear kernel projects the data into a flat hyperplane, favoring interpretability, while the RBF kernel enables non-linear decision boundaries by implicitly mapping features into a higher-dimensional space (Hsu et al., 2009). Hyperparameter

optimization was performed using grid search. The grid included penalty parameters $C \in \{0.1,1,10\}$ and kernel coefficients $\gamma \in \{\text{scale}, 0.01, 0.1\}$. To address class imbalance, the *balanced* class weight option was enabled.

5.2.3.3.2 XGBoost

XGBoost is a scalable and efficient implementation of gradient-boosted decision trees designed for structured data tasks (Chen & Guestrin, 2016). It operates by iteratively adding weak learners to correct the errors of prior learners, using second-order derivatives to optimize performance. XGBoost has been successfully used in recent studies to predict musculoskeletal injuries and concussion risk in elite athletes using diverse feature sets, making it a strong candidate for interpretable tabular classification (Leckey et al., 2025). The XGBoost classifier in this study was trained using a binary logistic objective and histogram-based tree building (*tree_method="hist"*), leveraging GPU acceleration. Grid search was used to tune the learning rate $\alpha \in \{0.01, 0.05, 0.1\}$, number of trees ($\in \{50, 100\}$) and maximum tree depth ($\in \{3, 5\}$). The *scale_pos_weight* parameter addressed class imbalance by up-weighting minority samples. SHAP (SHapley Additive exPlanations) values were computed to interpret feature importance in the final model (Lundberg & Lee, 2017). SHAP offers a unified framework that fairly distributes the prediction output among input features.

5.2.3.3.3 LSTM

LSTM, an advanced type of recurrent neural network (RNN), introduces a memory cell and gating mechanism (input, output, forget gates) that enables it to preserve long-term dependencies while mitigating issues like the vanishing gradient problem (Gers et al., 2000; Hochreiter & Schmidhuber, 1997). Previous studies have demonstrated the LSTM's utility in predicting lower-limb injuries and classifying abnormal movement patterns using inertial sensor or motion capture data (Han et al., 2024; L. Meng & Qiao, 2023). The LSTM model in this study processed full time-series kinematic data across all movement tasks (12 tasks × 300 frames × 17 joint features). Static and temporal features were processed through separate modules, a recurrent LSTM for sequential data and a feedforward network for static inputs, before being concatenated and passed through a

final classifier (Figure 5.2). The model was trained using the Adam optimizer, early stopping with a patience of 5, and a weighted binary cross-entropy loss function (BCEWithLogitsLoss) to address class imbalance.

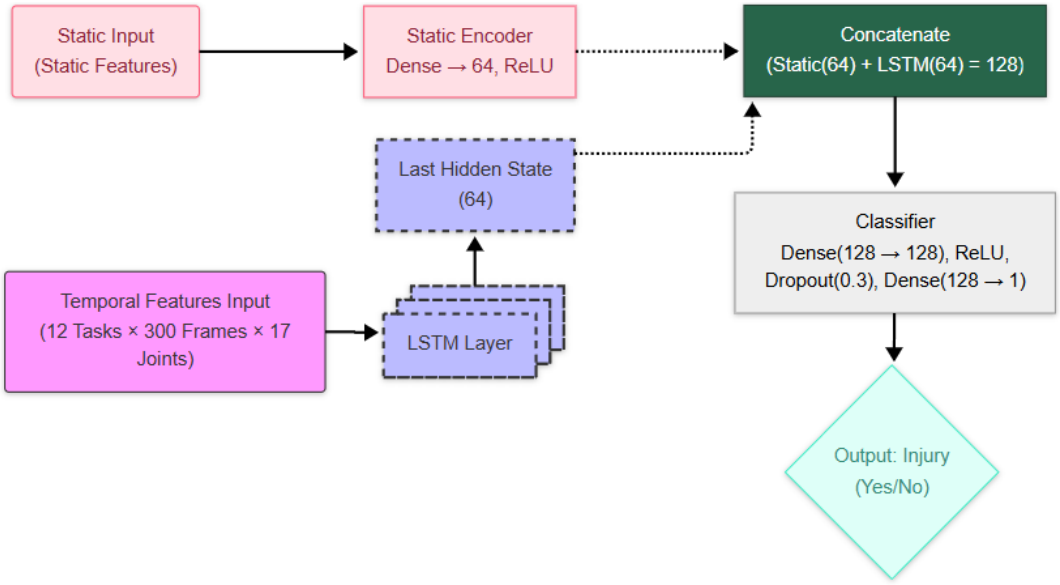

Figure 5.2: LSTM model architecture: static features are encoded via a 64-unit dense layer (ReLU). Temporal features pass through an LSTM, and its final 64-unit hidden state is concatenated with the static encoding to form a 128-unit vector. A classifier (Dense-ReLU-Dropout-Dense) then outputs the injury prediction (Yes/No).

5.2.3.3.4 Hybrid Transformer

The Transformer architecture utilizes self-attention mechanisms to model complex temporal dependencies in parallel, rather than sequentially as in RNNs (Vaswani et al., 2017). This makes them popular in sports science for their ability to extract features from complex time-series parallelly and have recently been applied in injury prediction (Wen, 2025). The Hybrid Transformer model in this work integrated static and temporal features using a dual-stream architecture (Figure 5.3).

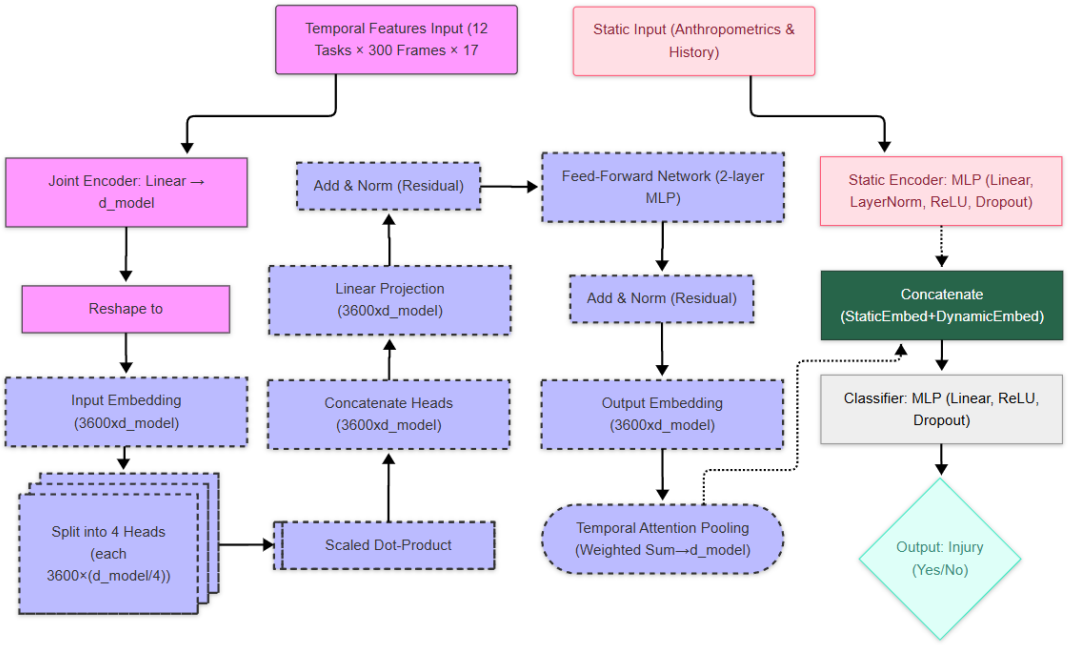

Figure 5.3: The hybrid Transformer processes temporal features (12 tasks × 300 frames × 17 joints) through a multihead self-attention encoder, followed by feed-forward layers and temporal pooling to produce a dynamic embedding. Static features pass through an MLP to produce a static embedding. These two embeddings are concatenated and fed into a final MLP classifier to predict injury (Yes/No).

Static features were embedded through a multi-layer perceptron (MLP), while joint-level kinematic data were encoded using a two-layer Transformer encoder with self-attention. In the self-attention mechanism, each time step in the sequence attends to all other time steps to capture long-range dependencies and dynamic interactions across movement patterns. Specifically, the mechanism computes attention weights by comparing query (Q), key (K), and value (V) matrices (Equation 5.1):

$$Attention(Q, K, V) = softmax\left(\frac{QK^T}{\sqrt{d_k}}\right)V \qquad (5.1)$$

where Q, K, and V are learned linear projections of the input sequence, and d_k is the dimensionality of the key vectors. This formulation enables the model to weigh the relevance of each frame relative to all others in the sequence, allowing it to focus on temporally salient events (e.g., landing phases).

After the Transformer layers, an attention pooling mechanism was applied across the full temporal span (12 tasks × 300 frames). This pooling operation learned a weighted sum of the temporal embeddings to form a single condensed representation of the participant's movement behavior. The resulting vector was concatenated with the static embedding and passed through a fully connected classifier for binary injury prediction.

To account for the class imbalance in injury labels, a weighted binary cross-entropy loss was used during training (Equation 5.2):

$$l = -\omega_1 \cdot y \cdot \log(p) - \omega_0 \cdot (1 - y) \cdot \log(1 - p) \quad (5.2)$$

where ω_1 and ω_0 are inverse-frequency weights computed as $\omega = \frac{N_{neg}}{N_{pos}}$, and $\boldsymbol{p}$ is the predicted probability. The Hybrid Transformer model was trained for a maximum of 30 epochs with early stopping based on validation loss (patience = 5), and five-fold Group K-Fold cross-validation was applied to ensure generalizability across participants.

5.2.3.4 Model performance evaluation

Model performance was evaluated using five-fold Group K-Fold cross-validation, ensuring that all data from the same participant (e.g., pre- and mid-season) were kept within a single fold. In each iteration, four folds were used for training and one fold for validation. The primary evaluation metric was the area under the receiver operating characteristic curve (AUC-ROC) which measures the model's ability to rank positive instances higher than negative ones across all thresholds. Additional metrics computed included accuracy, precision, recall, F1-score, and confusion matrices to capture different aspects of predictive quality (Sokolova & Lapalme, 2009): Accuracy reflects overall correct predictions but can be misleading with imbalanced classes. Precision quantifies how many predicted injuries were correct, while recall captures how many true injuries were identified. The F1-score balances precision and recall, especially important for imbalanced data. Confusion matrices provided a breakdown of true/false positives and negatives for each model.

To leverage built-in temporal attention mechanism of the Hybrid Transformer model, attention weights were extracted from the temporal attention pooling layer, which assigns a scalar weight to each time step in the encoded time-series representation. In practice, after passing the joint-encoded and transformer-processed dynamic input through the temporal attention pooling module, a 1D attention vector for each task was obtained, corresponding to the relative importance assigned to each of the 300 frames per trial. These vectors were retrieved per trial during the inference phase in the test fold using model hooks and stored for statistical analysis.

For task-level attention analysis, attention scores were first averaged across all 300 frames within each task and each trial to produce a mean attention value per task per participant. These average values were then grouped by injury status and assessed for normality using Shapiro–Wilk tests. Based on normality, group comparisons were conducted using either independent-samples t-tests or Mann-Whitney U tests (for non-parametric data). This analysis aimed to identify whether the model consistently focused more attention on specific movement tasks in the injured group.

For frame-level analysis, the same statistical procedure was applied to each task-frame pair (12 tasks × 300 frames), yielding a fine-grained temporal comparison of attention dynamics between groups. To control for interpretability in the visualization, statistically significant frame-wise differences ($p < .05$) were marked with asterisks in the corresponding plots. This two-tiered analysis enabled us to pinpoint not only which tasks drew more model attention in the injured vs. non-injured group, but also when within the movement sequence those differences were most pronounced.

5.3 Results

Given the modest and preprocessed dataset size, with no raw video or image input and minimal augmentation required, all models trained efficiently. Total training durations for SVM, XGBoost, and LSTM were consistently under two minutes. The Hybrid Transformer model required slightly more time, primarily due to its multi-head self-attention operations. Performance metrics for each model are presented in Table 5.5, with the Hybrid Transformer achieving the largest AUC, accuracy,

precision, recall and F1-Score.

Table 5.5: Summary of performance metrics for all models.

Model	AUC	Accuracy	Precision	Recall	F1-Score
SVM	0.342	54.0%	59.3%	44.7%	0.469
XGBoost	0.619	58.0%	56.1%	63.0%	0.576
LSTM	0.660	58.6%	71.9%	55.0%	0.566
Hybrid Transformer	0.740	67.6%	68.0%	60.4%	0.628

5.3.1 SVM

The SVM classifier yielded an accuracy of 54.0%, a precision of 59.3%, recall of 44.7%, and an F1-score of 0.469. The mean area under the ROC curve (AUC) was 0.342, computed from the averaged ROC curve across five-fold Group K-Fold validation folds (Figure 5.4, right). The cumulative confusion matrix across folds (Figure 5.4, left) showed 10 true positives, 17 true negatives, 14 false negatives, and 9 false positives.

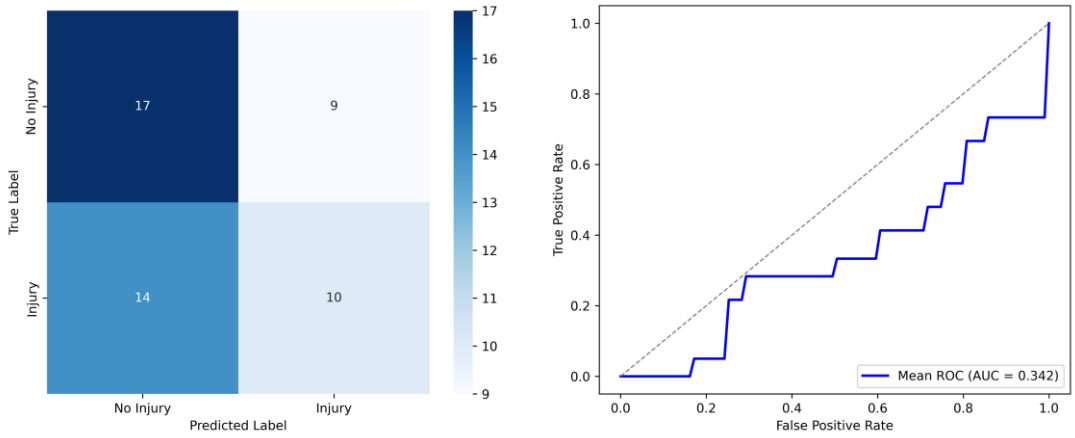

Figure 5.4: (Left) Confusion matrix aggregated across all folds from five-fold Group K-Fold cross-validation for the SVM classifier, with true labels on the vertical axis and predicted labels on the horizontal axis. (Right) Mean ROC curve computed by averaging the true positive rates (TPR) across interpolated false positive rate (FPR) values for each fold (AUC = 0.342).

5.3.2 XGBoost

The XGBoost model achieved an overall accuracy of 58.0%, with a precision of 56.1%, recall of 63.0%, and an F1-score of 0.576. The mean area under the ROC curve (AUC) was 0.619, based

on the average of ROC curves across five-fold Group K-Fold validation folds (Figure 5.5, right). The cumulative confusion matrix (Figure 5.5, left) showed 14 true negatives, 15 true positives, 12 false positives, and 9 false negatives.

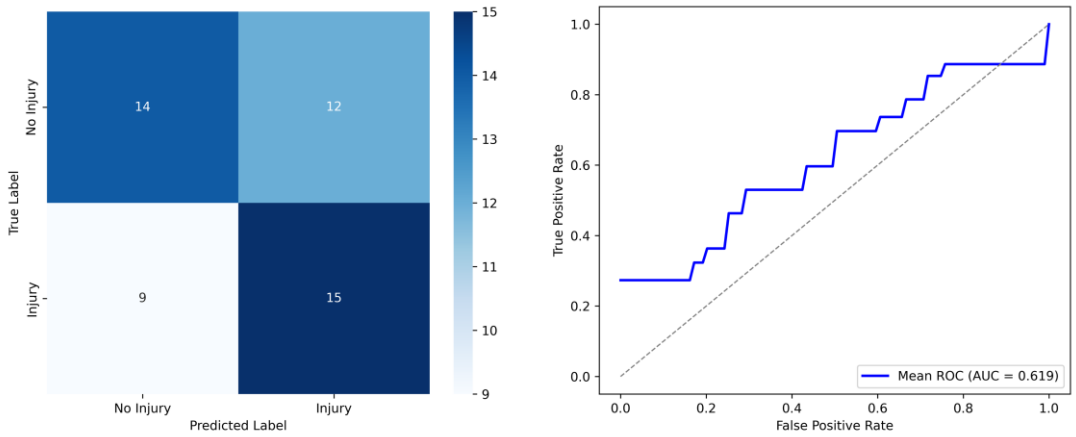

Figure 5.5: (Left) Cumulative confusion matrix for the XGBoost model aggregated across five Group K-Fold validation folds, with true labels on the vertical axis and predicted labels on the horizontal axis. (Right) Mean ROC curve computed by averaging the true positive rates (TPR) across interpolated false positive rate (FPR) values for each fold (AUC=0.619).

The top five most important features were identified for each cross-validation fold using SHAP analysis. Among these, four features consistently appeared across multiple folds: Right leg sway area with eyes open during T-balance (SA_EO_Right: 5 out of 5 folds), Veo (5/5), Complex reaction time lower limbs (CRT_LL: 2/5), and right leg vertical jump absolute peak power (VJ_PP_R: 2/5). Figure 5.6 presents the SHAP summary plot for a representative fold, illustrating the relative impact and directionality of the top five features on model predictions.

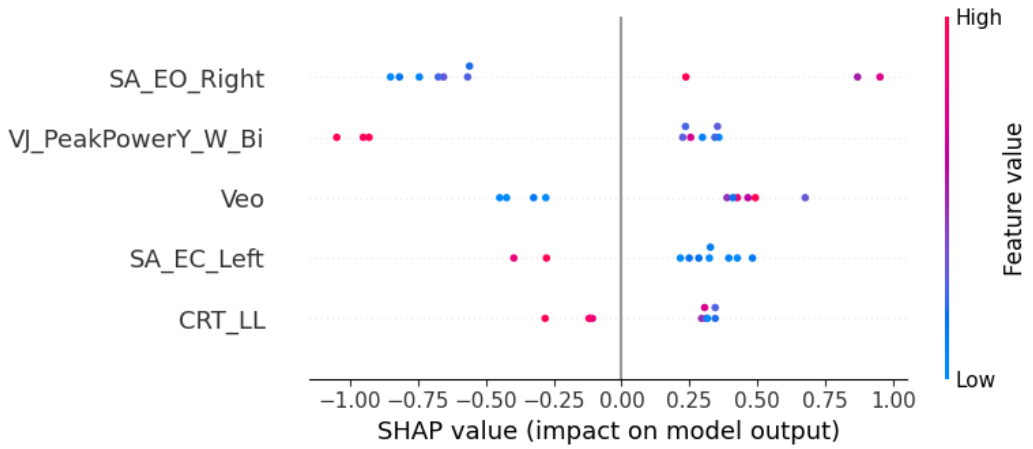

Figure 5.6: XGBoost model's SHAP values for the five most important features in a single cross-validation fold, ranked from top to bottom. SA_EO_Right = Right leg sway area with eyes open (T-balance); VJ_PeakPowerY_W_Bi = Bilateral vertical jump peak power; Veo = Intense Moments During Match Play; SA_EC_Left = Left leg sway area with eyes closed (T-balance); CRT_LL = Complex reaction time lower limbs. Each dot represents one participant's SHAP value for that feature, positive values push the model toward "injury" and negative values toward "no injury", and is colored by the original feature value (blue = low, red = high).

5.3.3 LSTM

The LSTM model yielded a mean AUC of 0.660 (Figure 5.7 right). The model achieved an accuracy of 58.6%, with a precision of 71.9%, recall of 55.0%, and an F1-score of 0.566. The cumulative confusion matrix (Figure 5.7 left) indicated that the model correctly classified 12 of 23 non-injured participants and 15 of 24 injured participants.

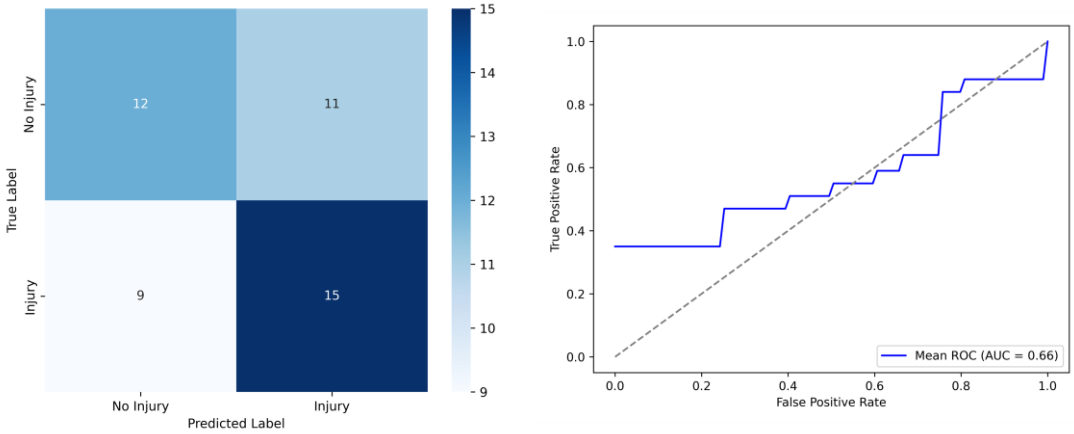

Figure 5.7: (Left) Cumulative confusion matrix aggregated across all folds from five-fold Group K-Fold cross-validation for the LSTM model, with true labels on the vertical axis and predicted

labels on the horizontal axis. (Right) Mean ROC curve computed by averaging the true positive rates (TPR) across interpolated false positive rate (FPR) values for each fold (AUC = 0.660).

5.3.4 Hybrid Transformer

The Hybrid Transformer model achieved a mean AUC of 0.74 (Figure 5.8 right). The model attained an accuracy of 67.6%, a precision of 68.0%, recall of 60.4%, and an F1-score of 0.628. The confusion matrix (Figure 5.8 left) showed that 17 of 23 non-injured participants and 15 of 24 injured participants were correctly identified.

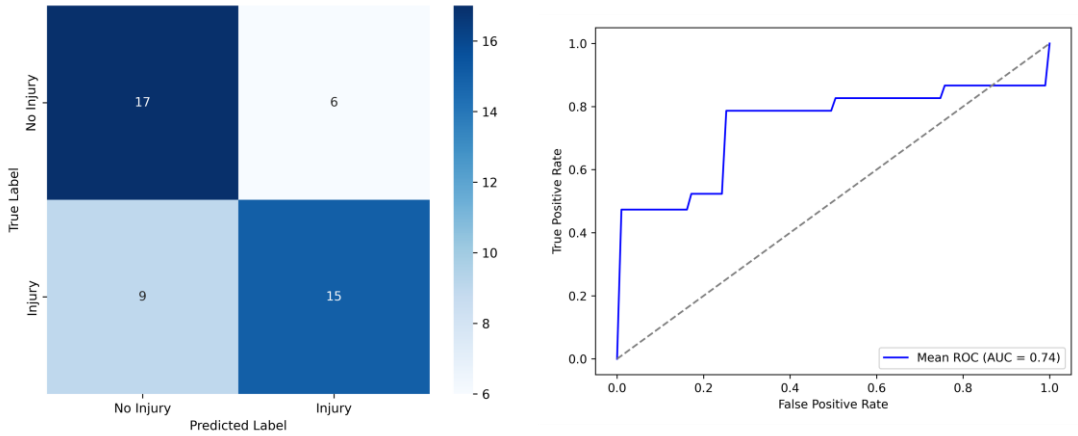

Figure 5.8: (Left) Cumulative confusion matrix aggregated across all folds from five-fold Group K-Fold cross-validation for the Hybrid Transformer model, with true labels on the vertical axis and predicted labels on the horizontal axis. (Right) Mean ROC curve computed by averaging the true positive rates (TPR) across interpolated false positive rate (FPR) values for each fold (AUC = 0.740).

Figure 5.9 displays the task-level attention distributions averaged over 300 frames per trial for each screening task, comparing injured and non-injured groups. The results showed that although overall task-level attention did not significantly differ between groups, notable trends were observed. Injured athletes exhibited elevated attention scores during right CMJ and right TB with eyes closed. In contrast, non-injured athletes showed slightly higher attention during balance tasks (e.g., Y-balance and T-balance).

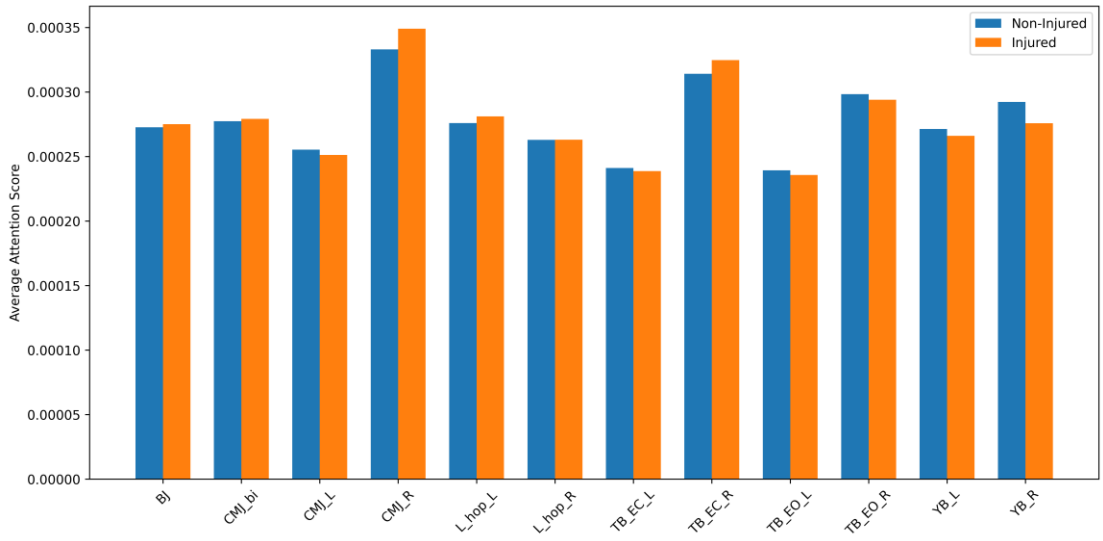

Figure 5.9: Average attention scores (y-axis) across folds for each movement task (x-axis), grouped by injury status (injured vs. non-injured). Higher scores indicate greater relative attention. No significant differences were observed at the task level.

To further localize temporal attention within specific movements, a frame-level attention analysis was performed across all 12 tasks and 300 time-normalized frames. As illustrated in Figure 5.10, injured participants exhibited significantly higher attention during the right-leg landing phase (frames 120-125) and left-leg push-off phase (frames 160-170) of the L-hop task. A similar pattern was observed in the right-leg CMJ, where injured athletes showed elevated attention during each of the three landing events (frames 80-90, 150-160, and 230-240).

In contrast, non-injured participants demonstrated greater attention during balance tasks (e.g., T-Balance and Y-Balance) and bilateral CMJ. Specifically, during right-leg T-Balance with both eyes open and eyes closed, significantly higher attention was allocated during the trunk's return from a horizontal to vertical posture (frames 205-220). In the bilateral CMJ, the non-injured group showed higher attention during the landing phase of the final repetition. Interestingly, although not statistically significant, the injured group exhibited a trend toward greater attention during the forward trunk flexion phase (frames 60-90) of the eyes-closed right T-Balance task.

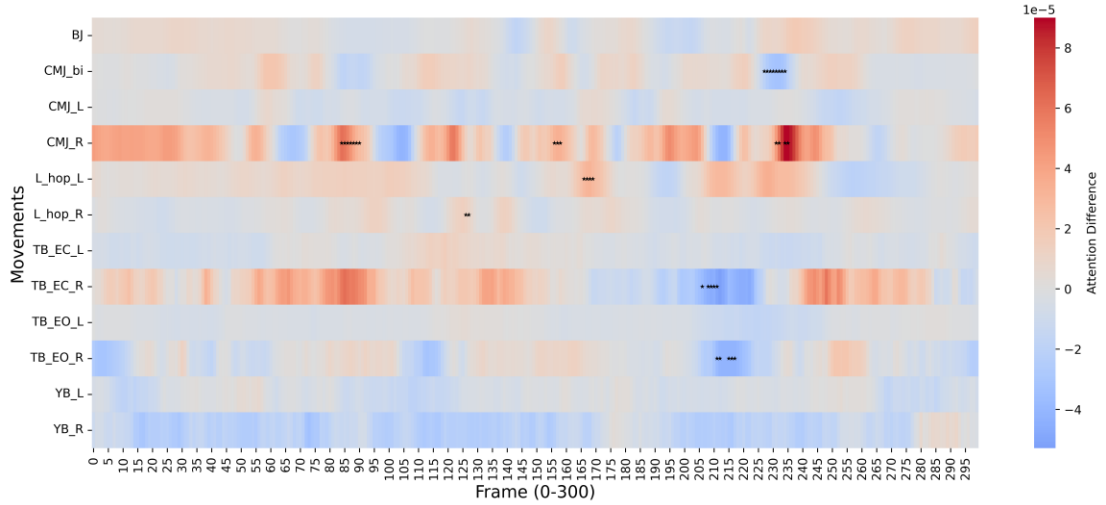

Figure 5.10: Heatmap illustrating frame-level attention differences across 12 movements (vertical axis) and 300 normalized frames (horizontal axis). Red indicates frames where injured participants received higher attention; blue indicates higher attention for non-injured participants. Statistically significant differences ($p < .05$) are marked by asterisks.

At the individual level, Figure 5.11 presents attention heatmaps from a representative injured participant (left) and a non-injured participant (right). These visualizations broadly reflect the group-level frame-wise findings. In the injured participant, attention scores were notably elevated during landing phases across multiple tasks, including the BJ, right-leg CMJ, and left-leg L-hop. In contrast, the non-injured participant exhibited a more evenly distributed attention pattern, with less emphasis on impact-related frames.

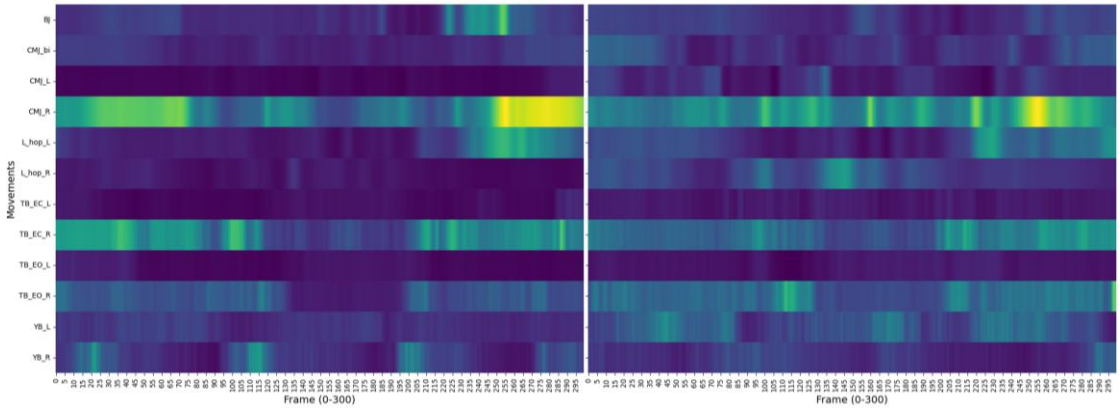

Figure 5.11: Example attention heatmap from the Hybrid Transformer model for two participant who did (left) and did not (right) sustain a non-contact injury. The y-axis represents the 12 movement screening tasks, and the x-axis shows the time-normalized (0 to 300 frames) for each

task. The color intensity reflects the magnitude of attention weights assigned to each frame by the temporal attention pooling layer, with brighter areas indicating greater model attention.

5.4 Discussion

This study evaluated the performance and interpretability of four widely used machine learning models (SVM, XGBoost, LSTM and Hybrid Transformer) for predicting non-contact lower limb injuries in female soccer athletes using multimodal biomechanical data. The results demonstrate that the Hybrid Transformer slightly outperformed traditional (SVM, XGBoost) and deep learning (LSTM) models across most performance metrics, achieving an AUC of 0.740, while also providing clinically meaningful insight through its built-in attention mechanisms.

Injury risk prediction remains a major challenge in soccer due to the multifactorial and non-linear nature of injury mechanisms (Bittencourt et al., 2016; Jarmann, 2023). Although previous work has explored statistical modeling and simpler machine learning algorithms (e.g., logistic regression, decision trees), these methods often require extensive feature engineering and struggle to capture dynamic, interdependent, and task-specific biomechanical information (Emery & Pasanen, 2019; Musat et al., 2024). Most importantly, from an injury prevention perspective in clinical settings, identifying injury risk based solely on unmodifiable or less modifiable factors, such as injury history or training load, which are commonly used inputs in many machine learning models, provides limited actionable insight for intervention. Unlike modifiable factors, they cannot guide specific training or rehabilitation strategies to mitigate risk.

The results support the hypothesis that the Hybrid Transformer would outperform the other models. The SVM classifier yielded the lowest performance among all models tested, with a mean AUC of 0.342. This suggests that the SVM struggled to capture the complex, non-linear relationships inherent in the biomechanical data. This aligns with prior findings where SVMs showed reduced efficacy on temporal or highly non-linear datasets due to their rigid decision boundaries and limited feature interaction modeling (Calderón-Díaz et al., 2023; Ribeiro et al., 2016). Moreover, while linear kernels may offer greater interpretability, they oversimplify the underlying patterns, and radial basis function kernels increase model complexity without native

interpretability.

The XGBoost model achieved moderate performance (AUC = 0.619), consistent with prior studies where XGBoost has been successfully applied to large, structured datasets for injury prediction using game-derived load metrics, such as distance covered and high-speed running (Gabbett, 2016; Leckey et al., 2025). However, in this study, which used laboratory-based biomechanical data, XGBoost likely lacked the temporal modeling capabilities to extract nuanced phase-specific patterns. While post-hoc interpretation using SHAP provided valuable insights, identifying SA_EO_Right, Veo, CRT_LL, and VJ_PP_Right as consistent contributors. These suggest that poorer balance with eyes closed, longer intense game exposure, slower complex reaction time of the lower limb, and lower absolute peak power during vertical jump may be associated with increased injury risk. This approach still required manual feature design and cannot reveal when in a movement sequence the injury risk features arise (Lundberg & Lee, 2017).

The LSTM model modestly outperformed XGBoost (AUC = 0.660), likely due to its inherent ability to model temporal sequences (Hochreiter & Schmidhuber, 1997). However, its recall was lower (55.0%), indicating limited ability to correctly identify injured participants. LSTMs are sensitive to hyperparameters, prone to vanishing gradients, and require sequential data processing, which increases training complexity and hinders interpretability (Che et al., 2018). Although SHAP has been adapted to RNNs (Zeng et al., 2022), such methods are computationally expensive and lack native task-level explainability.

The Hybrid Transformer demonstrated the strongest performance (AUC = 0.740) across most evaluation metrics and additionally offered direct interpretability through its built-in attention mechanism. While similar interpretability techniques (e.g., attention layers or SHAP) can be applied to LSTM models (Zeng et al., 2022), attention-based analysis was implemented only in the Hybrid Transformer pipeline due to its native temporal attention pooling architecture. This facilitated direct extraction of frame-level attention scores without additional modifications. Attention analysis revealed significantly different temporal focus between injured and non-injured athletes, particularly during high-demand tasks such as L-hop and unilateral countermovement

jumps. These findings align with prior literature linking such tasks with anterior cruciate ligament (ACL) injury risk, due to their demand for neuromuscular control and joint stability (Anicic et al., 2023; Kotsifaki et al., 2023; Siesmaa et al., 2022). Injured athletes exhibited greater attention weights during landing and push-off phases during right CMJ and left L-hop, suggesting that the model learned to prioritize frames associated with dynamic instability or compensatory movement strategies.

Although no task-level differences were statistically significant, frame-level analysis captured critical between-group divergences, emphasizing the Transformer's capacity to recognize subtle, phase-specific biomechanical patterns. This granular interpretability bridges a key gap in sports injury prediction, providing clinicians not just with binary predictions, but with interpretable visualizations of "when" and "why" an athlete may be at risk (Schilling et al., 2024). Such information can guide targeted interventions aimed at modifying risky movement patterns before injuries occur.

Additionally, the Hybrid Transformer architecture facilitates parallel sequence processing and multi-head self-attention, enabling the model to capture interactions across joints and movement segments simultaneously (Vaswani et al., 2017; Zheng et al., 2021). Unlike RNNs or LSTMs, which propagate information sequentially, Transformers allow for distributed representation of long-range biomechanical dependencies, such as compensations between hip and ankle or delayed landing responses across limbs (Dorschky et al., 2020; Kotsifaki et al., 2023).

Beyond model performance, this study also highlights the potential for transformer-based models to inform future biomechanical inquiry and clinical implementation. With larger, curated datasets, attention maps could be used to identify not only high-risk phases of movement but also joint- or axis-specific loading patterns (e.g., knee ab-/adduction moments), aiding early identification of injury-prone mechanics.

5.4.1 Limitations

Several limitations must be acknowledged. First, the small sample size (N = 47) limits the generalizability of results and increases the risk of overfitting, despite the use of Group K-fold

cross-validation and weighted loss functions. Second, the cohort consisted solely of collegiate female soccer players, potentially limiting applicability to other populations (e.g., youth or elite athletes). Third, while the temporal model (Hybrid Transformer) focused on modifiable kinematic features to inform preventive strategies, static physiological factors, such as hormone levels or joint laxity, were not included for further discussion. Hormonal variations linked to the menstrual cycle have been implicated in ACL injury risk (Reyes-Laredo et al., 2024) and should be considered in future work to improve personalization.

Additionally, while static features were incorporated into the Hybrid Transformer via an auxiliary MLP encoder, we chose not to integrate them with the XGBoost pipeline. This decision was based on their limited contribution to predictive performance (as revealed by SHAP analysis), and to avoid potential overfitting given the modest sample size. More importantly, this study does not aim to declare a universally superior model, but rather to compare the relative strengths and workflows of different modeling paradigms, kernel-based (SVM), tree-based (XGBoost), sequence-based (LSTM), and attention-based (Hybrid Transformer), each operating on appropriately preprocessed versions of the same dataset. Future work could explore hybrid ensemble approaches (e.g., combining deep temporal encoders with structured feature learners) to unify performance and interpretability across modalities.

The screening tasks used in this study were selected for their biomechanical relevance and practicality but may not be the most predictive for all injury types. Further exploration of different task combinations, as well as in-season biomechanical adaptations, could enhance model precision. Moreover, integrating in-game performance metrics or sport-specific time-series data, such as high-speed running or cutting, could improve generalizability, as such data better reflect real-world demands (Boone et al., 2021; Satvedi & Pyne, 2022).

Despite their potential, the application of transformer-based models in predicting non-contact injuries in female soccer remains largely unexplored. Previous work has primarily focused on male cohorts, retrospective electronic medical record (EMR) data, or single-sensor input (Mundt et al., 2020; Nassis et al., 2023), leaving a significant gap in applying advanced ML models to

multimodal screening data in high-risk female populations. Lastly, despite their promise, transformer models require substantial data and computation. Successful implementation in clinical or team settings will depend on simplified deployment pipelines and the availability of standardized datasets.

5.5 Conclusion

Traditional machine learning models such as SVM and XGBoost benefit from simplicity, computational efficiency, and straightforward implementation, making them suitable baseline choices for injury prediction. However, they rely heavily on manual feature engineering, a process which can be both time-consuming and influenced by personal expertise or bias. Deep learning approaches like LSTM and the Hybrid Transformer, on the other hand, reduce dependence on manual feature selection, thus minimizing personal interpretation biases. Nonetheless, these models demand considerable computational resources, particularly for extensive hyperparameter tuning and when applied to large datasets, potentially limiting their practical application in certain sports contexts.

Regarding interpretability and practical utility in sports settings, the XGBoost model complemented by SHAP analysis provides valuable insights into the relative importance of both modifiable (e.g., reaction time) and unmodifiable (e.g., injury history) factors contributing to injury risk. By contrast, the Hybrid Transformer model places greater emphasis on modifiable risk factors by leveraging built-in temporal attention mechanisms. Specifically, it identifies when during specific movements athletes may be at risk, thus enabling coaches and therapists to develop personalized, targeted neuromuscular training or rehabilitation interventions.

Collectively, this study demonstrates that Hybrid Transformer models can effectively predict non-contact lower limb injuries in female soccer athletes from biomechanical screening data and provide meaningful task- and frame-level interpretation. Clinically, this represents a significant advancement toward proactive, data-informed injury prevention. Instead of relying solely on subjective expert assessment or aggregated screening scores, practitioners can leverage objective

model-derived insights to pinpoint specific vulnerable movement phases and tailor interventions accordingly. For example, athletes identified as having increased injury risk during single-leg landings can benefit from targeted neuromuscular retraining or feedback-based training protocols.

With continued methodological refinement and access to larger, multi-season datasets, such modeling tools hold promises for shifting injury management strategies from reactive assessments toward proactive, real-time monitoring and personalized intervention. This shift has the potential to significantly reduce the injury burden and extend athletic careers in elite sport settings.

5.6 References

Alentorn-Geli, E., Myer, G. D., Silvers, H. J., Samitier, G., Romero, D., Lázaro-Haro, C., & Cugat, R. (2009). Prevention of Non-Contact Anterior Cruciate Ligament Injuries in Soccer Players. Part 1: Mechanisms of Injury and Underlying Risk Factors. *Knee Surgery, Sports Traumatology, Arthroscopy*, *17*(7), 705-729.

Anicic, Z., Janicijevic, D., Knezevic, O. M., Garcia-Ramos, A., Petrovic, M. R., Cabarkapa, D., & Mirkov, D. M. (2023). Assessment of Countermovement Jump: What Should We Report? *Life*, *13*(1), 190.

Bahr, R. (2003). Risk Factors for Sports Injuries - A Methodological Approach. *British Journal of Sports Medicine*, *37*(5), 384-392.

Bai, A., Song, H., Wu, Y., Dong, S., Feng, G., & Jin, H. (2025). Sliding-Window CNN + Channel-Time Attention Transformer Network Trained with Inertial Measurement Units and Surface Electromyography Data for the Prediction of Muscle Activation and Motion Dynamics Leveraging IMU-Only Wearables for Home-Based Shoulder Rehabilitation. *Sensors 2025, Vol. 25, Page 1275*, *25*(4), 1275.

Bennett, H., Davison, K., Arnold, J., Slattery, F., Martin, M., & Norton, K. (2017). Multicomponent Musculoskeletal Movement Assessment Tools: A Systematic Review and Critical Appraisal of Their Development and Applicability to Professional Practice. *Journal of Strength and Conditioning Research*, *31*(10), 2903-2919.

Bittencourt, N. F. N., Meeuwisse, W. H., Mendonça, L. D., Nettel-Aguirre, A., Ocarino, J. M., & Fonseca, S. T. (2016). Complex Systems Approach for Sports Injuries: Moving from Risk Factor Identification to Injury Pattern Recognition - Narrative Review and New Concept. *British Journal of Sports Medicine*, *50(21),* 1309-1314.

Boone, J. B., Vandusseldorp, T. A., Feito, Y., & Mangine, G. T. (2021). Relationships Between Sprinting, Broad Jump, and Vertical Jump Kinetics Are Limited in Elite, Collegiate Football Athletes. *Journal of Strength and Conditioning Research*, *35*(5), 1306-1316.

Bulow, A., Anderson, J. E., Leiter, J. R., MacDonald, P. B., & Peeler, J. (2019). The Modified Star Excursion Balance and Y-Balance Test Results Differ When Assessing Physically Active Healthy Adolescent Females. *International Journal of Sports Physical Therapy*, *14*(2), 192-203.

Calderón-Díaz, M., Silvestre Aguirre, R., Vásconez, J. P., Yáñez, R., Roby, M., Querales, M., & Salas, R. (2023). Explainable Machine Learning Techniques to Predict Muscle Injuries in Professional Soccer Players through Biomechanical Analysis. *Sensors 2024, Vol. 24, Page 119*, *24*(1), 119.

Che, Z., Purushotham, S., Cho, K., Sontag, D., & Liu, Y. (2018). Recurrent Neural Networks for Multivariate Time Series with Missing Values. *Scientific Reports*, *8*(1), 1-12.

Chehrehrazi, M., Sanjari, M. A., Mokhtarinia, H. R., Jamshidi, A. A., Maroufi, N., & Parnianpour, M. (2017). Goal Equivalent Manifold Analysis of Task Performance in Non-specific LBP and Healthy Subjects during Repetitive Trunk Movement: Effect of Load, Velocity, Symmetry. *Human Movement Science*, *51*, 72-81.

Chen, T., & Guestrin, C. (2016). XGBoost: A Scalable Tree Boosting System. *Proceedings of the ACM SIGKDD International Conference on Knowledge Discovery and Data Mining*, *13-17-August-2016*, 785-794.

Clagg, S., Paterno, M. V., Hewett, T. E., & Schmitt, L. C. (2015). Performance on the Modified Star Excursion Balance Test at the Time of Return to Sport Following Anterior Cruciate Ligament Reconstruction. *Journal of Orthopaedic & Sports Physical Therapy*, *45*(6), 444-452.

Cortes, C., Vapnik, V., & Saitta, L. (1995). Support-vector Networks. *Machine Learning 1995 20:3*, *20*(3), 273-297.

Cusumano, J. P., & Dingwell, J. B. (2013). Movement Variability Near Goal Equivalent Manifolds: Fluctuations, Control, and Model-based Analysis. *Human Movement Science*, *32*(5), 899-923.

de la Motte, S. J., Lisman, P., Gribbin, T. C., Murphy, K., & Deuster, P. A. (2019). Systematic Review of the Association Between Physical Fitness and Musculoskeletal Injury Risk: Part 3 - Flexibility, Power, Speed, Balance, and Agility. *Journal of Strength and Conditioning Research*, *33*(6), 1723-1735.

Dehghani, A., Glatard, T., & Shihab, E. (2019). *Subject Cross Validation in Human Activity Recognition*.

Dorschky, E., Nitschke, M., Martindale, C. F., van den Bogert, A. J., Koelewijn, A. D., & Eskofier, B. M. (2020). CNN-Based Estimation of Sagittal Plane Walking and Running Biomechanics from Measured and Simulated Inertial Sensor Data. *Frontiers in Bioengineering and Biotechnology*, *8*, 528071.

Emery, C. A., & Pasanen, K. (2019). Current trends in sport injury prevention. *Best Practice & Research Clinical Rheumatology*, *33*(1), 3-15.

Enright, K., Green, M., Hay, G., & Malone, J. J. (2020). Workload and Injury in Professional Soccer Players: Role of Injury Tissue Type and Injury Severity. *International Journal of Sports Medicine*, *41*(2), 89-97.

Furuki, D., & Takiyama, K. (2018). Detection of Task-relevant and Task-irrelevant Motion Sequences: Application to Motor Adaptation in Goal-directed and Whole-body Movements. *BioRxiv*, *April*, 339648.

Gabbett, T. J. (2016). The Training - Injury Prevention Paradox: Should Athletes Be Training Smarter and Harder? *British Journal of Sports Medicine*, *50*(5), 273-280.

Gebert, A., Gerber, M., Pühse, U., Gassmann, P., Stamm, H., & Lamprecht, M. (2018). Injuries in Formal and Informal Non-Professional Soccer - An Overview of Injury Context, Causes, And Characteristics. *European Journal of Sport Science*, *18*(8), 1168-1176.

Gers, F. A., Schmidhuber, J., & Cummins, F. (2000). Learning to Forget: Continual Prediction with LSTM. *Neural Computation*, *12*(10), 2451- 2471.

Ghasemzadeh, H., Amini, N., Saeedi, R., & Sarrafzadeh, M. (2015). Power-Aware Computing in Wearable Sensor Networks: An Optimal Feature Selection. *IEEE Transactions on Mobile Computing*, *14*(4), 800-812.

González-Fernández, F. T., Martínez-Aranda, L. M., Falces-Prieto, M., Nobari, H., & Clemente, F. M. (2022). Exploring The Y-Balance-Test Scores and Inter-Limb Asymmetry in Soccer Players: Differences Between Competitive Level and Field Positions. *BMC Sports Science, Medicine and Rehabilitation*, *14*(1), 1-13.

Gulgin, H., & Hoogenboom, B. (2014). The Functional Movement Screening (FMS)TM: An Inter-Rater Reliability Study Between Raters of Varied Experience. *International Journal of Sports Physical Therapy*, *9*(1), 14-20.

Han, R., Qi, F., Wang, H., & Yi, M. (2024). Innovative Machine Learning Approach for Analysing Biomechanical Factors in Running-Related Injuries. *Molecular & Cellular Biomechanics*, *21*(3), 530-530.

Hochreiter, S., & Schmidhuber, J. (1997). Long Short-Term Memory. *Neural Computation*, *9*(8), 1735-1780.

Hsu, C. W., Chang, C. C., & Lin, C. J. (2009). *A Practical Guide to Support Vector Classification*.

Huang, Y., Huang, S., Wang, Y., Li, Y., Gui, Y., & Huang, C. (2022). A Novel Lower Extremity Non-Contact Injury Risk Prediction Model Based on Multimodal Fusion and Interpretable Machine Learning. *Frontiers in Physiology*, *13*, 937546.

Jarmann, A. L. (2023). *Identifying Injury Risk Factors for Elite Soccer Teams Using Survival Analysis*.

Jauhiainen, S., Kauppi, J. P., Krosshaug, T., Bahr, R., Bartsch, J., & Äyrämö, S. (2022). Predicting ACL Injury Using Machine Learning on Data from an Extensive Screening Test Battery of

880 Female Elite Athletes. *The American Journal of Sports Medicine*, *50*(11), 2917.

Kotsifaki, R., Sideris, V., King, E., Bahr, R., & Whiteley, R. (2023). Performance and Symmetry Measures During Vertical Jump Testing at Return to Sport After ACL Reconstruction. *British Journal of Sports Medicine*, *57*(20), 1304-1310.

Lawrence, D. W., Comper, P., & Hutchison, M. G. (2016). Influence of Extrinsic Risk Factors on National Football League Injury Rates. *Orthopaedic Journal of Sports Medicine*, *4*(3), 232596711663922.

Leckey, C., Van Dyk, N., Doherty, C., Lawlor, A., & Delahunt, E. (2025). Machine Learning Approaches to Injury Risk Prediction in Sport: A Scoping Review with Evidence Synthesis. *British Journal of Sports Medicine*, *59*(7), 491-500.

Lundberg, S. M., & Lee, S. I. (2017). A Unified Approach to Interpreting Model Predictions. *Advances in Neural Information Processing Systems*, *2017-December*, 4766-4775.

Markwick, W. J., Bird, S. P., Tufano, J. J., Seitz, L. B., & Haff, G. G. (2015). The Intraday Reliability of the Reactive Strength Index Calculated from a Drop Jump in Professional Men's Basketball. *International Journal of Sports Physiology and Performance*, *10*(4), 482-488.

Mavor, M. P., Chan, V. C. H., Gruevski, K. M., Bossi, L. L. M., Karakolis, T., & Graham, R. B. (2023). Assessing the Soldier Survivability Tradespace Using a Single IMU. *IEEE Access*, *11*, 69762-69772.

Mavor, M. P., Mir-Orefice, A., Chan, V. C. H., Bose, G., Maclean, H. J., Mestre, T., Grimes, D., Freedman, M. S., & Graham, R. B. (2025). Validation Of an Instrumented Shoe Insole Framework for Analyzing Spatiotemporal Gait Metrics in Healthy and Neurodegenerative Populations. *MedRxiv*, 2025.05.06.25326646.

McCall, A., Carling, C., Davison, M., Nedelec, M., Le Gall, F., Berthoin, S., & Dupont, G. (2015). Injury Risk Factors, Screening Tests and Preventative Strategies: A Systematic Review of the Evidence That Underpins the Perceptions and Practices Of 44 Football (Soccer) Teams from Various Premier Leagues. In *British Journal of Sports Medicine* (Vol. 49, Issue 9, pp. 583-589).

McKeown, I., Taylor-McKeown, K., Woods, C., & Ball, N. (2014). Athletic Ability Assessment: A Movement Assessment Protocol for Athletes. *International Journal of Sports Physical Therapy*, *9*(7), 862-873.

Meng, L., & Qiao, E. (2023). Analysis And Design of Dual-Feature Fusion Neural Network for Sports Injury Estimation Model. *Neural Computing and Applications*, *35*(20), 14627-14639.

Mundt, M., Koeppe, A., David, S., Bamer, F., Potthast, W., & Markert, B. (2020). Prediction Of Ground Reaction Force and Joint Moments Based on Optical Motion Capture Data During Gait. *Medical Engineering & Physics*, *86*, 29-34.

Murdoch, W. J., Singh, C., Kumbier, K., Abbasi-Asl, R., & Yu, B. (2019). Interpretable Machine

Learning: Definitions, Methods, And Applications. *Proceedings of the National Academy of Sciences of the United States of America*, *116*(44), 22071-22080.

Musat, C. L., Mereuta, C., Nechita, A., Tutunaru, D., Voipan, A. E., Voipan, D., Mereuta, E., Gurau, T. V., Gurău, G., & Nechita, L. C. (2024). Diagnostic Applications of AI in Sports: A Comprehensive Review of Injury Risk Prediction Methods. *Diagnostics*, *14*(22), 2516.

Myer, G. D., Ford, K. R., Khoury, J., Succop, P., & Hewett, T. E. (2010). Development and Validation of a Clinic-Based Prediction Tool to Identify Female Athletes at High Risk for Anterior Cruciate Ligament Injury. *The American Journal of Sports Medicine*, *38*(10), 2025.

Nassis, G. P., Verhagen, E., Brito, J., Figueiredo, P., & Krustrup, P. (2023). A Review of Machine Learning Applications in Soccer with An Emphasis on Injury Risk. *Biology of Sport*, *40*(1), 233-239.

Onate, J. A., Dewey, T., Kollock, R. O., Thomas, K. S., Van Lunen, B. L., Demaio, M., & Ringleb, S. I. (2012). Real-Time Intersession and Interrater Reliability of The Functional Movement Screen. *Journal of Strength and Conditioning Research*, *26*(2), 408-415.

Plisky, P. J., Gorman, P. P., Butler, R. J., Kiesel, K. B., Underwood, F. B., & Elkins, B. (2009). The Reliability of an Instrumented Device for Measuring Components of the Star Excursion Balance Test. *North American Journal of Sports Physical Therapy: NAJSPT*, *4*(2), 92.

Randell, R. K., Clifford, T., Drust, B., Moss, S. L., Unnithan, V. B., De Ste Croix, M. B. A., Datson, N., Martin, D., Mayho, H., Carter, J. M., & Rollo, I. (2021). Physiological Characteristics of Female Soccer Players and Health and Performance Considerations: A Narrative Review. *Sports Medicine 2021 51:7*, *51*(7), 1377-1399.

Reyes-Laredo, F., Pareja-Blanco, F., López-Lluch, G., & Rodríguez-Bies, E. (2024). The Evolution of Physical Performance throughout an Entire Season in Female Football Players. *Sports 2024, Vol. 12, Page 52*, *12*(2), 52.

Ribeiro, M. T., Singh, S., & Guestrin, C. (2016). "Why Should I Trust You?" Explaining The Predictions of Any Classifier. *Proceedings of the ACM SIGKDD International Conference on Knowledge Discovery and Data Mining*, *13-17-August-2016*, 1135-1144.

Robotti, G., Draghi, F., Bortolotto, C., & Canepa, M. G. (2020). Ultrasound Of Sports Injuries of The Musculoskeletal System: Gender Differences. In *Journal of Ultrasound* (Vol. 23, Issue 3, pp. 279-285).

Satvedi, A., & Pyne, R. (2022). Injury Prediction for Soccer Players Using Machine Learning. *International Journal of Sport and Health Sciences*, *16*(3), 21-27.

Schilling, A., Anurathan, J., Mühlberger, J., Gerschner, F., Rössle, M., Theissler, A., & Klaiber, M. (2024). Querying Football Matches for Event Data: Towards Using Large Language Models. *Lecture Notes in Computer Science (Including Subseries Lecture Notes in Artificial Intelligence and Lecture Notes in Bioinformatics)*, *14794 LNCS*, 216-227.

Sha, Z., Zhou, Z., & Dai, B. (2021). Analyses of Countermovement Jump Performance in Time and Frequency Domains. *Journal of Human Kinetics*, *78*(1), 41.

Siesmaa, E., Twomey, D., Needham, C., & Herrington, L. (2022). Cutting Movement Assessment Scores during Anticipated and Unanticipated 90-Degree Sidestep Cutting Manoeuvres within Female Professional Footballers. *Sports 2022, Vol. 10, Page 128*, *10*(9), 128.

Smith, H. C., Vacek, P., Johnson, R. J., Slauterbeck, J. R., Hashemi, J., Shultz, S., & Beynnon, B. D. (2012). Risk Factors for Anterior Cruciate Ligament Injury: A Review of the Literature-Part 2: Hormonal, Genetic, Cognitive Function, Previous Injury, and Extrinsic Risk Factors. *Sports Health* (Vol. 4, Issue 2, pp. 15-161).

Sokolova, M., & Lapalme, G. (2009). A Systematic Analysis of Performance Measures for Classification Tasks. *Information Processing & Management*, *45*(4), 427-437.

Vaswani, A., Shazeer, N., Parmar, N., Uszkoreit, J., Jones, L., Gomez, A. N., Kaiser, Ł., & Polosukhin, I. (2017). Attention Is All You Need. *Advances in Neural Information Processing Systems*, *2017-December*, 5999-6009.

Wen, B. (2025). A Multimodal Transformer Framework with Biomechanical Constraints for Injury Prediction and Human Motion Analysis. *Journal of Computational Methods in Sciences and Engineering*.

Zeng, Z., Tang, X., Liu, Y., He, Z., & Gong, X. (2022). Interpretable Recurrent Neural Network Models for Dynamic Prediction of The Extubation Failure Risk in Patients with Invasive Mechanical Ventilation in The Intensive Care Unit. *BioData Mining*, *15*(1).

Zheng, C., Zhu, S., Mendieta, M., Yang, T., Chen, C., & Ding, Z. (2021). 3D Human Pose Estimation with Spatial and Temporal Transformers. *Proceedings of the IEEE International Conference on Computer Vision*, 11636-11645.

Chapter 6. Study 3: Evaluating the Influence of Two-Camera View Configurations on Markerless 3D Joint Angle Estimation Across Athletic Movements.

*Submitted to *Journal of Sports Biomechanics**

Xiong Zhao[1], Ryan B. Graham[1]

[1]*School of Human Kinetics, Faculty of Health Sciences, University of Ottawa, Ottawa, Ontario, Canada*

Abstract

Objectives: This study aimed to validate 2-camera markerless motion capture pipelines for estimating lower-limb joint kinematics in female varsity soccer athletes and to identify optimal camera configurations for practical deployment in applied sports settings.

Methods: Twenty-three female soccer athletes performed a series of movement screening tasks, including bilateral squats, countermovement jumps, broad jumps, lateral hops, and Y-balance tests. Movements were simultaneously recorded using an 8-camera markerless motion capture system (Theia3D), serving as the 3D reference. Each pairwise combination of the eight cameras (28 total configurations) was processed using a custom Pose2Sim pipeline to compute 3D joint angles. Validity was assessed both against the 3D reference system and within the 2-camera combinations using root mean square error (RMSE), mean absolute error (MAE), bias, and coefficient of multiple correlation (CMC).

Results: Joint angles in the sagittal plane, especially hip and knee flexion/extension, consistently showed high accuracy (RMSE < 8°, CMC ≈ 1.00). Conversely, coronal and transverse plane angles showed greater errors (RMSE >10°, CMC <0.60). Combinations from the Front, Back and Right groups, yielded consistently superior performance, while Diagonal or Same-quadrant combinations performed poorly. A consistent offset in hip flexion/extension angles, aligning with

previous findings, and reduced tracking fidelity during limb-crossing tasks (e.g., Y-balance) highlighted specific limitations in camera placement and task selection.

Conclusion: Validated 2-camera markerless motion capture pipelines can reliably estimate lower-limb joint kinematics during functional screening in female athletes, particularly for sagittal-plane movements. Optimal configurations, such as those from the Front and Back groups, provided wider views and greater overlap, resulting in consistently higher accuracy. Configurations with poor angular separation (e.g., same-quadrant or diagonal views) should be avoided, and camera placement below 3 meters is recommended to improve foot tracking and overall system fidelity.

6.1 Introduction

Movement screening has become a foundational component of pre-season evaluation in sports, designed to identify biomechanical risk factors, optimize training strategies, and inform targeted injury prevention efforts. This is especially critical in women's soccer, where athletes face a disproportionately high incidence of musculoskeletal injuries, particularly non-contact anterior cruciate ligament (ACL) injuries, compared to their male counterparts (Gabbett, 2016; Hewett et al., 2005). Addressing this disparity requires screening tools that are not only accessible and efficient but also biomechanically valid and reliable.

Various screening protocols have been developed to assess movement quality, including general assessments like the Functional Movement Screen (Cook et al., 2006) and more sport-specific tools such as jump-landing and dynamic balance tests. However, these tools often exhibit limited reliability, particularly when based on visual observation, resulting in poor inter-rater and intra-rater agreement (Kraus et al., 2014; Teyhen et al., 2015).

To improve the objectivity and sensitivity of movement screening, researchers have increasingly adopted motion capture systems. Traditional marker-based systems provide highly accurate three-dimensional joint kinematics and have played a key role in identifying biomechanical patterns associated with injury risk (Alentorn-Geli et al., 2009; Krosshaug et al.,

2016). However, their widespread use is limited by high costs, technical complexity, and time-consuming setup procedures, restricting their application to controlled laboratory settings.

Recent advancements in computer vision (CV) and deep learning have led to the emergence of markerless motion capture systems, which estimate human pose without the use of reflective markers. These systems offer a substantial reduction in operational demands and have shown strong potential for application in both sports and clinical environments (Needham et al., 2021). Multi-camera markerless systems, such as Theia3D (Theia Markerless Inc., Kingston, ON, Canada), have demonstrated good validity relative to marker-based systems (Kanko et al., 2021). Beyond their high cost, these systems still require synchronized multi-camera setups, precise calibration, and controlled capture conditions, which limits their routine use in team or field settings.

To balance accuracy with practicality, systems such as OpenCap have emerged, leveraging just two smartphone cameras in combination with automated OpenSim-based workflows to estimate joint kinematics (Delp et al., 2007; Uhlrich et al., 2022). These tools significantly reduce setup complexity and cost and have shown promising validity in gait and sport-specific movements when compared to traditional optical motion capture systems (Horsak et al., 2023; Lima et al., 2024; Svetek et al., 2025a; Turner et al., 2024). However, most current pipelines rely on pre-defined camera placements, and few studies have systematically examined how the choice of camera configuration influences 3D joint angle estimation in dynamic, sport-relevant tasks. Additionally, OpenCap requires users to upload video recordings to a cloud-based platform for post-processing, which may not be ideal in settings where data privacy is prioritized. In space-constrained environments such as clinical rooms or smaller training spaces, ideal 2-camera placement may also be unachievable. Pose2Sim offers a flexible alternative by enabling similar processing pipelines to OpenCap while running entirely on local machines, thereby increasing accessibility and data control.

The present study addresses these gaps by validating a 2-camera markerless motion capture pipeline using Pose2Sim for estimating 3D joint kinematics during common movement screening

tasks in female varsity soccer players. Specifically, we evaluated the validity of all 28 possible 2-camera combinations against a validated 8-camera markerless baseline (Theia3D) across a battery of functional tasks, including bilateral squats, jumps, and balance assessments. In addition to comparing each camera combination against the baseline by joint and task, we examined agreement across subgroups defined by camera placement (e.g., front, back, diagonal) to identify which configurations most reliably capture lower-limb joint kinematics during dynamic and quasi-static movement tasks.

It is hypothesized that camera combinations with greater view separation and wider overlap, such as front-back configurations, will yield more accurate joint angle estimations, particularly for movements occurring primarily in the sagittal plane. In contrast, combinations from diagonal or same-quadrant placements are expected to perform less reliably due to limited depth perception and increased occlusion. Furthermore, reduced accuracy is anticipated for joint angles in the frontal and transverse planes, such as hip internal/external rotation and ankle inversion/eversion, where precise 3D tracking is more sensitive to perspective and camera positioning.

6.2 Methods

6.2.1 Participants

Twenty-five female varsity soccer players recruited from the University of Ottawa's women's soccer team, but only twenty-three of them (mean age: 20.40 ± 1.98 years; height: 1.66 ± 0.06 m; mass: 63.31 ± 7.94 kg; BMI: 22.90 ± 2.30) participated the pre-season testing. Participants met the following inclusion criteria: (1) ≥ 18 years of age; (2) able to understand English instructions; (3) fully cleared for athletic participation with no current musculoskeletal injury or concussion; and (4) able to complete 40 bilateral bodyweight squats. This study was approved by the Research Ethics Board at University of Ottawa (file #: H-07-24-10628). Participants were informed of their right to withdraw at any time without consequence, and all data were anonymized prior to analysis to ensure confidentiality.

6.2.2 Protocol

Upon arriving at the laboratory, participants read and signed the informed consent form, and had their leg length, height, and weight measured. Once familiar with the lab and movements, they performed a single trial of T-balance with eyes open and Y-balance bilaterally, one trial of L-hop bilaterally, three repetitions of single-leg and bilateral countermovement jumps, and three broad jumps in a randomized order. After a minimum 5-minute rest, participants completed 35 repetitions of bodyweight squats at 40 beats per minute (BPM) to a metronome (Appendix A). Whole-body kinematics were recorded using an 8-camera markerless motion capture system (Theia Markerless Inc., Kingston, ON, Canada) at sampling frequencies of 60 Hz. The camera configuration, illustrated in Figure 6.1, remained consistent across all testing sessions throughout the season. However, the system was recalibrated prior to each data collection session to ensure measurement accuracy. During the same data collection session, participants also completed two reaction time tasks. These assessments were part of a broader testing battery but are beyond the scope of the present analysis. The full testing protocol, excluding consent form and questionnaire, was repeated at mid- and post-season.

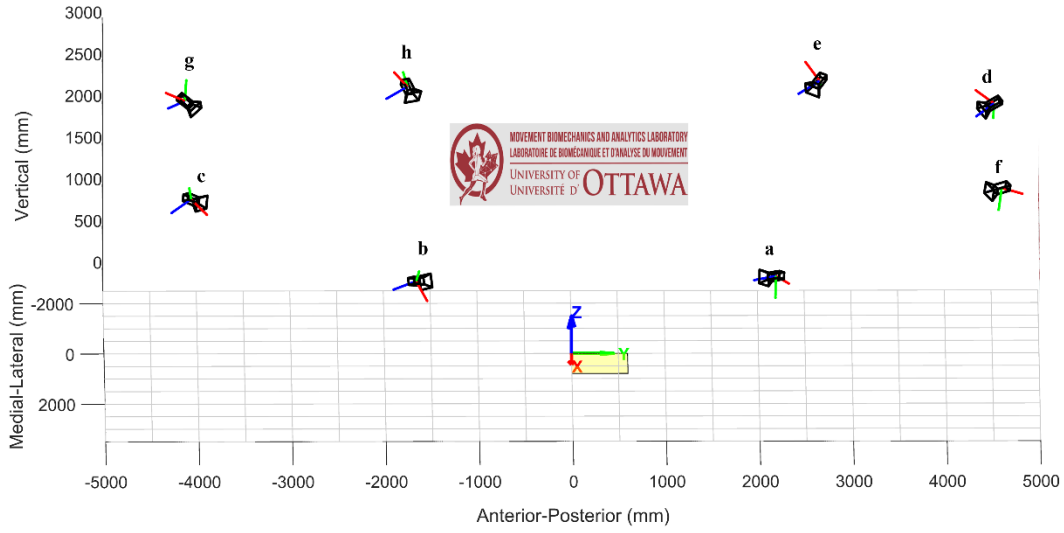

Figure 6.1: Laboratory configuration used in this study. Eight cameras (a-h) are arranged around the capture volume to enable 3D tracking, with their individual coordinate systems shown. The global coordinate system is centered on the force plates (yellow rectangle), with the Y-axis aligned anterior-posterior, X-axis medial-lateral, and Z-axis vertical (mm).

6.2.3 Data processing

For validation purposes, only seven pre-season tasks were analyzed: a single trial of Y-balance (YB) bilaterally, one trial of L-hop bilaterally, one repetition of bilateral countermovement jumps (CMJ), one broad jump (BJ). Bilateral bodyweight squats were chosen for comparison, covering cutting, jumping horizontally and vertically, squatting and balance movements. For the squat task, three repetitions were selected from each 35-rep trial for analysis. Repetitions were trimmed based on vertical center of mass trajectories and synchronized across systems using the start and end of the movement cycle. Broad jump analysis included only one successful trial per participant.

6.2.3.1 Theia3D data

Videos from all eight camera views (Figure 6.2) were transferred and analyzed using Theia 3D (Theia Markerless Inc., Kingston, ON, Canada) and Visual 3D (C-Motion Inc., Germantown, MD) to obtain 3D joint kinematics for each movement task. The built-in musculoskeletal model allows for 3 rotational degrees of freedom (DoF) at the hip and ankle, and 2 at the knee. Final joint kinematics were exported to MATLAB R2019b (The MathWorks Inc., Natick, MA, USA), where they were low-pass filtered using a fourth-order zero-lag Butterworth filter with a 6 Hz cutoff frequency. These processed joint angles served as the reference for validating the 2-camera combinations.

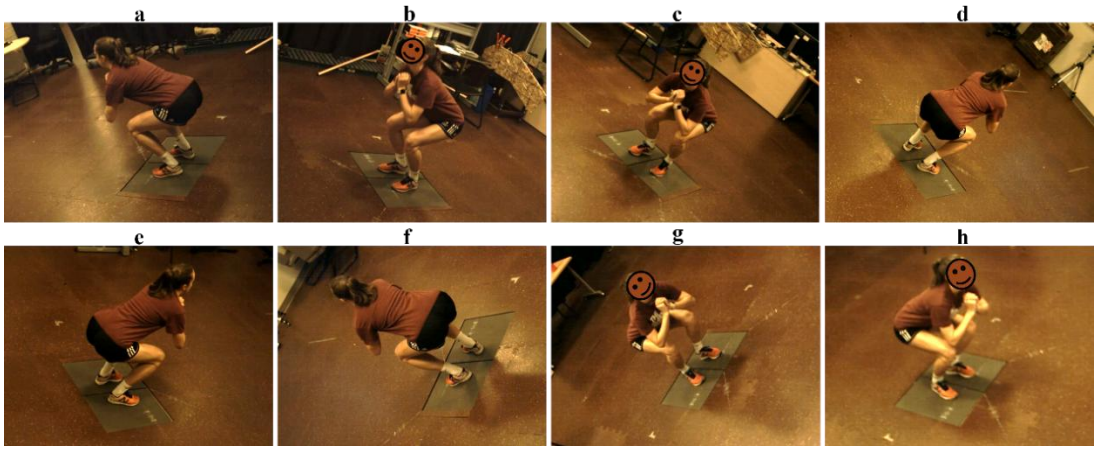

Figure 6.2: Screenshots of the view of each camera (a-h) during squat. The numbering of the view is corresponding to the numbering of the camera in Figure 6.1.

6.2.3.2 Two-camera data

For 2-camera motion capture pipeline, videos from every two of the eight camera views ($C_8^2 = 28\ combinations$) were processed independently using a custom Python 3.10 script on Ubuntu 22.04 LTS. Each combination was treated as an individual input into a Pose2Sim (Pagnon & Kim, 2024) workflow in Figure 6.3.

Within the workflow, first, camera calibration was performed for each 2-camera configuration using the same calibration file used in Theia3D system, with only the two relevant cameras retained per combination. Following calibration, human pose estimation was conducted using RTMPose (Jiang et al., 2023), a 2D keypoint detector. The detected keypoints were triangulated to obtain 3D coordinates using methods implemented in the Pose2Sim framework. To enhance the spatial resolution of the triangulated data, a pretrained Long Short-Term Memory (LSTM) model was applied to predict the positions of 52 anatomically relevant markers from the original 27 sparse keypoints (Falisse et al., 2024). The resulting 3D coordinates were then low-pass filtered using a fourth-order zero-lag Butterworth filter with a 6 Hz cutoff frequency. Filtered marker trajectories were saved in OpenSim-compatible .trc format and imported into OpenSim 4.5 (Delp et al., 2007). A scaled musculoskeletal model was used to perform inverse kinematics with 3 DoF at the hip, 1 DoF at the knee and 2 DoF at the ankle, and the resulting joint angles were calculated for further analysis.

From both systems, joint angles from the following degrees of freedom were extracted for both left and right limbs for comparison: hip (flexion/extension, add-/ab-duction, internal/external rotation), knee (flexion/extension) and ankle (plantar-/dorsi-flexion, inversion/eversion). For each task, joint angle data from both Theia3D (reference) and each of the 28 2-camera combinations were trimmed from beginning and end of the task based on the same criteria and time-normalized to 100 frames to enable temporal alignment and error computation. Trials with unsuccessful pose estimation or triangulation, and incomplete tasks tracking from the 2-camera combinations were excluded.

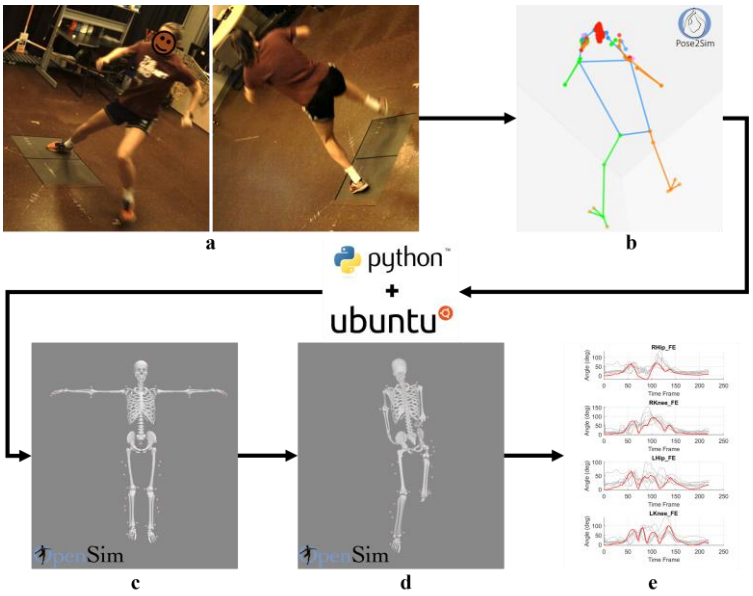

Figure 6.3: Overview of the workflow. (a) 2D image frames from two cameras during a movement task; (b) 3D pose estimation using the Pose2Sim pipeline with RTMPose; (c) scaling of a musculoskeletal model in OpenSim based on the estimated 3D pose; (d, e) computation of joint angles via inverse kinematics.

6.2.4 Statistical analysis

6.2.4.1 Theia3D vs. 2-camera combinations

Root mean square error (RMSE) and mean absolute error (MAE) were calculated for each individual trial, median RMSE and median MAE were calculated to quantify the magnitude of pointwise differences across the time-normalized joint angle trajectories. Median coefficient of multiple correlation (CMC) was calculated to assess waveform similarity across the movement cycle, as it captures both temporal alignment and amplitude patterns. Bland-Altman analyses were also performed on the peak joint angle values to assess systematic bias and define limits of agreement (LoA) between systems. Each of these metrics was computed between each 2-camera combination and the theia3d baseline.

6.2.4.2 Within 2-camera combinations

Median RMSE and CMC values were then extracted for each joint and task. Since no gold-standard reference was available, and the number of combinations varied across groups, pairwise

comparisons were conducted rather than comparisons to a group mean. Specifically, all possible pairwise differences in RMSE were computed within each group to characterize the internal consistency of joint estimates. The median and 25^{th}-75^{th} interquartile range (IQR) of these pairwise RMSEs and CMCs were used to summarize the agreement and correlation. This approach allowed for a more direct evaluation of variability within each group, independent of group size or any central tendency that may be skewed by outliers.

To assess the consistency and agreement between two systems and within the 2-camera combinations, all 28 different 2-camera combinations were divided into 6 subgroups based on camera placement (see supplementary material 1). To interpret the strength of waveform agreement, CMC values were categorized according to established guidelines (Schober & Schwarte, 2018): values below 0.10 were considered negligible, 0.10-0.39 as weak, 0.40-0.69 as moderate, 0.70-0.89 as strong, and values from 0.90-1.00 as very strong. In parallel, RMSE and MAE were used as measures of prediction accuracy, with lower values indicating greater proximity between the joint angle outputs of the 2-camera combinations and those of the reference system (Horsak et al., 2023; Kanko, Laende, Davis, et al., 2021; Wren et al., 2023). All analyses were conducted in MATLAB R2019b (The MathWorks Inc., Natick, MA, USA).

6.3 Results

Out of a total of 4,508 possible trials (23 participants × 7 tasks × 28 two-camera combinations), 3,999 trials (88.71%) were successfully retained for analysis. The remaining 11.29% were excluded due to data quality issues such as tracking failure, or signal dropout in one or both cameras. Table 6.1 presents the percentage of dropped trials across the seven tasks (BJ, CMJ, L-hop, YB, and Squat) for each camera group. Left and right in bilateral tasks, L-hop and YB, were combined into one. For clarity, the term "between systems" refers to comparisons between the Theia3D system and each individual 2-camera combination, while "within combinations" refers to comparisons among different 2-camera configurations. These terms will be used throughout the paper hereafter for consistency and convenience.

Table 6.1: Summary of the dropout rates by camera group and task for 2-camera combinations.

Group	Task				
	BJ	L-hop	YB	Squat	CMJ
Front	2.48%	1.09%	7.61%	0.93%	0.00%
Back	1.09%	4.97%	5.43%	0.00%	0.00%
Left	0.93%	6.21%	4.04%	0.78%	0.16%
Right	1.40%	0.78%	6.68%	0.93%	0.31%
Diagonal	1.09%	2.80%	6.99%	1.32%	0.08%
Same quadrant	1.24%	1.09%	5.59%	0.78%	0.00%

Note: Front/Back: both cameras positioned anteriorly/ posteriorly (left and right); Left/Right: both cameras on the left/right side (front-left/right and back-left/right); Diagonal: two cameras placed diagonally; Same quadrant: both cameras positioned in the same quadrant (e.g., both front-left). BJ: Broad Jump, YB: Y-balance, CMJ: Countermovement Jump.

6.3.1 Between systems

6.3.1.1 By joint

When averaging across participants, task and combinations, joint angle estimation performance varies depending on the anatomical plane of motion and the combination. In general, joint angles in the sagittal plane, including flexion/extension at the hip and knee, as well as ankle plantarflexion/dorsiflexion, demonstrated the lowest RMSE, MAE, and Bias values. However, hip flexion/extension consistently showed a substantial constant offset across all tasks, with RMSE ranging from 17.16° to 27.51°, MAE from 14.13° to 26.08°, and Bias from 10.23° to 26.71°, despite showing high waveform similarity with CMC values exceeding 0.85.

In contrast, joint angles in the coronal and transverse planes (e.g., hip abduction/adduction, hip internal/external rotation, and ankle inversion/eversion) exhibited lower RMSE, MAE, and Bias, yet showed only moderate waveform agreement, with CMC values typically around 0.60. The poorest performance in terms of waveform similarity was observed for ankle inversion/eversion, where CMC values approached zero, indicating minimal alignment with the reference signal. These patterns are visualized in Figure 6.4, highlighting both joint-specific trends in accuracy and agreement.

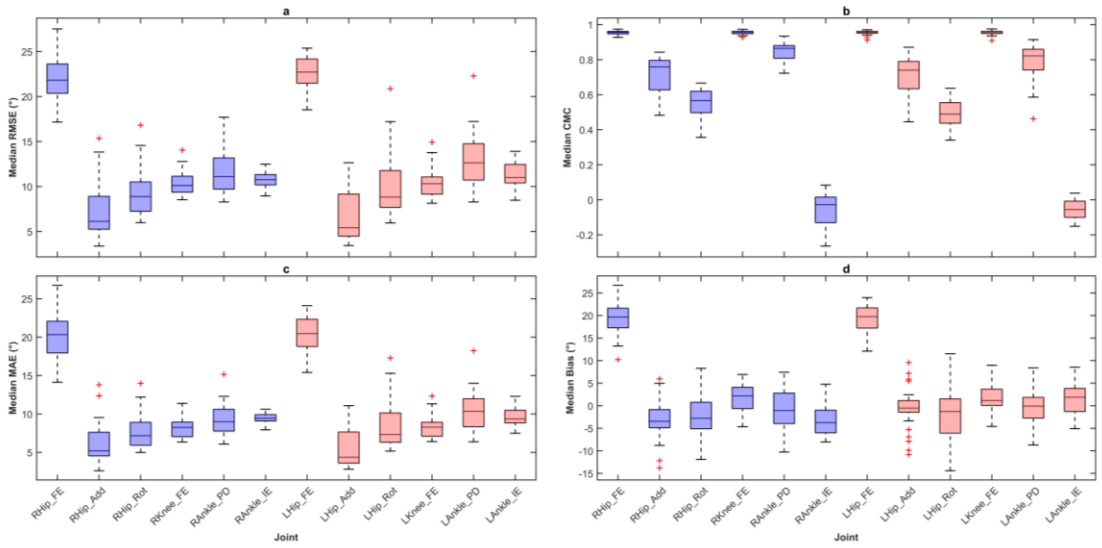

Figure 6.4: Boxplots of the four validation metrics comparing Theia3D and 2-camera markerless estimates across joints. (a) Root Mean Square Error (RMSE), (b) Coefficient of Multiple Correlation (CMC), (c) Mean Absolute Error (MAE), and (d) Bias. Values represent median metrics across all tasks and participants. Blue boxes indicate the right limb, and red boxes indicate the left limb. Red "+" symbols represent outliers.

Among the 28 two-camera configurations analyzed, combinations belonging to the Front and Back groups generally demonstrated better performance, while those categorized as Diagonal or within the Same quadrant showed poorer agreement with the 3D baseline. Notably, the *b_h* combination (Back) consistently demonstrated superior accuracy and waveform similarity when compared to the 3D baseline. As shown in Table 6.2, *b_h* yielded lower RMSE and MAE values across most joints, particularly in the sagittal and coronal planes. For instance, hip abduction/adduction demonstrated an RMSE of 3.38° (1.98-7.12°), MAE of 2.61° (1.65-6.05°), and a CMC of 0.84 (0.54-0.94), accompanied by minimal bias (-1.22°, -3.06 to -0.08°). Similarly, ankle inversion/eversion under *b_h* showed more favorable error metrics than other configurations, although waveform similarity was limited (CMC = -0.04).

In contrast, the *a_f* combination (Same quadrant) was among the weakest performers. It consistently produced higher errors and weaker agreement across multiple joints. For instance, hip abduction/adduction showed an RMSE of 8.86° (6.79-12.11°), MAE of 7.74° (5.92-10.40°), and a low CMC of 0.48 (0.11-0.73). For ankle inversion/eversion, RMSE reached 13.83° (11.81-

16.86°), with CMC values close to zero, indicating poor tracking fidelity. Notably, hip rotation under *a_f* also showed elevated errors (RMSE = 11.70°; CMC = 0.50), with a systematic underestimation bias of -8.48° (-11.43 to -4.18°).

Table 6.2: Validation metrics for best (*b_h*) and worst (*a_f*) 2-camera combination by joint angle.

Joint	Combo	RMSE (°)	MAE (°)	CMC	Bias (°)
Hip FE	b_h	**20.94** (14.26-25.88)	**19.08** (13.80-23.82)	**0.96** (0.91,0.98)	**18.73** (13.21,22.88)
	a_f	**27.35** (23.44-34.28)	**26.76** (22.09-32.80)	**0.93** (0.87,0.98)	**26.71** (21.93,32.47)
Hip Ad/Ab	b_h	**3.72** (3.21,4.51)	**2.92** (2.50,3.66)	**0.82** (0.72,0.88)	**-0.88** (-1.68,0.04)
	a_f	**8.86** (6.79,12.11)	**7.74** (5.92,10.40)	**0.48** (0.11,0.73)	**-5.00** (-7.84,-2.51)
Hip Rot	b_h	**6.61** (4.60,10.04)	**5.50** (3.85,8.33)	**0.66** (0.42,0.83)	**1.00** (-1.28,3.51)
	a_f	**11.70** (8.33,14.43)	**10.07** (7.19,12.40)	**0.50** (0.22,0.68)	**-8.48** (-11.43,-4.18)
Knee FE	b_h	**10.31** (6.67,15.58)	**7.87** (5.47,12.17)	**0.98** (0.91,0.99)	**5.51** (3.63,8.77)
	a_f	**12.66** (9.96,16.95)	**10.19** (7.72,12.87)	**0.93** (0.84,0.97)	**-0.35** (-3.34,5.62)
Ankle PD	b_h	**9.28** (6.86,13.10)	**7.80** (5.47,10.91)	**0.90** (0.78,0.97)	**5.37** (2.97,8.45)
	a_f	**17.70** (15.35,21.26)	**15.14** (12.06,18.83)	**0.77** (0.58,0.87)	**-10.27** (-16.12,-4.65)
Ankle IE	b_h	**9.54** (7.42,13.43)	**8.22** (6.25,11.13)	**-0.06** (-0.43,0.22)	**1.80** (-2.62,-5.72)
	a_f	**13.83** (11.81,16.86)	**12.30** (9.84,14.67)	**0.04** (-0.35,0.34)	**6.05** (0.95,10.66)

Note: Values are reported as median (IQR). CMC = Coefficient of Multiple Correlation; MAE = Mean Absolute Error; RMSE = Root Mean Square Error; Bias = Mean difference with 95% limits of agreement (LoA) in parentheses. Combo = Combination. The limb with the larger errors and lower agreement was selected and reported for each joint.

For example, the overall tracking performance is illustrated by the joint angle waveforms during the squat task shown in Figure 6.5. Complete performance metrics for all joints across

combinations are provided in Supplementary Table S1.

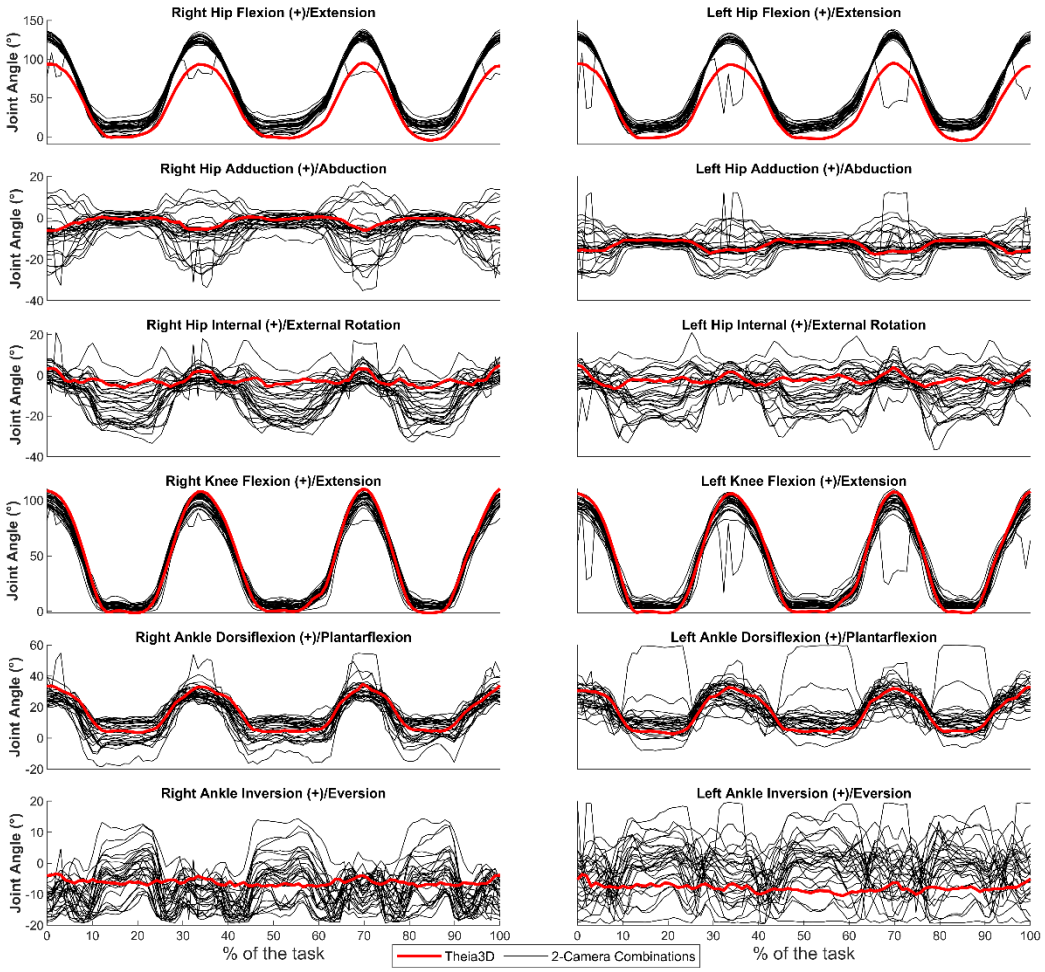

Figure 6.5: Example of lower limb joint angles during the squat task, comparing the Theia3D baseline (red) with outputs from all 2-camera combinations (black). Each black line represents the joint angle trajectory from a different camera combination. The x-axis denotes the percentage of the task cycle, and the y-axis indicates joint angle in degrees.

6.3.1.2 By task

When examining the agreement between systems across tasks, notable variations in performance emerged depending on the task and the camera combination. Overall, camera combinations such as *d_f* (Front), *b_h* (Back), and *a_b* (Right) consistently produced joint kinematics across multiple tasks (Squat, BJ and CMJ) with relatively low RMSE and MAE, high waveform similarity, and minimal systematic bias. In contrast, combinations like *a_f* (Same

quadrant), *c_d* (Diagonal) performed poorly in most tasks, particularly in unilateral tasks (L-hop and YB) where waveform agreement was reduced and bias was more pronounced.

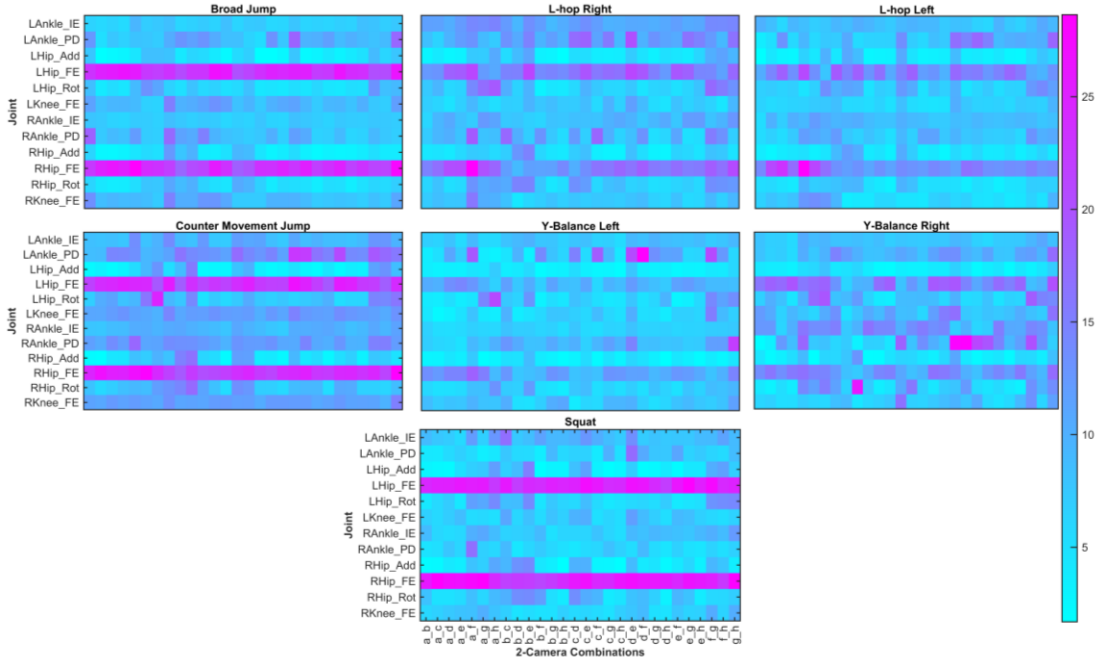

Figure 6.6: Heatmap of median RMSE values across joints and camera combinations by task. Lighter colors indicate lower errors. The x-axis represents the camera combinations, and the y-axis represents the joints.

Among the best-performing combinations, *b_h* (Back) and *a_b* (Right) showed strong agreement in Squat, BJ, and CMJ tasks, with consistently high CMC values and low errors across metrics (Figures 6.6-6.9). Combinations such as *a_c* (Right) and *d_f* (Front) also yielded favorable results in these tasks and performed moderately well in L-hop. Additionally, *c_h*, *b_g* and *f_h* from group Back provided adequate tracking in symmetric tasks, though performance varied more by joint. These combinations were effective for lower limb sagittal-plane movements but lacked consistency in frontal and transverse planes.

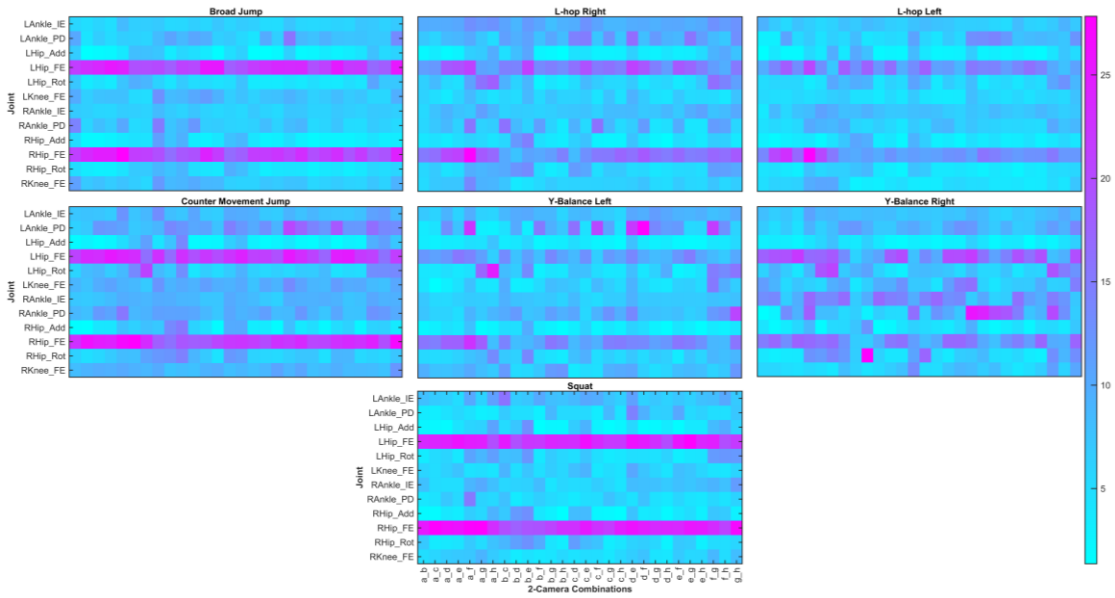

Figure 6.7: Heatmap of median MAE values across joints and camera combinations by task. Lighter colors indicate lower errors. The x-axis represents the camera combinations, and the y-axis represents the joints.

In contrast, combinations such as *a_f and h_g* (Same quadrant), and *c_d* (Diagonal) exhibited reduced performance across most tasks, especially in Y-balance and L-hop, where waveform agreement (CMC) was often poor and RMSE exceeded 15°. These diagonal and same-quadrant combinations frequently resulted in elevated bias values, as visualized in Figure 6.9.

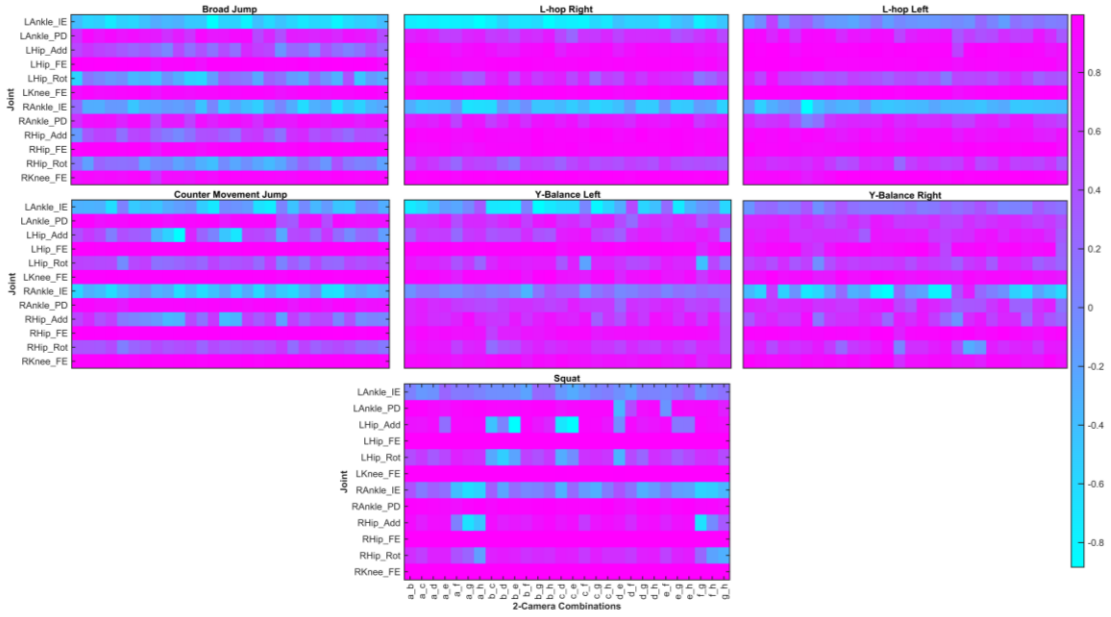

Figure 6.8: Heatmap of median CMC values across joints and camera combinations by task. Lighter colors indicate lower agreement. The x-axis represents the camera combinations, and the y-axis represents the joints.

Among the tasks, Squat and BJ were generally captured more reliably across most camera combinations, indicated by higher overall CMCs and lower RMSEs. In contrast, tasks involving unilateral movements, such as Y-balance and L-hop, exhibited greater variability in performance depending on the camera combination. For instance, few configurations consistently performed well across all four metrics in left YB or right L-hop. Detailed task- and combination-specific validation metrics, including RMSE, MAE, CMC, and Bias, are provided in Supplementary Table S2.

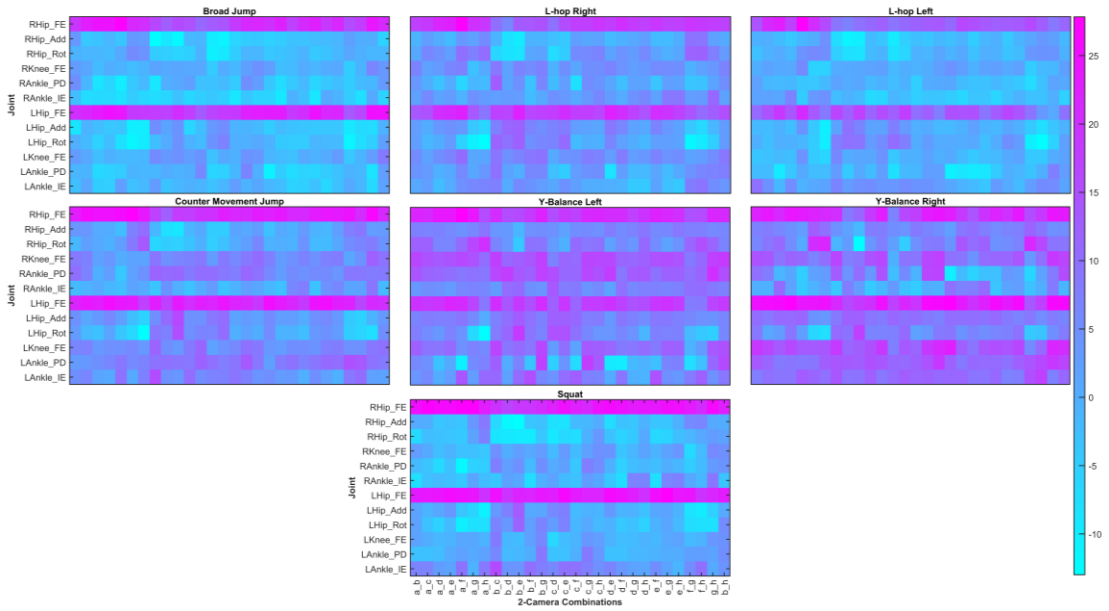

Figure 6.9: Heatmap of median Bias values across joints and camera combinations by task. Lighter colors indicate lower errors. The x-axis represents the camera combinations, and the y-axis represents the joints.

6.3.2 Within combinations

6.3.2.1 By joint

When analyzing agreement within 2-camera combinations, performance by joint, task, and subgroup was evaluated. Across all joints and combinations (Table 6.3), flexion/extension in the sagittal plane, particularly at the hip and knee, showed the highest agreement. Median RMSE values for right and left hip flexion/extension were 7.71° (5.23-11.25°) and 7.39° (5.01-10.81°), respectively, with waveform similarity (CMC = 0.99). Knee flexion/extension followed a similar trend with RMSEs of 7.37° and 7.94° and CMCs of 0.99 for both limbs. In contrast, greater variability and lower CMCs were found in the frontal and transverse planes. Hip abduction/adduction and ankle inversion/eversion showed RMSEs in the 8-10° range and moderate to weak CMCs (0.53-0.71), especially in the left limb.

Table 6.3: Summary of joint angle median RMSE and CMC values averaged across all 2-camera combinations.

Joint	Median RMSE (IQR)		Median CMC (IQR)	
	Right	Left	Right	Left

Hip_FE	**7.71** (5.23, 11.25)	**7.39** (5.01, 10.81)	**0.99** (0.95, 1.00)	**0.99** (0.95, 1.00)
Hip_Add	**7.98** (5.05, 11.71)	**8.28** (5.21, 12.17)	**0.71** (0.26, 0.91)	**0.65** (0.18, 0.88)
Hip_Rot	**9.46** (6.10, 14.06)	**10.75** (6.97, 15.96)	**0.74** (0.45, 0.90)	**0.67** (0.34, 0.85)
Knee_FE	**7.37** (4.97, 10.72)	**7.94** (5.34, 11.64)	**0.99** (0.96, 1.00)	**0.99** (0.95, 1.00)
Ankle_PD	**11.27** (7.49, 17.04)	**12.92** (8.54, 19.35)	**0.88** (0.69, 0.96)	**0.81** (0.56, 0.94)
Ankle_IE	**8.88** (6.03, 12.42)	**10.05** (7.20, 13.58)	**0.56** (0.22, 0.80)	**0.53** (0.20, 0.77)

Note: Values represent the median RMSE (in degrees) and CMC with interquartile ranges (IQR) for each joint angle, averaged across all 2-camera combinations and tasks. Results are reported separately for the right and left limbs. Higher CMC and lower RMSE values indicate better agreement.

6.3.2.2 By task

When comparing performance by task averaged across all camera combinations (Supplementary Table S3), squat consistently yielded the most accurate joint angle estimations, with lower RMSEs and very high waveform agreement across most joints. Specifically, right and left hip flexion/extension demonstrated RMSEs of 5.44° and 5.40°, respectively, with CMCs of 1.00. Right and left knee flexion/extension followed closely with RMSEs of 6.19° and 6.11°, and CMCs also reaching 1.00. Ankle plantarflexion/dorsiflexion on both limbs showed RMSEs of 6.85° (right) and 6.25° (left), with CMCs ranging from 0.96 to 0.98. The CMJ also showed strong performance in sagittal joints, with hip flexion/extension RMSEs of 6.36° (right) and 5.90° (left), and CMCs of 0.99. Knee flexion/extension during CMJ resulted in RMSEs of 7.34° (right) and 7.06° (left), with CMCs between 0.98 and 0.99. In contrast, the YB tasks showed larger errors and reduced CMCs, particularly in non-sagittal joints. For example, right ankle inversion/eversion RMSEs exceeded 12°, with corresponding CMCs falling as low as 0.21.

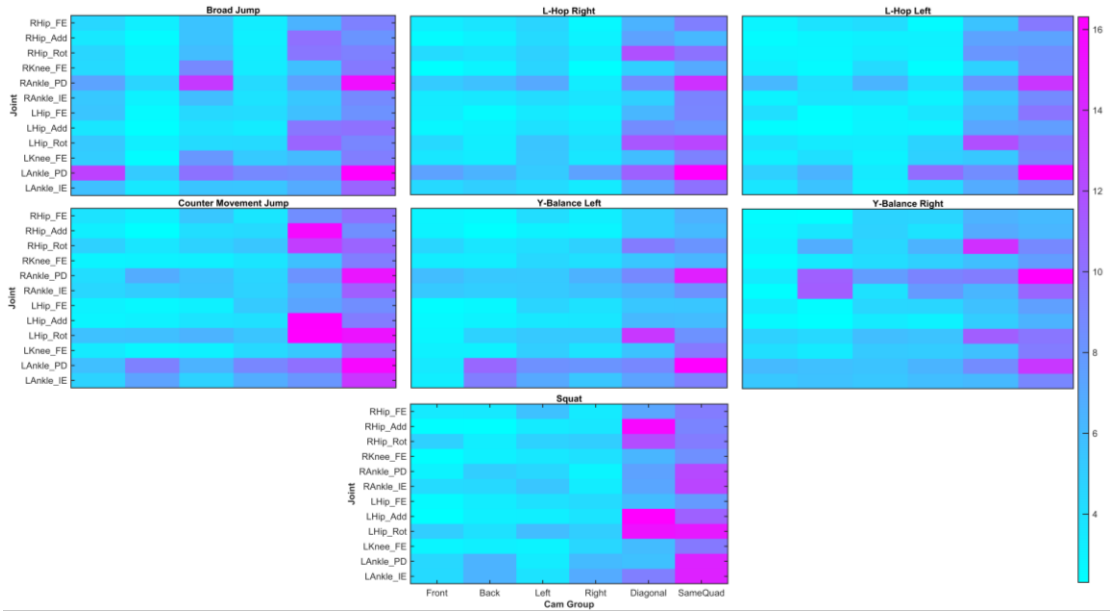

Figure 6.10: Heatmap of median RMSE values for each joint across camera subgroup configurations and movement tasks. The x-axis represents camera subgroups (Front, Back, Left, Right, Diagonal, Same Quadrant), and the y-axis lists the joint angles analyzed. Each subplot corresponds to a specific task. Lighter colors indicate lower RMSE values, reflecting better agreement within the group.

6.3.2.3 Within each subgroup

Subgroup analysis (Front, Back, Left, Right, Diagonal, and Same Quadrant) based on camera placement further illustrated that the spatial relationship between cameras substantially influences accuracy. When averaged across tasks, the Front and Back groups produced the most accurate results across joints, particularly for sagittal plane motion. RMSE values for right hip flexion/extension were 4.20° (Front) and 3.87° (Back), with corresponding CMCs ≥ 0.99. Similar trends were seen for knee flexion/extension. Conversely, Same Quadrant configurations yielded the weakest performance, especially for joints in the transverse and frontal planes. In this group, left hip rotation RMSE reached 15.77° with a CMC of 0.43, while left ankle inversion/eversion had an RMSE of 14.76° and CMC of 0.33.

Diagonal configurations yielded moderate performance, performing better than Same Quadrant but worse than Front or Back pairs. Right and left hip flexion/extension RMSEs in this

group were 8.74° and 10.58°, with CMCs of 0.99 and 0.96, respectively. Ankle and hip transverse angles continued to show reduced agreement in this group.

Left and Right groups exhibited variable performance. While sagittal plane angles such as hip flexion/extension remained accurate, frontal and transverse angles showed modest to poor agreement. For instance, right hip rotation in the Right group showed an RMSE of 5.56° and CMC of 0.79, while the Left group recorded an RMSE of 6.07° and CMC of 0.91.

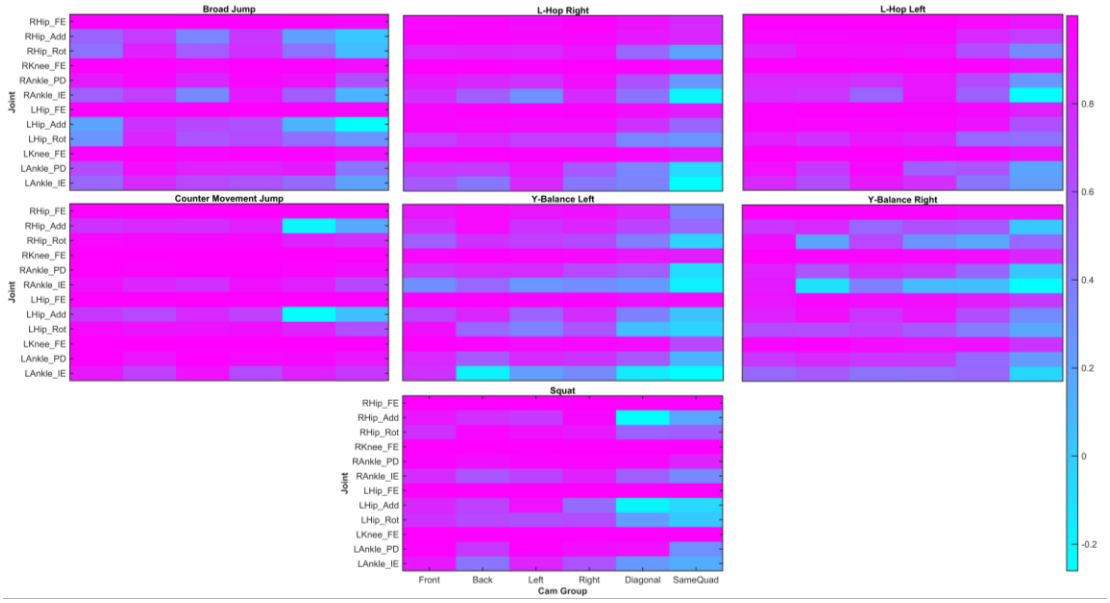

Figure 6.11: Heatmap of median CMC values for each joint across camera subgroup configurations and movement tasks. The x-axis represents camera subgroups (Front, Back, Left, Right, Diagonal, Same Quadrant), and the y-axis lists the joint angles analyzed. Each subplot corresponds to a specific task. Lighter colors indicate lower CMC values, reflecting weaker agreement within group.

In summary, the accuracy of 2-camera joint angle estimation is highly dependent on both the type of movement and the spatial configuration of the cameras (Figure 6.10-6.11). Best results were achieved for sagittal plane movements during symmetrical tasks (Squat and CMJ), especially when cameras were placed directly in front of or behind the participant. Suboptimal configurations, Same Quadrant, resulted in significantly higher errors and lower waveform agreement.

Detailed subgroup validation metrics, including RMSE and CMC, are provided in Supplementary Table S4 and full results by task and subgroup are provided in Supplementary Table S5 (subgroups in sub sheets).

6.4 Discussion

This study validated 28 different 2-camera markerless motion capture configurations using the Pose2Sim pipeline for estimating lower-limb joint kinematics during common screening tasks in female varsity soccer athletes. The outputs from each 2-camera combination were evaluated both against a widely used 8-camera markerless motion capture system (Theia3D) and through comparisons within the 2-camera configurations.

Of the 4,508 potential trials, 3,999 (88.71%) were successfully retained for analysis. The L-hop task exhibited the highest dropout rates within the Back (4.97%) and Left (6.21%) camera groups. Overall, the YB tasks demonstrated the greatest dropout rates, ranging from 4.04% to 7.61% across all camera groups. The BJ task had a dropout rate of 2.48% in the Front group, with substantially lower rates observed in other groups. All other tasks, particularly the CMJ, showed dropout rates approaching zero across all configurations. Upon visual inspection, the elevated dropout in L-hop trials was primarily due to participants jumping out of the frame, a similar issue observed for BJ trials in the Front group. In contrast, the higher dropout observed during YB tasks appeared to result from self-occlusion, likely caused by limb crossing and pelvic occlusion inherent to the movement.

6.4.1 Between systems

Across tasks, joint-specific comparisons revealed that sagittal-plane joint angles, particularly knee flexion/extension, consistently demonstrate greater accuracy relative to the 3D baseline, with RMSE values generally below 8° and CMC values approaching 1.00. In contrast, joint angles in the coronal and transverse planes exhibited higher RMSE and lower waveform agreement. A consistent offset was observed in hip flexion/extension angles, with Theia3D systematically yielding lower values across tasks and combinations (RMSE = 17-27°), despite high waveform similarity (CMC > 0.90). This pattern is consistent with previous findings in which optical motion capture systems reported larger hip flexion/extension angles compared to markerless systems, approximately 11° during gait (Kanko et al., 2021; Wren et al., 2023) and 6.7-13.8° during

dynamic athletic tasks (Song et al., 2023). These discrepancies may be attributed to differences in pelvis segment definitions between systems, with Theia3D adopting a more neutral pelvic orientation, as described in Theia3D's technical documentation. Although the current 2-camera pipeline employed a markerless workflow, the LSTM-based marker augmentation algorithm was trained primarily on optical marker data, which may have contributed to systematic differences. Additionally, variation in pose estimation models (e.g., RTMPose vs. Theia3D's proprietary model) likely introduced further divergence in these joint angle outputs. Another plausible source of discrepancy is the difference in joint DoF between systems: the OpenSim model imposed tighter constraints at the lower limb, whereas Theia3D permits an additional rotational DoF at the knee and ankle. Constraining the knee to a single flexion/extension DoF is common, especially with sparse camera views (Turner et al., 2024; Svetek et al., 2025), because it stabilizes inverse kinematics, but it can under-represent frontal/transverse motion and may miss varus/valgus patterns in cutting or pivoting tasks. Future work should harmonize joint definitions and DoFs with optical motion-capture (gold-standard) models and, where feasible, include sensitivity analyses across DoF configurations. Nevertheless, the between-system differences observed in this study are similar to those reported in prior Theia3D-optical motion-capture validation studies (Song et al., 2023; Kanko et al., 2021; Wren et al., 2023).

By task, the YB task, which involves substantial lower limb crossing and quasi-static postures, demonstrated the poorest performance across camera combinations. Notably, only combinations within the Front group achieved overall RMSE values below 10° for sagittal-plane joints (excluding the hip, where a consistent offset was observed). Unilateral tasks such as the L-hop exhibited considerable variability in accuracy depending on camera placement, while bilateral tasks (e.g., squats and CMJ) generally yielded more consistent and accurate results across combinations. Previous studies validating markerless motion capture systems like OpenCap have primarily focused on dynamic, non-crossing movements such as single-leg hops, drop jumps, and gait, and have not typically included complex tasks like YB that involve limb crossing (Svetek et al., 2025; Turner et al., 2024).

Overall, camera combinations from Front (*a_e, d_f*), Back (*b_h, c_g*), Right (*a_b, c_f*), and Left (*e_h, d_g*) groups offered higher accuracy and waveform similarity during bilateral tasks. These configurations likely benefited from broader fields of view and greater visual overlap between the two cameras. In contrast, configurations such as *a_f* (Same quadrant) and *b_e* (Diagonal) consistently exhibited poorer performance, characterized by larger errors and reduced waveform agreement, likely due to restricted perspective and limited view overlap. In prior research, most 2-camera systems were configured with both cameras positioned in front of the participant, angled approximately 45-60° from the sagittal axis to optimize view overlap and depth reconstruction (Cronin et al., 2023; Lima et al., 2024; Svetek et al., 2025; Turner et al., 2024).

6.4.2 Within combinations

Across all tasks and camera combinations, joint angles in the sagittal plane demonstrated the most favorable agreement, with median RMSE values below 10 degrees and very strong waveform similarity as reflected by high median CMC values (Table 6.3). In contrast, ankle inversion/eversion consistently yielded the lowest median CMC values. This result aligns with prior research suggesting that foot tracking remains a persistent challenge in markerless motion capture systems using 2-camera configurations (Kanko et al., 2021). Indeed, foot joint angles have historically shown the poorest accuracy in both markerless and marker-based systems, largely due to the complex anatomy and dynamic behavior of the foot, which require dense marker sets for precise tracking (Nester et al., 2007).

Squat movements, which involve fixed foot positions and largely sagittal-plane motion (e.g., plantarflexion/dorsiflexion), showed good agreement in nearly all lower limb joints bilaterally, as illustrated in Figure 6.5. The limited accuracy observed at the ankle may also be attributed to the elevated placement of cameras in this study (approximately 3 meters high), which could reduce visibility and tracking fidelity at the foot segment. If ground reaction forces were to be estimated from these kinematic datasets, such ankle tracking limitations could introduce substantial error (Martin et al., 2023).

Unlike single-camera systems that are susceptible to severe viewpoint constraints, 2-camera setups provide a balanced trade-off between ease of deployment and biomechanical fidelity (Boldo et al., 2024). Our findings suggest that validated 2-camera markerless motion capture pipelines have strong potential to enable practical and scalable biomechanical assessments. When implemented with accessible hardware such as smartphones or tablets, these systems may allow coaches and clinicians to conduct meaningful joint-level analyses during routine training sessions or match play. Importantly, the ability to capture detailed biomechanical data during context-specific movements, such as passing, shooting, or dynamic balance tasks, could greatly enhance individualized injury risk profiling and real-time intervention strategies (Darapaneni et al., 2022; Kolodziej et al., 2022).

6.4.3 Limitations

Several limitations should be acknowledged. First, while Theia3D is widely used and accepted in biomechanical research, it is not considered a definitive gold standard. Therefore, the reported between-system accuracy may be affected by inherent uncertainties within the reference system itself. Future work validating these 2-camera pipelines directly against optical motion capture systems would provide stronger evidence of their biomechanical accuracy. Nonetheless, both OpenCap and Pose2Sim are independently validated 2-camera markerless systems, and the within-combination comparisons in this study offer valuable insights into the influence of camera placement on kinematic accuracy.

Second, the experimental setup differed from typical field or clinical environments. Cameras were mounted approximately 3 meters above the ground, higher than conventional placements (1.5-2.0 m), which may have introduced perspective distortions or occlusions, particularly at the distal segments (e.g., feet). However, elevated camera positioning is common in sports settings (e.g., to avoid occlusion by other players), especially in team-based environments. The increasing use of camera systems and CV technology in sport to capture critical gameplay moments reflects this trend (Ghosh et al., 2023; Thulasya Naik et al., 2021). Still, the application of 2-camera markerless setups for tracking multiple athletes in dynamic sports contexts, such as soccer, requires

further validation. A recent study applying a 2-camera OpenCap system to long jump performance during live events reported poor agreement and unrealistic biomechanical outputs (Cronin et al., 2023), underscoring the need for rigorous validation in real-world sports contexts.

Lastly, although the 2-camera workflow reduces setup complexity, it remains susceptible to challenges such as occlusion and limited angular separation, especially for movements in the coronal and transverse planes. Additionally, tasks involving limb crossing or quasi-static control, such as the Y-Balance, demonstrated notably lower agreement. This may reflect fundamental limitations of 2-camera systems in capturing complex out-of-plane motions, regardless of configuration. These findings emphasize the importance of strategic camera placement and task-specific considerations when implementing markerless motion capture pipelines in applied settings.

6.5 Conclusion

This study demonstrated that select 2-camera markerless motion capture configurations can accurately and reliably capture lower-limb 3D joint kinematics during functional screening tasks in female varsity soccer athletes. Configurations from the Front, Back, and Right camera groups, particularly those with wider view overlap, consistently achieved high accuracy for sagittal-plane movements. In contrast, combinations from the Same Quadrant and Diagonal groups showed reduced agreement, particularly for coronal and transverse plane motions.

In clinical or performance assessment settings where space is constrained, but motion accuracy is essential, the validated 2-camera setups identified in this study offer practical guidance for implementation. Field deployment should avoid poorly performing configurations, and camera height should remain below 3 meters to improve foot tracking, particularly for tasks requiring accurate distal joint kinematics.

By identifying optimal camera placements that balance biomechanical fidelity with logistical feasibility, this work advances the development of accessible, field-ready motion analysis tools. The findings support the use of task-specific and resource-efficient movement screening protocols,

particularly in female athlete populations, which have historically been underrepresented in biomechanical research and injury prevention efforts.

6.6 References

Alentorn-Geli, E., Myer, G. D., Silvers, H. J., Samitier, G., Romero, D., Lázaro-Haro, C., & Cugat, R. (2009). Prevention Of Non-Contact Anterior Cruciate Ligament Injuries in Soccer Players. Part 1: Mechanisms Of Injury and Underlying Risk Factors. *Knee Surgery, Sports Traumatology, Arthroscopy*, *17*(7), 705-729.

Boldo, M., Di Marco, R., Martini, E., Nardon, M., Bertucco, M., & Bombieri, N. (2024). On The Reliability of Single-Camera Markerless Systems for Overground Gait Monitoring. *Computers in Biology and Medicine*, *171*, 108101.

Cook, G., Burton, L., & Hoogenboom, B. (2006). Pre-Participation Screening: The Use of Fundamental Movements as An Assessment of Function - Part 1. *North American Journal of Sports Physical Therapy: NAJSPT*, *1*(2), 62-72.

Cronin, N. J., Walker, J., Tucker, C. B., Nicholson, G., Cooke, M., Merlino, S., & Bissas, A. (2023). Feasibility Of OpenPose Markerless Motion Analysis in A Real Athletics Competition. *Frontiers in Sports and Active Living*, *5*, 1298003.

Darapaneni, N., Kumar, P., Malhotra, N., Sundaramurthy, V., Thakur, A., Chauhan, S., Thangeda, K. C., & Paduri, A. R. (2022). *Detecting Key Soccer Match Events to Create Highlights Using Computer Vision*.

Delp, S. L., Anderson, F. C., Arnold, A. S., Loan, P., Habib, A., John, C. T., Guendelman, E., & Thelen, D. G. (2007). OpenSim: Open-Source Software to Create and Analyze Dynamic Simulations of Movement. *IEEE Transactions on Biomedical Engineering*, *54*(11), 1940-1950.

Falisse, A., Uhlrich, S. D., Chaudhari, A. S., Hicks, J. L., & Delp, S. L. (2024). Marker Data Enhancement for Markerless Motion Capture. *BioRxiv*, 2024.07.13.603382.

Gabbett, T. J. (2016). The Training-Injury Prevention Paradox: Should Athletes Be Training Smarter and Harder? *British Journal of Sports Medicine*, *50*(5), 273-280.

Ghosh, I., Ramasamy Ramamurthy, S., Chakma, A., & Roy, N. (2023). Sports Analytics Review: Artificial Intelligence Applications, Emerging Technologies, And Algorithmic Perspective. *Wiley Interdisciplinary Reviews: Data Mining and Knowledge Discovery*, *13*(5), e1496.

Hewett, T. E., Myer, G. D., Ford, K. R., Heidt, R. S., Colosimo, A. J., McLean, S. G., Van Den Bogert, A. J., Paterno, M. V., & Succop, P. (2005). Biomechanical Measures of Neuromuscular Control and Valgus Loading of The Knee Predict Anterior Cruciate Ligament Injury Risk in Female Athletes: A Prospective Study. *American Journal of Sports Medicine*, *33*(4), 492–501.

Horsak, B., Eichmann, A., Lauer, K., Prock, K., Krondorfer, P., Siragy, T., & Dumphart, B. (2023). Concurrent Validity of Smartphone-Based Markerless Motion Capturing to Quantify Lower-Limb Joint Kinematics in Healthy and Pathological Gait. *Journal of Biomechanics*, *159*, 111801.

Jiang, T., Lu, P., Zhang, L., Ma, N., Han, R., Lyu, C., Li, Y., & Chen, K. (2023). *RTMPose: Real-Time Multi-Person Pose Estimation based on MMPose*.

Kanko, R. M., Laende, E. K., Davis, E. M., Selbie, W. S., & Deluzio, K. J. (2021). Concurrent Assessment of Gait Kinematics Using Marker-Based and Markerless Motion Capture. *Journal of Biomechanics*, *127*, 110665.

Kolodziej, M., Willwacher, S., Nolte, K., Schmidt, M., & Jaitner, T. (2022). Biomechanical Risk Factors of Injury-Related Single-Leg Movements in Male Elite Youth Soccer Players. *Biomechanics 2022, Vol. 2, Pages 281-300*, *2*(2), 281-300.

Kraus, K., Schutz, E., Taylor, W. R., & Doyscher, R. (2014). Efficacy Of the Functional Movement Screen: A Review. *Journal Of Strength and Conditioning Research*, *28*(12), 3571-3584.

Krosshaug, T., Steffen, K., Kristianslund, E., Nilstad, A., Mok, K.-M., Myklebust, G., Andersen, T. E., Holme, I., Engebretsen, L., & Bahr, R. (2016). The Vertical Drop Jump Is a Poor Screening Test for ACL Injuries in Female Elite Soccer and Handball Players. *The American Journal of Sports Medicine*, *44*(4), 874-883.

Lima, Y. L., Collings, T., Hall, M., Bourne, M. N., & Diamond, L. E. (2024). Validity and Reliability of Trunk and Lower-Limb Kinematics During Squatting, Hopping, Jumping and Side-Stepping Using Opencap Markerless Motion Capture Application. *Journal of Sports Sciences*, *42*(19), 1847-1858.

Lu, P., Jiang, T., Li, Y., Li, X., Chen, K., & Yang, W. (2023). *RTMO: Towards High-Performance One-Stage Real-Time Multi-Person Pose Estimation*.

Martin, C., Touzard, P., Horvais, N., Puchaud, P., Kulpa, R., Bideau, B., & Sorel, A. (2023). Influence Of Shoe Torsional Stiffness on Foot and Ankle Biomechanics During Tennis Forehand Strokes. *European Journal of Sport Science*, *23*(6), 914-924.

Needham, L., Evans, M., Cosker, D. P., Wade, L., McGuigan, P. M., Bilzon, J. L., & Colyer, S. L. (2021). The Accuracy of Several Pose Estimation Methods For 3D Joint Centre Localisation. *Scientific Reports 2021 11:1*, *11*(1), 1-11.

Nester, C., Jones, R. K., Liu, A., Howard, D., Lundberg, A., Arndt, A., Lundgren, P., Stacoff, A., & Wolf, P. (2007). Foot Kinematics During Walking Measured Using Bone and Surface Mounted Markers. *Journal of Biomechanics*, *40*(15), 3412-3423.

Pagnon, D., & Kim, H. (2024). Sports2D: Compute 2D Human Pose and Angles from A Video or A Webcam. *Journal of Open Source Software*, *9*(101), 6849.

Schober, P., & Schwarte, L. A. (2018). Correlation Coefficients: Appropriate Use and

Interpretation. *Anesthesia and Analgesia*, *126*(5), 1763-1768.

Song, K., Hullfish, T. J., Scattone Silva, R., Silbernagel, K. G., & Baxter, J. R. (2023). Markerless Motion Capture Estimates of Lower Extremity Kinematics and Kinetics Are Comparable to Marker-Based Across 8 Movements. *Journal of Biomechanics*, *157*, 111751.

Svetek, A., Morgan, K., Burland, J., & Glaviano, N. R. (2025). Validation of Opencap on Lower Extremity Kinematics During Functional Tasks. *Journal of Biomechanics*, *183*, 112602.

Teyhen, D. S., Shaffer, S. W., Butler, R. J., Goffar, S. L., Kiesel, K. B., Rhon, D. I., Williamson, J. N., & Plisky, P. J. (2015). What Risk Factors Are Associated with Musculoskeletal Injury in US Army Rangers? A Prospective Prognostic Study. *Clinical Orthopaedics & Related Research*, *473*(9), 2948-2958.

Thulasya Naik, B., Farukh Hashmi, M., Author, C., & Farukh Hashmi mdfarukh, M. (2021). *Ball and Player Detection & Tracking in Soccer Videos Using Improved YOLOV3 Model*.

Turner, J. A., Chaaban, C. R., & Padua, D. A. (2024). Validation of Opencap: A Low-Cost Markerless Motion Capture System for Lower-Extremity Kinematics During Return-to-Sport Tasks. *Journal of Biomechanics*, *171*.

Uhlrich, S. D., Falisse, A., Kidziński, Ł., Muccini, J., Ko, M., Chaudhari, A. S., Hicks, J. L., Delp, S. L., & Uhlrich, S. (2022). OpenCap: 3D Human Movement Dynamics from Smartphone Videos. *BioRxiv*, *650*, 2022.07.07.499061.

Wren, T. A. L., Isakov, P., & Rethlefsen, S. A. (2023). Comparison of Kinematics Between Theia Markerless and Conventional Marker-Based Gait Analysis in Clinical Patients. *Gait & Posture*, *104*, 9-14.

6.7 Supplementary material 1

Figure 6.12 illustrates a bird's-eye view of the laboratory camera configuration. All eight cameras are labeled alphabetically, and the capture volume is divided into four quadrants relative to the participant's orientation and the world coordinate system. "Front" indicates the direction faced by the participant during task execution, while "Right" refers to the participant's right-hand side.

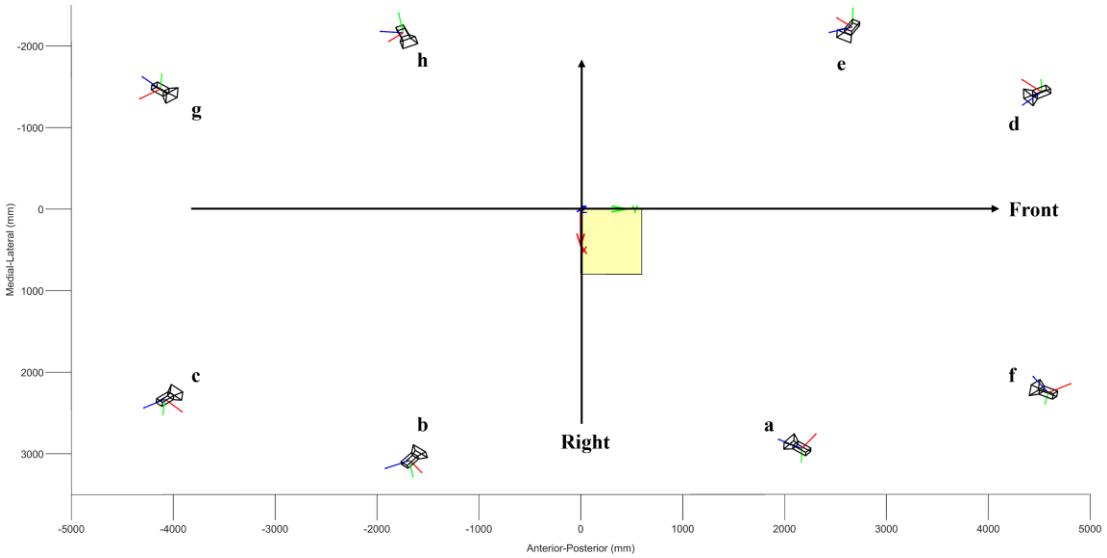

Figure 6.12: Bird's-eye view of the laboratory camera configuration. Eight cameras (a-h) are positioned around the capture volume, which is manually divided into four quadrants. The global coordinate system (in mm) is centered on the force plates (yellow rectangle), with the Y-axis oriented anterior-posterior, X-axis medial-lateral, and Z-axis vertically upward.

Table 6.4 shows how the subgroups of the camera combinations are defined. The combinations correspond to camera labels (a-h) shown in Figure 6.12.

Table 6.4: Definition of camera combination subgroups.

Group	**Combination**			
Front	a-e	a-d	f-e	f-d
Back	b-h	b-g	c-h	c-g
Left	d-h	d-g	e-h	e-g
Right	f-b	f-c	a-b	a-c
Same quadrant	a-f	e-d	b-c	g-h
Diagonal	a-h	a-g	f-h	f-g
	c-d	c-e	b-d	b-e

Note: Front: Both cameras in the front half (left-front and right-front); Back: Both cameras in the back half (left-back and right-back); Left: One camera in the left-back and one in the left-front; Right: One camera in the right-back and one in the right-front; Diagonal: Cameras positioned diagonally across opposite quadrants (left-back & right-front or left-front & right-back); Same quadrant: Both cameras located within the same quadrant.

Chapter 7. General Discussion

This doctoral thesis brings together four complementary studies that collectively advance an integrated, evidence-based framework for monitoring movement pattern and preventing non-contact injuries in female varsity soccer. By aligning season-long biomechanical assessment, quantification of movement pattern, explainable machine-learning pipelines, and field-friendly markerless motion capture, the work contributes to addressing three persistent challenges in sports biomechanics: the scarcity of female-specific longitudinal data, the difficulty of scaling biomechanical monitoring beyond the laboratory, and the "black-box" nature of many predictive models.

7.1 Summary of findings

A first major contribution is the establishment of a season-long, multimodal dataset in varsity women's soccer. Although previous studies have characterised pre-season risk factors (Hewett et al., 2005) or described single-time-point relationships between neuromuscular control and injury (Pappas et al., 2016), longitudinal work in female athletes remains sparse. By capturing laboratory biomechanics, on-field sprint performance, and injury record at three time points, the present design reveals the temporal windows in which neuromuscular fatigue, performance decline, and injury burden converge. In line with epidemiological data showing peak soft-tissue injury rates during periods of fixture congestion, when teams play multiple matches with limited recovery time (Randell et al., 2021), Study 1a shows that mid-season is accompanied by slower 10-40 m sprint times, depressed countermovement-jump height, and elevated knee-ankle coordination variability, all of which normalise partially by post-season. These trajectories provide actionable benchmarks that coaches can use to adjust training load and recovery strategies.

A second advance stems from the extension of the Goal Equivalent Manifold framework to three dimensions. Standard 2D GEM analyses partition variability into task-relevant and task-irrelevant components, yet they ignore timing error, an execution variable of obvious importance in rhythmic tasks. By embedding timing alongside displacement and velocity, Study 1b

demonstrates that players with a history of concussion retain lower GEM performance index scores across an entire season, echoing laboratory findings of prolonged motor-control impairment after mild traumatic brain injury (Bussey et al., 2023; Howell et al., 2019). Crucially, these deficits were not detectable via conventional variability metrics or static balance tests, underscoring the added sensitivity of the 3D approach for return-to-play monitoring.

Third, the thesis evaluates four machine-learning pipelines under identical cross-validation splits and shows that a Hybrid Transformer outperforms classical Support Vector Machines, XGBoost, and Long-Short-Term Memory networks. Transformers have proved powerful in biomechanical pose estimation (Zhao et al., 2023) and activity recognition (Kim et al., 2022), but their application to athlete injury prediction is new. Study 2 not only demonstrates superior discrimination (ROC-AUC = 0.740) but, through attention maps, localises risk-critical phases such as early landing and push-off, corroborating video-analysis studies linking valgus collapse during landing to ACL injury (Krosshaug et al., 2016). Such transparency satisfies growing calls for interpretable artificial intelligence in sports medicine (Hahn et al., 2024; Ramkumar et al., 2022).

Finally, Study 3 shows that reliable sagittal-plane kinematics can be obtained from only two strategically placed cameras. Although recent work has validated multi-camera markerless systems in controlled settings (Drazan et al., 2021), field deployment is hindered by cost and setup complexity. Mapping errors for every two-camera combination of an eight-camera array revealed that wide-baseline, front-back pairs produce root-mean-square errors below 8° and coefficients of multiple correlation near 1 for hip and knee flexion-extension. These findings reduce the technical barrier to routine on-field biomechanical screening, complementing wearable-sensor solutions that remain limited by drift and soft-tissue artefact (Robert-Lachaine et al., 2017).

Collectively, the four studies demonstrate a viable end-to-end workflow: rapid two-camera capture, automated kinematics, GEM- or summary-feature extraction, interpretable Transformer prediction, and season-over-season tracking. The pipeline aligns with contemporary models of "precision sport" that advocate continuous, individualised monitoring (Thornton et al., 2019).

7.2 Limitations

First, notwithstanding its contributions, the thesis has several limitations. The cohort comprised only twenty-five athletes, which provided adequate power for biomechanical comparisons but limited the precision of injury-prediction models, particularly for rarer pathologies. Although stratified Group K-Fold cross-validation mitigated overfitting, external validation on larger multi-team datasets is essential for clinical deployment, in line with best-practice guidelines for prognostic modelling (Collins et al., 2015).

Second, the competitive window was 15 weeks, typical of Canadian university play but shorter than professional or international calendars that often exceed 30 weeks (FIFPro, 2022). Adaptive responses over longer periods, including cumulative fatigue and squad-rotation effects, therefore remain unknown.

Third, Theia3D served as the reference for camera-configuration validation, yet it is itself a markerless system with documented biases, chiefly an offset in hip flexion/extension angles (Kanko et al., 2021). Optical marker-based benchmarks would provide an even more conservative test of pipeline validity.

Fourth, concussion histories were heterogeneous: time since most recent concussion ranged from six months to over two years, making it difficult to disentangle acute from chronic effects. Future studies should stratify by recency and incorporate neuro-cognitive or vestibular metrics, as recommended by consensus statements on sport-related concussion (McCrory et al., 2017).

Lastly, external load, hormonal, and psychosocial factors were not integrated, even though menstrual-cycle phase (Dos'Santos et al., 2023) and training monotony (Gabbett, 2016) modulate neuromuscular performance and injury risk. Including these dimensions would yield a more holistic risk-profiling tool.

7.3 Future directions

7.3.1 Data type

Future work should extend the dataset across multiple universities, semi-professional clubs,

and consecutive seasons to enhance statistical power and enable subgroup analyses by playing position or maturation status. Multi-site consortia would facilitate federated learning, allowing sensitive medical data to remain local while still contributing to a global model (Moshawrab et al., 2023).

Richer multimodal inputs should be considered. Surface electromyography (EMG) can quantify muscle-activation strategies, while wearable load sensors and salivary cortisol provide insights into physiological stress. Integrating self-reported wellness and psychological readiness scales may capture the biopsychosocial context in which movement patterns emerge.

7.3.2 Advanced modeling and real-time implementation

The adoption of multi-task learning frameworks may enable simultaneous injury prediction, performance monitoring, and return-to-play assessment. Real-time deployment using embedded AI or cloud-connected systems could allow for on-field injury risk flagging and timely intervention. Markerless motion capture pipelines should also be optimized for more complex sport-specific tasks (e.g., change-of-direction, agility drills) and extended to hybrid kinetic-kinematic frameworks for richer biomechanical profiling.

From a deployment standpoint, the two-camera pipeline could be compiled into an edge-AI smartphone application, enabling real-time feedback within seconds of task completion. Complementary work in basketball has already shown that single-smartphone capture can inform jump-landing mechanics with acceptable error (Balsalobre-Fernández et al., 2015).

The set of validated tasks should be broadened beyond sagittal-plane jumps and squats to multidirectional cutting, pivoting, and reactive agility drills, movements responsible for the majority of ACL injuries in women's sport (Griffin et al., 2006). Physics-informed neural networks that couple kinematics to kinetics could estimate joint moments directly from video, providing a richer mechanical context for injury prediction.

7.3.3 Female athlete-specific considerations

Female-specific model personalisation warrants attention. Hormonal fluctuations across the

menstrual cycle alter ligament laxity and neuromuscular control (Parker et al., 2024). Embedding cyclical covariates into the Transformer architecture may uncover risk profiles that sex-agnostic algorithms overlook.

7.3.4 In-field collection

Although laboratory validation is a critical step, future studies should test the markerless system in real-world environments such as on-field training or competition settings to better assess ecological validity and practical feasibility.

7.4 Conclusions

Across four studies, this thesis shows that interpretable, portable, and sex-aware analytics are feasible within the resource constraints of varsity sport. Seasonal monitoring revealed mid-season dips in power and sprint capacity; 3D GEM analysis detected durable post-concussion coordination deficits; a Hybrid Transformer provided both accurate and transparent injury predictions; and Front/Back/Right groups of two-camera configurations captured sagittal-plane kinematics with acceptable fidelity. Together, these advances lay the groundwork for continuous athlete-monitoring ecosystems that move laboratory-grade insight onto the sideline and into everyday coaching practice.

The findings indicate that transformer models, when equipped with temporal self-attention, deliver the optimal balance of predictive accuracy and clinical interpretability for non-contact injury risk in female soccer. Persistent deficits following concussion can be quantified through 3D GEM metrics, even when traditional screening suggests full recovery. Two strategically placed cameras suffice for reliable sagittal-plane joint-angle estimation during routine screening, making high-quality biomechanics accessible to programmes without motion-analysis laboratories.

Based on these findings, pre-season testing for varsity women's soccer should prioritize countermovement jumps, T-Balance, L-hop, complex lower-limb reaction-time tests, and repetitive bilateral body-weight squats. These measures capture key physical and neuromuscular domains, explosive performance, stability, and cognitive-motor integration, that were shown in

this thesis to vary meaningfully across the season and to relate to injury risk. Incorporating these tasks into routine pre-season screening provides a practical foundation for individualized monitoring and early identification of athletes who may require targeted intervention or load management.

By combining biomechanical feature extraction with machine-learning interpretation and season-long surveillance, the thesis establishes a scalable, actionable framework for injury prevention in varsity women's soccer and sets an agenda for integrating physiological, hormonal, and psychological variables into next-generation sport health analytics.

Chapter 8. General References

Alipour Ataabadi, Y., Sadeghi, H., Hosein Alizadeh, M., Khaleghi, M., & Alipour Ataabadi, C. Y. (2019). Comparing Biomechanical Risk Factors of Anterior Cruciate Ligament Injury of Elite Female Soccer Players During the Shearing Maneuver and Header on the Natural Grass and Artificial Turf. *Sport Sciences and Health Research*, *11*(1), 51-60.

Allen, M. M., Pareek, A., Krych, A. J., Hewett, T. E., Levy, B. A., Stuart, M. J., & Dahm, D. L. (2016). Are Female Soccer Players at an Increased Risk of Second Anterior Cruciate Ligament Injury Compared with Their Athletic Peers? *American Journal of Sports Medicine*, *44*(10),2492-2498.

Alsubaie, A. M., Mazaheri, M., Martinez-Valdes, E., & Falla, D. (2021). Is Movement Variability Altered in People with Chronic Non-Specific Low Back Pain: A Protocol for A Systematic Review. *BMJ Open*, *11*(5), e046064.

Ayala, R. E. D., Granados, D. P., Gutiérrez, C. A. G., Ruíz, M. A. O., Espinosa, N. R., & Heredia, E. C. (2024). Novel Study for the Early Identification of Injury Risks in Athletes Using Machine Learning Techniques. *Applied Sciences 2024, Vol. 14, Page 570*, *14*(2), 570.

Bahr, R. (2005). Understanding Injury Mechanisms: A Key Component of Preventing Injuries in Sport. *British Journal of Sports Medicine*, *39*(6), 324-329.

Bahr, R. (2016). Why Screening Tests to Predict Injury Do Not Work-And Probably Never Will: A Critical Review. In *British Journal of Sports Medicine* (Vol. 50, Issue 13, pp. 776-780).

Balsalobre-Fernández, C., Glaister, M., & Lockey, R. A. (2015). The Validity and Reliability of an iPhone App for Measuring Vertical Jump Performance. *Journal of Sports Sciences*, *33*(15), 1574-1579.

Bartlett, R., Wheat, J., & Robins, M. (2007). Is Movement Variability Important for Sports Biomechanists? *Sports Biomechanics*, *6*(2), 224-243.

Bernardina, G. R. D., Monnet, T., Cerveri, P., & Silvatti, A. P. (2019). Moving System with Action Sport Cameras: 3D Kinematics of The Walking and Running in A Large Volume. *PLoS ONE*, *14*(11).

Bishop, C., Abbott, W., Brashill, C., Loturco, I., Beato, M., & Turner, A. (2022). Seasonal Variation of Physical Performance, Bilateral Deficit, and Interlimb Asymmetry in Elite Academy Soccer Players: Which Metrics Are Sensitive to Change? *Journal of Strength and Conditioning Research*, *37*, 358-365.

Bishop, C., Read, P., Lake, J., Chavda, S., & Turner, A. (2018). Interlimb Asymmetries: Understanding How to Calculate Differences from Bilateral and Unilateral Tests. *Strength and Conditioning Journal*, *40*(4), 1-6.

Bollars, P., Claes, S., Vanlommel, L., Van Crombrugge, K., Corten, K., & Bellemans, J. (2014).

The Effectiveness of Preventive Programs in Decreasing the Risk of Soccer Injuries in Belgium. *The American Journal of Sports Medicine*, *42*(3), 577-582.

Bonazza, N. A., Smuin, D., Onks, C. A., Silvis, M. L., & Dhawan, A. (2017). Reliability, Validity, and Injury Predictive Value of the Functional Movement Screen. In *American Journal of Sports Medicine* (Vol. 45, Issue 3, pp. 725-732).

Britt, E., Ouillette, R., Edmonds, E., Chambers, H., Johnson, K., Bastrom, T., & Pennock, A. (2020). The Challenges of Treating Female Soccer Players with ACL Injuries: Hamstring Versus Bone-Patellar Tendon-Bone Autograft. *Orthopaedic Journal of Sports Medicine*, *8*(11).

Bulow, A., Anderson, J. E., Leiter, J. R., MacDonald, P. B., & Peeler, J. (2019). The Modified Star Excursion Balance And Y-Balance Test Results Differ When Assessing Physically Active Healthy Adolescent Females. *International Journal of Sports Physical Therapy*, *14*(2), 192-203.

Bussey, M. D., Pinfold, J., Romanchuk, J., & Salmon, D. (2023). Anticipatory Head Control Mechanisms in Response to Impact Perturbations: An Investigation of Club Rugby Players with and without A History of Concussion Injury. *Physical Therapy in Sport*, *59*, 7-16.

Butler, R. J., Lehr, M. E., Fink, M. L., Kiesel, K. B., & Plisky, P. J. (2013). Dynamic Balance Performance and Noncontact Lower Extremity Injury in College Football Players: An Initial Study. *Sports Health*, *5*(5), 417-422.

Caccese, J. B., Bryk, K. N., Porfido, T., Bretzin, A. C., Peek, K., Kaminski, T. W., Kontos, A. P., Chrisman, S. P. D., Putukian, M., Buckley, T. A., Broglio, S. P., McAllister, T. W., McCrea, M. A., Pasquina, P. F., & Esopenko, C. (2023). Cognitive and Behavioral Outcomes in Male and Female NCAA Soccer Athletes across Multiple Years: A CARE Consortium Study. *Medicine and Science in Sports and Exercise*, *55*(3), 409-417.

Can, İ., Beka YASAR, A., Bayrakdaroglu, S., & Yildiz, B. (2019). *Fitness Profiling in Women Soccer: Performance Characteristics of Elite Turkish Women Soccer Players*.

Cao, Z., Hidalgo, G., Simon, T., Wei, S.-E., & Sheikh, Y. (2021). OpenPose: Realtime Multi-Person 2D Pose Estimation Using Part Affinity Fields. *IEEE Transactions on Pattern Analysis and Machine Intelligence*, *43*(1), 172-186.

Chaaban, C. R., Berry, N. T., Armitano-Lago, C., Kiefer, A. W., Mazzoleni, M. J., & Padua, D. A. (2021). Combining Inertial Sensors and Machine Learning to Predict vGRF and Knee Biomechanics during a Double Limb Jump Landing Task. *Sensors 2021, Vol. 21, Page 4383*, *21*(13), 4383.

Chen, T., Xu, D., Zhou, Z., Zhou, H., Shao, S., & Gu, Y. (2025). Prediction of Vertical Ground Reaction Forces Under Different Running Speeds: Integration of Wearable IMU with CNN-xLSTM. *Sensors 2025, Vol. 25, Page 1249*, *25*(4), 1249.

Claudino, J. G., Capanema, D. de O., de Souza, T. V., Serrão, J. C., Machado Pereira, A. C., & Nassis, G. P. (2019). Current Approaches to the Use of Artificial Intelligence for Injury Risk

Assessment and Performance Prediction in Team Sports: A Systematic Review. *Sports Medicine - Open*, *5*(1), 28.

Clouthier, A. L., Ross, G. B., & Graham, R. B. (2020). Sensor Data Required for Automatic Recognition of Athletic Tasks Using Deep Neural Networks. *Frontiers in Bioengineering and Biotechnology*, *7*.

Collins, G. S., Reitsma, J. B., Altman, D. G., & Moons, K. G. M. (2015). Transparent Reporting of A Multivariable Prediction Model for Individual Prognosis or Diagnosis (TRIPOD): The TRIPOD Statement. *Annals of Internal Medicine*, *162*(1), 55-63.

Colombel, J., Bonnet, V., Daney, D., Dumas, R., Seilles, A., & Charpillet, F. (2020). Physically Consistent Whole-Body Kinematics Assessment Based on an RGB-D Sensor. Application to Simple Rehabilitation Exercises. *Sensors*, *20*(10), 2848.

Colyer, S. L., Evans, M., Cosker, D. P., & Salo, A. I. T. (2018). A Review of the Evolution of Vision-Based Motion Analysis and the Integration of Advanced Computer Vision Methods Towards Developing a Markerless System. In *Sports Medicine - Open* (Vol. 4, Issue 1, p. 24).

Cook, G., Burton, L., & Hoogenboom, B. (2006). Pre-Participation Screening: The Use of Fundamental Movements as An Assessment of Function - Part 1. *North American Journal of Sports Physical Therapy: NAJSPT*, *1*(2), 62-72.

Cowin, J., Nimphius, S., Fell, J., Culhane, P., & Schmidt, M. (2022). A Proposed Framework to Describe Movement Variability within Sporting Tasks: A Scoping Review. Sports medicine - open, 8(1), 85.

Crisco, J. J., Jokl, P., Heinen, G. T., Connell, M. D., & Panjabi, M. M. (1994). A Muscle Contusion Injury Model: Biomechanics, Physiology, and Histology. *The American Journal of Sports Medicine*, *22*(5), 702-710.

Cusumano, J. P., & Dingwell, J. B. (2013). Movement Variability Near Goal Equivalent Manifolds: Fluctuations, Control, and Model-based Analysis. *Human Movement Science*, *32*(5), 899-923.

De, A., Fernandes, A., Diniz Da Silva, C., Teoldo Da Costa, I., Carlos, J., & Marins, B. (2015). The "FIFA 11+" Warm-Up Programme for Preventing Injuries in Soccer Players: A Systematic Review. *Fisioterapia Em Movimento*, *28*(2), 397-405.

De Brabandere, A., Emmerzaal, J., Timmermans, A., Jonkers, I., Vanwanseele, B., & Davis, J. (2020). A Machine Learning Approach to Estimate Hip and Knee Joint Loading Using a Mobile Phone-Embedded IMU. *Frontiers in Bioengineering and Biotechnology*, *8*, 320.

Di Paolo, S., Nijmeijer, E., Bragonzoni, L., Dingshoff, E., Gokeler, A., & Benjaminse, A. (2023). Comparing Lab and Field Agility Kinematics in Young Talented Female Football Players: Implications for ACL Injury Prevention. *European Journal of Sport Science*, *23*(5), 859-868.

Díaz-Ochoa, A., Gómez-Renaud, M., Hoyos-Flores, J. R., Hernández-Cruz, G., (FEADEF), F. E. de A. de D. de E. F. (F E. F. E. de A. de D. de E. F. sica, & (México), A. U. of N. L. (México)

A. U. of N. L. (2023). *Variations in Physical Performance During a Competitive Season in Mexican Female Varsity Soccer Players by Playing Position*.

Difiori, J. P., Benjamin, H. J., Brenner, J. S., Gregory, A., Jayanthi, N., Landry, G. L., & Luke, A. (2014). Overuse Injuries and Burnout in Youth Sports: A Position Statement from The American Medical Society for Sports Medicine. *British Journal of Sports Medicine*, *48*(4), 287-288.

Dingwell, J. B., John, J., & Cusumano, J. P. (2010). Do Humans Optimally Exploit Redundancy to Control Step Variability in Walking? *PLoS Computational Biology*, *6*(7), e1000856.

Dingwell, J. B., & Marin, L. C. (2006). Kinematic Variability and Local Dynamic Stability of Upper Body Motions When Walking at Different Speeds. *Journal of Biomechanics*, *39*(3), 444-452.

D'Onofrio, R., Alashram, A. R., Annino, G., Masucci, M., Romagnoli, C., Padua, E., & Manzi, V. (2023). Prevention of Secondary Injury after Anterior Cruciate Ligament Reconstruction: Relationship between Pelvic-Drop and Dynamic Knee Valgus. *International Journal of Environmental Research and Public Health*, *20*(4), 3063.

Dos, T., Thomas, C., & Jones, P. A. (2021). The Effect of Angle on Change of Direction Biomechanics: Comparison and Inter-Task Relationships. *Journal of Sports Sciences*, *39*, 2618-2631.

Dos'Santos, T., Stebbings, G. K., Morse, C., Shashidharan, M., Daniels, K. A. J., & Sanderson, A. (2023). Effects of the Menstrual Cycle Phase on Anterior Cruciate Ligament Neuromuscular and Biomechanical Injury Risk Surrogates in Eumenorrheic and Naturally Menstruating Women: A Systematic Review. *PLoS ONE*, *18*(1 January).

Drazan, J. F., Phillips, W. T., Seethapathi, N., Hullfish, T. J., & Baxter, J. R. (2021). Moving Outside the Lab: Markerless Motion Capture Accurately Quantifies Sagittal Plane Kinematics During the Vertical Jump. *Journal of Biomechanics*, *125*, 110547.

Emery, C. A., Roy, T. O., Whittaker, J. L., Nettel-Aguirre, A., & Van Mechelen, W. (2015). Neuromuscular Training Injury Prevention Strategies in Youth Sport: A Systematic Review and Meta-Analysis. *British Journal of Sports Medicine*, *49*(13), 865-870.

Engebretsen, L., Soligard, T., Steffen, K., Alonso, J. M., Aubry, M., Budgett, R., Dvorak, J., Jegathesan, M., Meeuwisse, W. H., Mountjoy, M., Palmer-Green, D., Vanhegan, I., & Renström, P. A. (2013). Sports Injuries and Illnesses During the London Summer Olympic Games 2012. *British Journal of Sports Medicine*, *47*(7), 407-414.

Fältström, A., Kvist, J., Gauffin, H., & Hägglund, M. (2019). Female Soccer Players with Anterior Cruciate Ligament Reconstruction Have a Higher Risk of New Knee Injuries and Quit Soccer to a Higher Degree Than Knee-Healthy Controls. *The American Journal of Sports Medicine*, *47*(1), 31-40.

Frost, D. M., Beach, T. A. C., Callaghan, J. P., & McGill, S. M. (2015). FMS Scores Change with

Performers' Knowledge of The Grading Criteria - Are General Whole-Body Movement Screens Capturing "Dysfunction"? *Journal of Strength and Conditioning Research*, *29*(11), 3037-3044.

Gabbett, T. J. (2016). The Training - Injury Prevention Paradox: Should Athletes Be Training Smarter and Harder? *British Journal of Sports Medicine*, *50*(5), 273-280.

Garrett, J. (1996). Muscle Strain Injuries. In *American Journal of Sports Medicine* (Vol. 24, Issue SUPPL.).

Gates, D. H., & Dingwell, J. B. (2008). The Effects of Neuromuscular Fatigue on Task Performance During Repetitive Goal-Directed Movements. *Experimental Brain Research*, *187*(4), 573-585.

Gathercole, R., Sporer, B., Stellingwerff, T., & Sleivert, G. (2015). Alternative Countermovement-Jump Analysis to Quantify Acute Neuromuscular Fatigue. *International Journal of Sports Physiology and Performance*, *10*(1), 84-92.

Giza, E., & Micheli, L. J. (2005). Soccer Injuries. In *Medicine and sport science* (Vol. 49, pp. 140-169).

Griffin, L. Y., Albohm, M. J., Arendt, E. A., Bahr, R., Beynnon, B. D., DeMaio, M., Dick, R. W., Engebretsen, L., Garrett, W. E., Hannafin, J. A., Hewett, T. E., Huston, L. J., Ireland, M. L., Johnson, R. J., Lephart, S., Mandelbaum, B. R., Mann, B. J., Marks, P. H., Marshall, S. W., … Yu, B. (2006). Understanding and Preventing Noncontact Anterior Cruciate Ligament Injuries: A Review of The Hunt Valley II Meeting, January 2005. *American Journal of Sports Medicine*, *34*(9), 1512-1532.

Gulgin, H., & Hoogenboom, B. (2014). The Functional Movement Screening (FMS)TM: An Inter-Rater Reliability Study Between Raters of Varied Experience. *International Journal of Sports Physical Therapy*, *9*(1), 14-20.

Guskiewicz, K. M., Ross, S. E., & Marshall, S. W. (2001). Postural Stability and Neuropsychological Deficits After Concussion in Collegiate Athletes. *Journal of Athletic Training*, *36*(3), 263.

Gustavsson, A., Neeter, C., Thomeé, P., Grävare Silbernagel, K., Augustsson, J., Thomeé, R., & Karlsson, J. (2006). A Test Battery for Evaluating Hop Performance in Patients with An ACL Injury and Patients Who Have Undergone ACL Reconstruction. *Knee Surgery, Sports Traumatology, Arthroscopy*, *14*(8), 778-788.

Haase, F. K., Prien, A., Douw, L., Feddermann-Demont, N., Junge, A., & Reinsberger, C. (2023). Cortical Thickness and Neurocognitive Performance in Former High-Level Female Soccer and Non-Contact Sport Athletes. *Scandinavian Journal of Medicine & Science in Sports*, *33*(6), 921-930.

Hägglund, M., Waldén, M., & Ekstrand, J. (2006). Previous Injury as A Risk Factor for Injury in Elite Football: A Prospective Study Over Two Consecutive Seasons. *British Journal of Sports*

Medicine, *40*(9), 767-772.

Hahn, J., Giansanti, D., Review, S., & Allen, B. (2024). The Promise of Explainable AI in Digital Health for Precision Medicine: A Systematic Review. *Journal of Personalized Medicine 2024, Vol. 14, Page 277*, *14*(3), 277.

Han, R., Qi, F., Wang, H., & Yi, M. (2024). Innovative Machine Learning Approach for Analysing Biomechanical Factors in Running-Related Injuries. *Molecular & Cellular Biomechanics*, *21*(3), 530-530.

Harsted, S., Holsgaard-Larsen, A., Hestbæk, L., Boyle, E., & Lauridsen, H. H. (2019). Concurrent Validity of Lower Extremity Kinematics and Jump Characteristics Captured in Pre-School Children by A Markerless 3D Motion Capture System. *Chiropractic and Manual Therapies*, *27*(1), 1-16.

Hassanmirzaei, B., Fahimipour, F., Haratian, Z., Moghadam, N., Hassanmirzaei, B., Fahimipour, F., Haratian, Z., Moghadam, N., Hassanmirzaei, B., Fahimipour, F., Haratian, Z., Moghadam, N., Hassanmirzaei, B., Fahimipour, F., Haratian, Z., Moghadam, N., Hassanmirzaei, B., Fahimipour, F., Haratian, Z., & Moghadam, N. (2021). The Association of Visual Impairments of Elite Soccer Players with Concussion and Sports Injuries: A Prospective Cohort Study. *Asian Journal of Sports Medicine 2021 12:2*, *12*(2).

Herman, D. C., Jones, D., Harrison, A., Moser, M., Tillman, S., Farmer, K., Pass, A., Clugston, J. R., Hernandez, J., & Chmielewski, T. L. (2017). Concussion May Increase the Risk of Subsequent Lower Extremity Musculoskeletal Injury in Collegiate Athletes. *Sports Medicine (Auckland, N.Z.)*, *47*(5), 1003-1010.

Hewett, T. E., Myer, G. D., Ford, K. R., Heidt, R. S., Colosimo, A. J., McLean, S. G., Van Den Bogert, A. J., Paterno, M. V., & Succop, P. (2005). Biomechanical Measures of Neuromuscular Control and Valgus Loading of The Knee Predict Anterior Cruciate Ligament Injury Risk in Female Athletes: A Prospective Study. *American Journal of Sports Medicine*, *33*(4), 492-501.

Howell, D. R., Lynall, R. C., Buckley, T. A., & Herman, D. C. (2018). Neuromuscular Control Deficits and the Risk of Subsequent Injury after a Concussion: A Scoping Review. *Sports Medicine 2018 48:5*, *48*(5), 1097-1115.

Howell, D. R., Myer, G. D., Grooms, D., Diekfuss, J., Yuan, W., & Meehan, W. P. (2019). Examining Motor Tasks of Differing Complexity After Concussion in Adolescents. *Archives of Physical Medicine and Rehabilitation*, *100*(4), 613-619.

Huang, Y., Huang, S., Wang, Y., Li, Y., Gui, Y., & Huang, C. (2022). A Novel Lower Extremity Non-Contact Injury Risk Prediction Model Based on Multimodal Fusion and Interpretable Machine Learning. *Frontiers in Physiology, 13*.

Huang, X., Yan, Z., Ma, Y., & Liu, H. (2023). The Influence of Different Levels of Physical Activity and Sports Performance on The Accuracy of Dynamic Lower Limbs Balance

Assessment Among Chinese Physical Education College Students. *Frontiers in Physiology*, *14*, 1184340.

Hulme, A., Thompson, J., Nielsen, R. O., Read, G. J. M., & Salmon, P. M. (2019). Towards A Complex Systems Approach in Sports Injury Research: Simulating Running-Related Injury Development with Agent-Based Modelling. *British Journal of Sports Medicine*, *53*(9), 560-569.

Hutchison, M., Comper, P., Mainwaring, L., & Richards, D. (2011). The Influence of Musculoskeletal Injury on Cognition: Implications for Concussion Research. *American Journal of Sports Medicine*, *39*(11), 2331-2337.

Janisch, J., Kirven, J., Schapker, N., Myers, L. C., Shapiro, L. J., & Young, J. W. (2024). Protocol To Record and Analyze Primate Leaping in Three Dimensions in The Wild. *Journal of Experimental Zoology Part A: Ecological and Integrative Physiology*, *341*(9), 965-976.

Joos, V., Somers, V., & Standaert, B. (2024). *TrackLab*. Github repository.

Kakavas, G., Malliaropoulos, N., Skarpas, G., & Forelli, F. (2025). The Impact of Concussions on Neuromuscular Control and Anterior Cruciate Ligament Injury Risk in Female Soccer Players: Mechanisms and Prevention - A Narrative Review. *Journal of Clinical Medicine 2025, Vol. 14, Page 3199*, *14*(9), 3199.

Kaneko, S., Sasaki, S., Hirose, N., Nagano, Y., Fukano, M., Fukubayashi, T., Kaneko, S., Sasaki, S., Hirose, N., Nagano, Y., Fukano, M., Fukubayashi, T., Kaneko, S., Sasaki, S., Hirose, N., Nagano, Y., Fukano, M., Fukubayashi, T., Kaneko, S., … Fukubayashi, T. (2017). Mechanism of Anterior Cruciate Ligament Injury in Female Soccer Players. *Asian Journal of Sports Medicine 2017 8:1*, *8*(1).

Kanko, R. M., Laende, E. K., Davis, E. M., Selbie, W. S., & Deluzio, K. J. (2021). Concurrent Assessment of Gait Kinematics Using Marker-Based and Markerless Motion Capture. *Journal of Biomechanics*, *127*, 110665.

Kim, D., Lee, J., Cho, M., & Kwak, S. (2022). Detector-Free Weakly Supervised Group Activity Recognition. *Proceedings of the IEEE Computer Society Conference on Computer Vision and Pattern Recognition*, *2022-June*, 20051-20061.

Kolodziej, M., Willwacher, S., Nolte, K., Schmidt, M., & Jaitner, T. (2022). Biomechanical Risk Factors of Injury-Related Single-Leg Movements in Male Elite Youth Soccer Players. *Biomechanics 2022, Vol. 2, Pages 281-300*, *2*(2), 281-300.

Komar, J., Seifert, L., & Thouvarecq, R. (2015). What Variability Tells Us About Motor Expertise: Measurements and Perspectives from A Complex System Approach. *Movement & Sport Sciences - Science & Motricité*, *89*, 65-77.

Krosshaug, T., Steffen, K., Kristianslund, E., Nilstad, A., Mok, K.-M., Myklebust, G., Andersen, T. E., Holme, I., Engebretsen, L., & Bahr, R. (2016). The Vertical Drop Jump Is a Poor Screening Test for ACL Injuries in Female Elite Soccer and Handball Players. *The American*

Journal of Sports Medicine, *44*(4), 874-883.

Li, C., Ivarsson, A., Lam, L. T., & Sun, J. (2019). Basic Psychological Needs Satisfaction and Frustration, Stress, And Sports Injury Among University Athletes: A Four-Wave Prospective Survey. *Frontiers in Psychology*, *10*(MAR), 450619.

López-Valenciano, A., Ruiz-Pérez, I., Garcia-Gómez, A., Vera-Garcia, F. J., De Ste Croix, M., Myer, G. D., & Ayala, F. (2020). Epidemiology of Injuries in Professional Football: A Systematic Review and Meta-Analysis. *British Journal of Sports Medicine* (Vol. 54, Issue 12, pp. 711-718).

Lynall, R. C., Mauntel, T. C., Padua, D. A., & Mihalik, J. P. (2015). Acute Lower Extremity Injury Rates Increase after Concussion in College Athletes. *Medicine and Science in Sports and Exercise*, *47*(12), 2487-2492.

John, G., AlNadwi, A., Georges Abi Antoun, T., & Ahmetov, I. I. (2025). Injury Prevention Strategies in Female Football Players: Addressing Sex-Specific Risks. Sports (Basel, Switzerland), 13(2), 39.

Maemichi, T., & Kumai, T. (2025). Long-Term Injury Survey in a Japanese University Women's Soccer Team. *International Journal of Sports Physical Therapy*, *20*(4), 572-582.

Maldonado, G., Bailly, F., Souères, P., & Watier, B. (2018). On The Coordination of Highly Dynamic Human Movements: An Extension of The Uncontrolled Manifold Approach Applied to Precision Jump in Parkour. *Scientific Reports*, *8*(1), 12219.

Malone, S., Owen, A., Newton, M., Mendes, B., Collins, K. D., & Gabbett, T. J. (2017). The Acute:Chonic Workload Ratio in Relation to Injury Risk in Professional Soccer. *Journal of Science and Medicine in Sport*, *20*(6), 561-565.

Markovic, G., Dizdar, D., Jukic, I., & Cardinale, M. (2004). Reliability And Factorial Validity of Squat and Countermovement Jump Tests. *Journal of Strength and Conditioning Research*, *18*(3), 551-555.

Martin, V., Reimann, H., & Schöner, G. (2019). A Process Account of The Uncontrolled Manifold Structure of Joint Space Variance in Pointing Movements. *Biological Cybernetics*, *113*(3), 293-307.

Mathis, A., Schneider, S., Lauer, J., & Mathis, M. W. (2020). A Primer on Motion Capture with Deep Learning: Principles, Pitfalls, and Perspectives. *Neuron*, *108*(1), 44-65.

McCall, A., Carling, C., Davison, M., Nedelec, M., Le Gall, F., Berthoin, S., & Dupont, G. (2015). Injury Risk Factors, Screening Tests and Preventative Strategies: A Systematic Review of The Evidence That Underpins the Perceptions and Practices of 44 Football (Soccer) Teams from Various Premier Leagues. *British Journal of Sports Medicine* (Vol. 49, Issue 9, pp. 583-589).

McCall, A., Dupont, G., & Ekstrand, J. (2016). Injury Prevention Strategies, Coach Compliance and Player Adherence of 33 of the UEFA Elite Club Injury Study Teams: A Survey of Teams'

Head Medical Officers. *British Journal of Sports Medicine*, *50*(12), 725-730.

McCrory, P., Meeuwisse, W., Dvořák, J., Aubry, M., Bailes, J., Broglio, S., Cantu, R. C., Cassidy, D., Echemendia, R. J., Castellani, R. J., Davis, G. A., Ellenbogen, R., Emery, C., Engebretsen, L., Feddermann-Demont, N., Giza, C. C., Guskiewicz, K. M., Herring, S., Iverson, G. L., … Vos, P. E. (2017). Consensus Statement on Concussion in Sport - The 5th International Conference on Concussion in Sport Held in Berlin, October 2016. *British Journal of Sports Medicine*, *51*(11), 838-847.

McCunn, R., aus der Fünten, K., Fullagar, H. H. K., McKeown, I., & Meyer, T. (2016). Reliability And Association with Injury of Movement Screens: A Critical Review. *Sports Medicine, 46(6)*, 763-781.

McDevitt, S., Hernandez, H., Hicks, J., Lowell, R., Bentahaikt, H., Burch, R., Ball, J., Chander, H., Freeman, C., Taylor, C., & Anderson, B. (2022). Wearables for Biomechanical Performance Optimization and Risk Assessment in Industrial and Sports Applications. *Bioengineering*, *9*(1).

McKeown, I., Taylor-McKeown, K., Woods, C., & Ball, N. (2014). Athletic Ability Assessment: A Movement Assessment Protocol for Athletes. *International Journal of Sports Physical Therapy*, *9*(7), 862-873.

Meng, Y., Bíró, I., & Sárosi, J. (2023). Markerless Measurement Techniques for Motion Analysis in Sports Science. *Analecta Technica Szegedinensia*, *17*(2), 24-31.

Mooney, J., Self, M., Refaey, K., Elsayed, G., Chagoya, G., Bernstock, J. D., & Johnston, J. M. (2020). Concussion in Soccer: A Comprehensive Review of The Literature. *Concussion*, *5*(3).

Moshawrab, M., Adda, M., Bouzouane, A., Ibrahim, H., & Raad, A. (2023). Reviewing Federated Machine Learning and Its Use in Diseases Prediction. *Sensors 2023, Vol. 23, Page 2112*, *23*(4), 2112.

Mündermann, L., Corazza, S., & Andriacchi, T. P. (2006). The Evolution of Methods for The Capture of Human Movement Leading to Markerless Motion Capture for Biomechanical Applications. In *Journal of NeuroEngineering and Rehabilitation* (Vol. 3, Issue 1, pp. 1-11).

Myer, G. D., Ford, K. R., Paterno, M. V., Nick, T. G., & Hewett, T. E. (2008). The Effects of Generalized Joint Laxity on Risk of Anterior Cruciate Ligament Injury in Young Female Athletes. *The American Journal of Sports Medicine*, *36*(6), 1073-1080.

Nakahira, Y., Taketomi, S., Kawaguchi, K., Mizutani, Y., Hasegawa, M., Ito, C., Uchiyama, E., Ikegami, Y., Fujiwara, S., Yamamoto, K., Nakamura, Y., Tanaka, S., & Ogata, T. (2022). Kinematic Differences Between the Dominant and Nondominant Legs During a Single-Leg Drop Vertical Jump in Female Soccer Players. *American Journal of Sports Medicine*, *50*(10), 2817-2823.

Nakamoto, H., & Mori, S. (2008). Sport-Specific Decision-Making in a Go/Nogo Reaction Task: Difference among Nonathletes and Baseball and Basketball Players. *Perceptual and Motor*

Skills, *106*(1), 163-170.

Nakano, N., Sakura, T., Ueda, K., Omura, L., Kimura, A., Iino, Y., Fukashiro, S., & Yoshioka, S. (2020). Evaluation of 3D Markerless Motion Capture Accuracy Using OpenPose with Multiple Video Cameras. *Frontiers in Sports and Active Living*, *2*.

Nawasreh, Z. H., Yabroudi, M. A., Darwish, A. A., Debes, W. A., & Bashaireh, K. M. (2022). Player Sex and Playing Surface Are Individual Predictors of Injuries in Professional Soccer Players. *Pathophysiology 2022, Vol. 29, Pages 619-630*, *29*(4), 619-630.

Newell, K. M., & Slifkin, A. B. (1998). The Nature of Movement Variability. In *Motor Behavior and Human Skill* (pp. 143-159).

Niyonsenga, J. D., & Phillips, J. S. (2013). Factors Associated with Injuries Among First-Division Rwandan Female Soccer Players. *African Health Sciences*, *13*(4), 1021-1026.

Noyes, F. R., Barber, S. D., & Mangine, R. E. (1991). Abnormal Lower Limb Symmetry Determined by Function Hop Tests After Anterior Cruciate Ligament Rupture. *The American Journal of Sports Medicine*, *19*(5), 513-518.

Oliveira, L. Á., Melendi, D., & García, R. (2024). Comparing Tactical Analysis Methods in Women's Soccer Using Positioning Data from Electronic Performance and Tracking Systems. *Electronics 2024, Vol. 13, Page 1876*, *13*(10), 1876.

Paillard, T., & Noé, F. (2006). Effect Of Expertise and Visual Contribution on Postural Control in Soccer. *Scandinavian Journal of Medicine and Science in Sports*, *16*(5), 345-348.

Pappas, E., Shiyko, M. P., Ford, K. R., Myer, G. D., & Hewett, T. E. (2016). Biomechanical Deficit Profiles Associated with ACL Injury Risk in Female Athletes. *Medicine and Science in Sports and Exercise*, *48*(1), 107-113.

Parker, E. A., Duchman, K. R., Meyer, A. M., Wolf, B. R., & Westermann, R. W. (2024). Menstrual Cycle Hormone Relaxin and ACL Injuries in Female Athletes: A Systematic Review. *The Iowa Orthopaedic Journal*, *44*(1), 113.

Paterno, M. V., Taylor-Haas, J. A., Myer, G. D., & Hewett, T. E. (2013). Prevention Of Overuse Sports Injuries in The Young Athlete. In *Orthopedic Clinics of North America* (Vol. 44, Issue 4, pp. 553-564).

Plisky, P. J., Rauh, M. J., Kaminski, T. W., & Underwood, F. B. (2006). Star Excursion Balance Test as A Predictor of Lower Extremity Injury in High School Basketball Players. *Journal of Orthopaedic and Sports Physical Therapy*, *36*(12), 911-919.

Prien, A., Besuden, C., Junge, A., Feddermann-Demont, N., Brugger, P., & Verhagen, E. (2020). Cognitive Ageing in Top-Level Female Soccer Players Compared to a Normative Sample from the General Population: A Cross-sectional Study. *Journal of the International Neuropsychological Society*, *26*(7), 645-653.

Rad, N. F., Alimoradi, M., Antohe, B., Uysal, H. Ş., Korkmaz, S., & Mohammadian, Z. (2024).

Modeling of Ankle Joint Range of Motion and Landing Quality Scores in Female Soccer Players with Quantile Regression Approach.

Ralston, B., Arthur, J., Makovicka, J. L., Hassebrock, J., Tummala, S., Deckey, D. G., Patel, K., Chhabra, A., & Hartigan, D. (2020). Hip and Groin Injuries in National Collegiate Athletic Association Women's Soccer Players. *Orthopaedic Journal of Sports Medicine*, *8*(1).

Ramkumar, P. N., Luu, B. C., Haeberle, H. S., Karnuta, J. M., Nwachukwu, B. U., & Williams, R. J. (2022). Sports Medicine and Artificial Intelligence: A Primer. *American Journal of Sports Medicine*, *50*(4), 1166-1174.

Randell, R. K., Clifford, T., Drust, B., Moss, S. L., Unnithan, V. B., De Ste Croix, M. B. A., Datson, N., Martin, D., Mayho, H., Carter, J. M., & Rollo, I. (2021). Physiological Characteristics of Female Soccer Players and Health and Performance Considerations: A Narrative Review. *Sports Medicine 2021 51:7*, *51*(7), 1377-1399.

Renstrom, P., Ljungqvist, A., Arendt, E., Beynnon, B., Fukubayashi, T., Garrett, W., Georgoulis, T., Hewett, T. E., Johnson, R., Krosshaug, T., Mandelbaum, B., Micheli, L., Myklebust, G., Roos, E., Roos, H., Schamasch, P., Shultz, S., Werner, S., Wojtys, E., & Engebretsen, L. (2008). Non-Contact ACL Injuries in Female Athletes: An International Olympic Committee Current Concepts Statement. *British Journal of Sports Medicine*, *42*(6), 394-412.

Robert-Lachaine, X., Mecheri, H., Larue, C., & Plamondon, A. (2017). Accuracy And Repeatability of Single-Pose Calibration of Inertial Measurement Units for Whole-Body Motion Analysis. *Gait and Posture*, *54*, 80-86.

Roberts, D., Khan, H., Kim, J. H., Slover, J., & Walker, P. S. (2013). Acceleration-Based Joint Stability Parameters for Total Knee Arthroplasty That Correspond with Patient-Reported Instability. *Proceedings of the Institution of Mechanical Engineers, Part H: Journal of Engineering in Medicine*, *227*(10), 1104-1113.

Ross, G. B., Dowling, B., Troje, N. F., Fischer, S. L., & Graham, R. B. (2020). Classifying Elite from Novice Athletes Using Simulated Wearable Sensor Data. *Frontiers in Bioengineering and Biotechnology*, *8*.

Scholz, J. P., & Schöner, G. (1999). The Uncontrolled Manifold Concept: Identifying Control Variables for a Functional Task. *Experimental Brain Research*, *126*(3), 289-306.

Serrien, B., Witterzeel, E., & Baeyens, J.-P. P. (2018). The Uncontrolled Manifold Concept Reveals That the Structure of Postural Control in Recurve Archery Shooting Is Related to Accuracy. *Journal of Functional Morphology and Kinesiology*, *3*(3), 48.

Seshadri, D.R., Li, R.T., Voos, J.E. et al. Wearable Sensors for Monitoring the Internal and External Workload of The Athlete. npj Digit. Med. 2, 71 (2019).

Silvers-Granelli, H., Mandelbaum, B., Adeniji, O., Insler, S., Bizzini, M., Pohlig, R., Junge, A., Snyder-Mackler, L., & Dvorak, J. (2015). Efficacy of The FIFA 11+ Injury Prevention Program in The Collegiate Male Soccer Player. *American Journal of Sports Medicine*, *43*(11),

2628-2637.

Slembrouck, M., Luong, H., Gerlo, J., Schütte, K., Van Cauwelaert, D., De Clercq, D., Vanwanseele, B., Veelaert, P., & Philips, W. (2020). Multiview 3D Markerless Human Pose Estimation from OpenPose Skeletons. *Lecture Notes in Computer Science (Including Subseries Lecture Notes in Artificial Intelligence and Lecture Notes in Bioinformatics)*, *12002 LNCS*, 166-178.

Somers, V., Joos, V., Cioppa, A., Giancola, S., Ghasemzadeh, S. A., Magera, F., Standaert, B., Mansourian, A. M., Zhou, X., Kasaei, S., Ghanem, B., Alahi, A., Van Droogenbroeck, M., & De Vleeschouwer, C. (2024). *Soccernet Game State Reconstruction: End-To-End Athlete Tracking and Identification on A Minimap*.

Song, K., Hullfish, T. J., Scattone Silva, R., Silbernagel, K. G., & Baxter, J. R. (2023). Markerless Motion Capture Estimates of Lower Extremity Kinematics and Kinetics Are Comparable to Marker-Based Across 8 Movements. *Journal of Biomechanics*, *157*, 111751.

Spierer, D. K., Petersen, R. A., Duffy, K., Corcoran, B. M., & Tracye, R. M. (2010). Gender Influence on Response Time to Sensory Stimuli. *Journal of Strength and Conditioning Research*, *24*(4), 957-963.

Stergiou, N., & Decker, L. M. (2011). Human Movement Variability, Nonlinear Dynamics, And Pathology: Is There a Connection? *Human Movement Science*, *30*(5), 869-888.

Thornton, H. R., Delaney, J. A., Duthie, G. M., & Dascombe, B. J. (2019). Developing Athlete Monitoring Systems in Team Sports: Data Analysis and Visualization. *International Journal of Sports Physiology and Performance*, *14*(6), 698-705.

Ullah, K., Ahsan, M., Hasanat, S. M., Haris, M., Yousaf, H., Raza, S. F., Tandon, R., Abid, S., & Ullah, Z. (2024). Short-Term Load Forecasting: A Comprehensive Review and Simulation Study with CNN-LSTM Hybrids Approach. *IEEE Access*, *12*, 111858-111881.

Van Eetvelde, H., Mendonça, L. D., Ley, C., Seil, R., & Tischer, T. (2021). Machine Learning Methods in Sport Injury Prediction and Prevention: A Systematic Review. *Journal of Experimental Orthopaedics*, *8*(1).

Vedung, F., Hänni, S., Tegner, Y., Johansson, J., & Marklund, N. (2020). Concussion Incidence and Recovery in Swedish Elite Soccer - Prolonged Recovery in Female Players. *Scandinavian Journal of Medicine and Science in Sports*, *30*(5), 947-957.

Wade, L., Needham, L., McGuigan, P., & Bilzon, J. (2022). Applications And Limitations of Current Markerless Motion Capture Methods for Clinical Gait Biomechanics. *PeerJ*, *10*, e12995.

Weber, A. E., Trasolini, N. A., Bolia, I. K., Rosario, S., Prodromo, J. P., Hill, C., Romano, R., Liu, C. Y., Tibone, J. E., & Gamradt, S. C. (2020). Epidemiologic Assessment of Concussions in an NCAA Division I Women's Soccer Team. *Orthopaedic Journal of Sports Medicine*, *8*(5).

Wei, K., & Kording, K. P. (2018). Behavioral Tracking Gets Real. *Nature Neuroscience*, *21*(9), 1146-1147.

Weiner, A. R., Durbin, J. R., Lunardi, S. R., Li, A. Y., Hannah, T. C., Schupper, A. J., Gal, J. S., Jumreornvong, O., Spiera, Z., Ali, M., Marayati, N. F., Gometz, A., Lovell, M. R., & Choudhri, T. F. (2022). Incidence and Severity of Concussions Among Young Soccer Players Based on Age, Sex, and Player Position. *Orthopaedic Journal of Sports Medicine*, *10*(1).

Wisløff, U., Castagna, C., Helgerud, J., Jones, R., & Hoff, J. (2004). Strong Correlation of Maximal Squat Strength with Sprint Performance and Vertical Jump Height in Elite Soccer Players. *British Journal of Sports Medicine*, *38*(3), 285-288.

Xiao, M., Lemos, J. L., Hwang, C. E., Sherman, S. L., Safran, M. R., & Abrams, G. D. (2022). Increased Risk of ACL Injury for Female but Not Male Soccer Players on Artificial Turf Versus Natural Grass: A Systematic Review and Meta-Analysis. *Orthopaedic Journal of Sports Medicine*, *10*(8).

Xiao, M., Nguyen, J. N., Hwang, C. E., & Abrams, G. D. (2021). Increased Lower Extremity Injury Risk Associated with Player Load and Distance in Collegiate Women's Soccer. *Orthopaedic Journal of Sports Medicine*, *9*(10).

Xu, L., Liu, Y., Cheng, W., Guo, K., Zhou, G., Dai, Q., & Fang, L. (2018). FlyCap: Markerless Motion Capture Using Multiple Autonomous Flying Cameras. *IEEE Transactions on Visualization and Computer Graphics*, *24*(8), 2284-2297.

Yang, J., Tibbetts, A. S., Covassin, T., Cheng, G., Nayar, S., & Heiden, E. (2012). Epidemiology of overuse and acute injuries among competitive collegiate athletes. *Journal of Athletic Training*, *47*(2), 198-204.

Zago, M., Luzzago, M., Marangoni, T., De Cecco, M., Tarabini, M., & Galli, M. (2020). 3D Tracking of Human Motion Using Visual Skeletonization and Stereoscopic Vision. *Frontiers in Bioengineering and Biotechnology*, *8*, 181.

Zhao, Q., Zheng, C., Liu, M., Wang, P., & Chen, C. (2023). PoseFormerV2: Exploring Frequency Domain for Efficient and Robust 3D Human Pose Estimation. *Proceedings of the IEEE Computer Society Conference on Computer Vision and Pattern Recognition*, *2023-June*, 8877-8886.

Appendix A. Movement Tests

T-Balance

The athlete begins by standing on one leg with the opposite hip and knee flexed to 90° and the hands in a prayer position at nipple line (Figure A.1). This position is held for three seconds. In one fluid motion, the athlete hinges at the hip, extending the hip and knee, bringing the trunk parallel to the floor, while extending both of arms out to 90° of abduction at the shoulder, creating a T-shape with the arms and the trunk (Figure A.1b-c). The athlete rotates forward as far as possible, while maintaining balance. Once reaching the T-position, the athlete then returns to the starting position (Figure A.1d).

The athletes will undergo two trials for each condition, one with their eyes open and another with their eyes closed, for both sides.

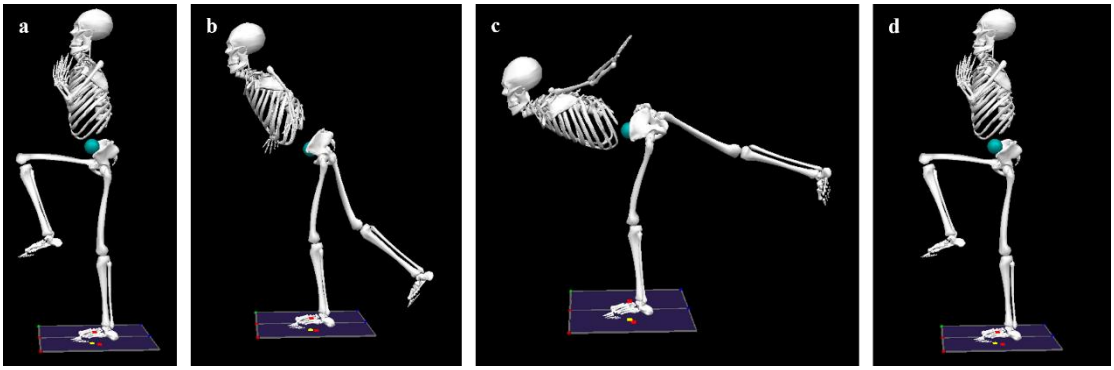

Figure A.1: T-Balance task: (a) stand on one leg with opposite hip and knee at 90° and hands in prayer; (b) hinge at the hip as the trunk lowers; (c) reach forward into the T-position with arms abducted 90° and non-stance leg extended; (d) return upright.

Y-Balance

The goal of this test is to maintain single-leg balance on one leg while reaching as far as possible with the contralateral leg in three different directions using a Y-balance kit (Figure A.2). The three movement directions are anterior, posteromedial and posterolateral, performed on each leg.

The starting position is standing on one leg at the stance plate with the toes of the foot at the red line, and the other leg touching down lightly just behind the plate (Figure A.3a). The non-

stance foot is reached out in the desired direction, pushing the reach indicator as far as they can while maintaining balance (Figure A.3b-d). The free foot must be returned to the starting position under control (Figure A.3e). The subject may not touch down the free leg during the movement to keep balance or put their foot on top of the reach indicator to gain support and cannot kick out the indicator.

Figure A.2: The Y-Balance Test kit, displaying the central platform with three reaching arms/reach indicator used to measure multidirectional reach distances.

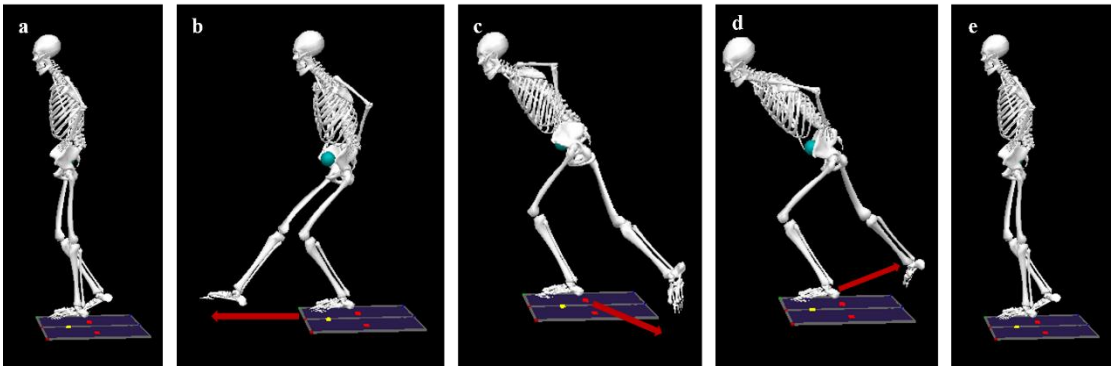

Figure A.3: Y-Balance test: (a) the subject stands on one leg with the toes aligned to the red start line and the contralateral foot lightly touching behind; (b-d) the free leg reaches as far as possible in the anterior, posteromedial, or posterolateral direction, pushing the reach indicator while maintaining single-leg balance; (e) the reaching foot returns under control to the start position.

L-Hop

The athlete starts standing on both legs and jumps horizontally as far as he/she is able to (Figure A.4a). Upon landing, the athlete lands on one foot and then jumps laterally as far as he/she can from the single planted foot (Figure A.4b-c) landing on the opposite foot (Figure A.4d).

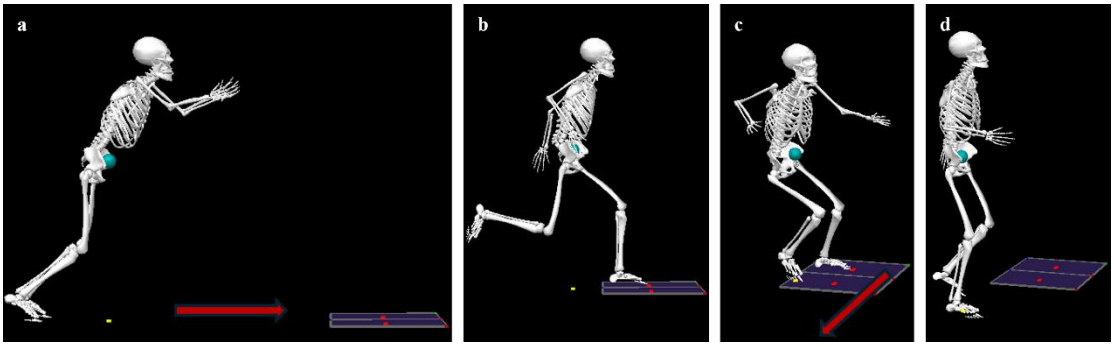

Figure A.4: L-Hop test: (a) athlete begins standing on both legs, jumps forward as far as possible; (b-c) upon landing on one foot, the athlete immediately jumps laterally as far as possible; (d) the athlete lands on the opposite foot.

Bilateral body-weight squat

Participants initiate the movement from an upright position with the knees and hips fully extended (Figure A.5a). They will be asked to elevate their arms in front of themselves. To allow participants to exhibit their movement variability, there will be no further restrictions of the movement. A full repetition involves descending until both thighs dropped below or parallel to the ground, keeping the heels on the floor, and returning to the upright position (Figure A.5b-e). After hearing a verbal command to begin, the participants will control their movement pace to the metronome beat (40 beats per minute; Figure 14 bottom) to the best of their ability. The movement will be repeated 35 times.

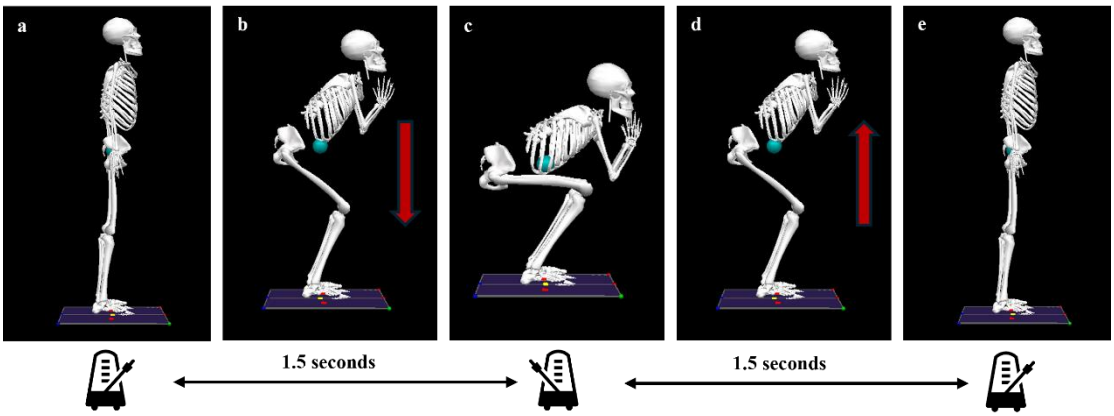

Figure A.5: Squat task: (a) start upright with hips and knees fully extended; (b) descent toward thighs at least parallel to the floor; (c) bottom position; (d) ascent from the bottom; (e) return to full extension.

Countermovement jump

This movement is performed both on a single leg (left/right) and bilaterally. The athlete starts by standing on two force plates (Figure A.6a). They then perform a quick downward movement (countermovement) before jumping as high as possible (Figure A.6b). The athlete uses both arms and single leg/legs to generate maximal force and height (Figure A.6c) and land on the force plates (Figure A.6d). The jump should be performed with consistent countermovement depth and arm swing, maintaining extended hip, knee, and ankle joints during flight.

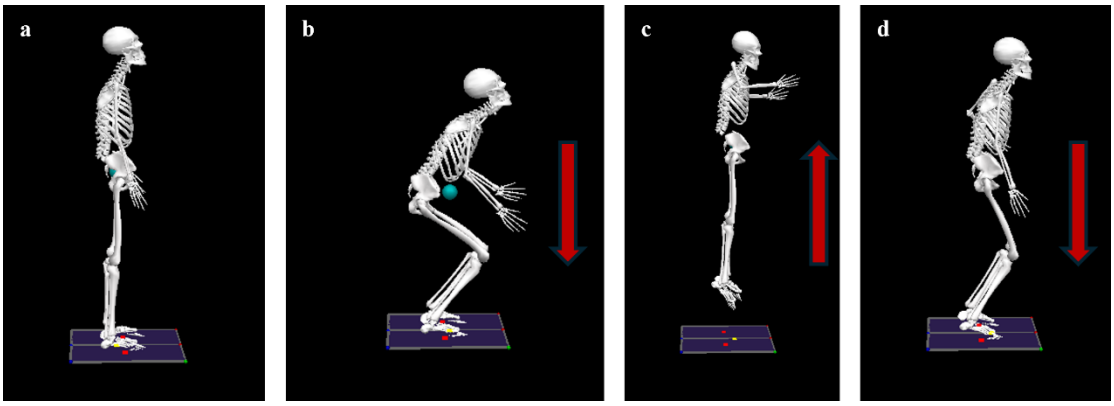

Figure A.6: Countermovement jump (single-leg and bilateral): (a) start upright on force plates; (b) rapid countermovement descent; (c) maximal vertical leap using arms and leg(s); (d) landing back onto the force plates. During flight, hips, knees, and ankles remain fully extended.

Broad jump

Participants stand on both of their feet, with each foot placed on a separate force plate (Figure A.7a). They will be instructed to perform a broad jump, aiming to jump as far as they can (Figure A.7b-d). Each participant will complete this jump three times, and all of the three attempts will be recorded for analysis.

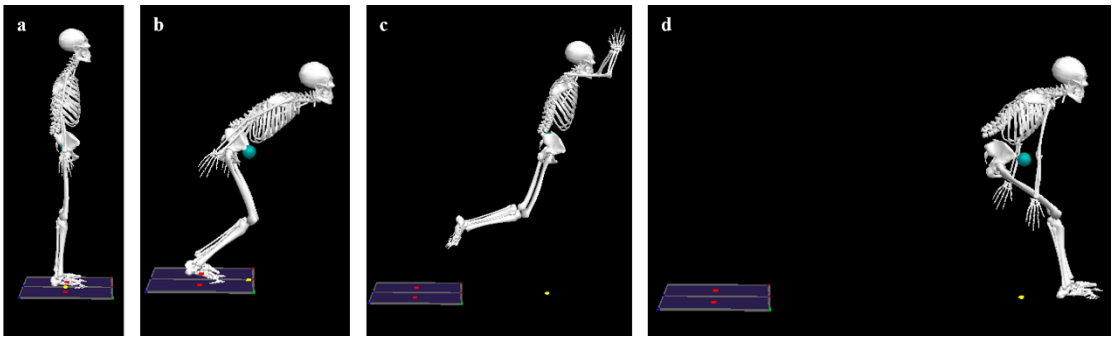

Figure A.7: Broad jump: (a) standing on both feet, one on each force plate; (b) countermovement phase as the athlete prepares to jump; (c) airborne flight phase reaching maximal horizontal distance; (d) landing on the floor.

Reaction time tasks

The FITLIGHT Trainer (FITLIGHT Sports Corp., Ontario, Canada) is used to measure the reaction time (RT). Four lights will be placed in front of the participant drawing a semicircle with the radius of half of their leg length at 0°, 45°,135°and 180° (Figure A.8).

To perform the task, the participant will stand at the origin of the semicircle, facing the lights with both their feet in contact with the floor. Two tests will be performed (simple RT and complex RT). The simple reaction test (SRT) and the complex reaction test (CRT) will be performed with both feet and consisted of 10 luminous stimuli. In this last one, the visual stimuli will be of two colors, blue or green; to the first, one has to tap with the left feet, while to the second, one has to tap with the right feet, while in the SRT, one needs to tap with the same foot during one trial. The setup for single leg SRT and CRT for lower limb is shown in Figure A.8a and Figure A.8b, respectively.

The same tasks will be performed by upper limbs. For the upper limbs, the Fitlights are fixed on the tripods at their waist height with the same configuration (Figure A.8c).

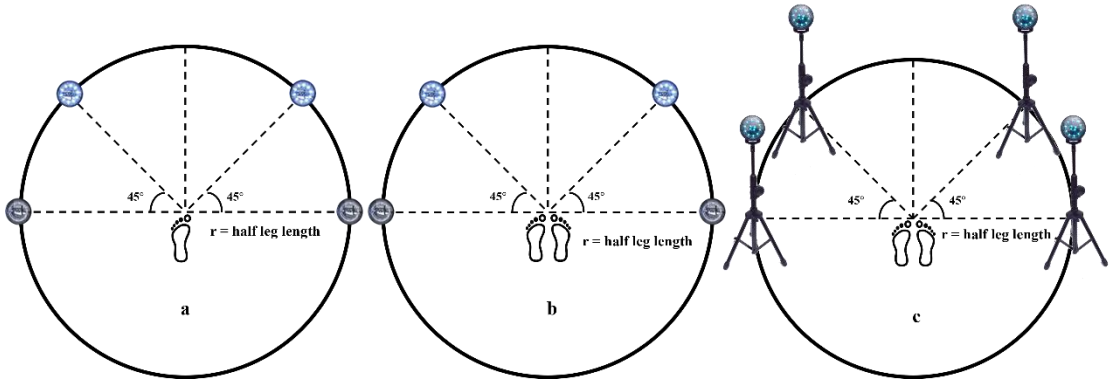

Figure A.8: Reaction-time task setups using the FITLIGHT Trainer in a semicircular arrangement (0°, 45°, 135°, 180°) at a radius equal to half the participant's leg length. (a), the lower-limb simple reaction time (SRT) task setup. (b), the lower-limb complex reaction time (CRT) task setup. (c), the upper-limb SRT/CRT tasks setup with the same semicircular layout mounted on tripods at waist height.

Appendix B. Data Collection Sheet

Date: _____ **Participant ID: _____**

Name of participant: _____ Sports team __Soccer__ Position: _____ Sex _____Age: _____ Height: _____ Weight: _____

Dominant hand: _____ Dominant foot: _____

Training History

Questions	**Answer**	
How old were you when you became active in competitive Sports?	Age	
How many hours do you train for your sport per week?	Hours	
How many hours do you train beyond normal training times for your sport? (i.e., on your own time outside of the structured practice training hours set)	Hours/Week	

Injury History

Concussions

Date (Month/Year)	**Time missed**	**Symptoms**

Additional notes:

_____

_____

Muscular/Skeletal injuries

Date (Month/Year)	**Time missed**	**Diagnosis (injury location)**	**Treatment**

Additional notes:

_____

_____

Broad Jump Distance

Distance (m)	

Y-Balance Results

Stance leg	**Leg length(m)**	**Anterior**	**Posteromedial**	**Posterolateral**
Right				
Left				

Reaction Time Tasks Results

Simple RT test

Moving segment	**Avg. reaction (s)**	**Time total (s)**
Left Leg		
Right Leg		
Left arm		
Right arm		

Complex RT test

Moving segment	**Avg. reaction (s)**	**Time total (s)**
Lower Limbs		
Upper Limbs		

Appendix C. Post-season Injury Information

Injury data to be collected by athletic therapists:

- Participant ID
- Date of injury
- Occurred in a game or practice
- Mechanism of injury
    - Traumatic
        - Contact
        - Non-Contact
    - Overuse
- Nature of injury
- Severity if applicable (grade 1, 2, 3)
- Participation status following injury
    - No change
    - Limited practice, no restrictions for games
    - Limited practice and games
    - No participation for < 7 days
    - No participation for > 7 days

Appendix D. Metrics from Veo Cam 3

Veo Analytics features.

Features	Description
Scoreboards	Display the score and timer of the game.
2D map	The 2D map shows the players' and referees' positions in real-time in a top radar view.
Match momentum	Provides an overview of situations in the game where the team is in attack or is being pushed back by the opponent.
Heatmaps	Visualize the average position of the players and the action during the game.
Match stats	All highlights in the recording will be counted, collected, and graphically presented in a list in the Highlights panel.
Shot map	Automatically shows where shots happened for each team and which of them were goals.
Pass strings	Automatically shows how many continuous passes happened for each team, broken down by the number of passes in the string.
Pass location	Automatically shows where successful passes happened for each team broken down by pitch location.

Note: detailed explanation can be found at https://support.veo.co/hc/en-us/articles/11873714080657-Analyze-your-games-with-Veo-Analytics

Appendix E. Ethics Certificate

06/08/2024

Université d'Ottawa
Bureau d'éthique et d'intégrité de la recherche

University of Ottawa
Office of Research Ethics and Integrity

CERTIFICAT D'APPROBATION ÉTHIQUE | CERTIFICATE OF ETHICS APPROVAL

Numéro du dossier / Ethics File Number	H-07-24-10628
Titre du projet / Project Title	Evaluating Movement Quality in Women's Collegiate Soccer
Type de projet / Project Type	Recherche de professeur / Professor's research project
Statut du projet / Project Status	Approuvé / Approved
Date d'approbation (jj/mm/aaaa) / Approval Date (dd/mm/yyyy)	06/08/2024
Date d'expiration (jj/mm/aaaa) / Expiry Date (dd/mm/yyyy)	05/08/2025

Équipe de recherche / Research Team

Chercheur / Researcher	Affiliation	Role
Ryan GRAHAM	École des sciences de l'activité physique / School of Human Kinetics	Chercheur Principal / Principal Investigator
Xiong ZHAO	École des sciences de l'activité physique / School of Human Kinetics	Assistant de recherche / Research Assistant
Janie COURNOYER	École des sciences de l'activité physique / School of Human Kinetics	Co-chercheur / Co-investigator

Conditions spéciales ou commentaires / Special conditions or comments

550, rue Cumberland, pièce 154
Ottawa (Ontario) K1N 6N5 Canada

550 Cumberland Street, Room 154
Ottawa, Ontario K1N 6N5 Canada

613-562-5387 • 613-562-5338 • ethique@uOttawa.ca / ethics@uOttawa.ca
www.recherche.uottawa.ca/deontologie | www.recherche.uottawa.ca/ethics

06/08/2024

Université d'Ottawa
Bureau d'éthique et d'intégrité de la recherche

University of Ottawa
Office of Research Ethics and Integrity

Le Comité d'éthique de la recherche (CÉR) de l'Université d'Ottawa, opérant conformément à l'*Énoncé de politique des Trois conseils* (2014) et toutes autres lois et tous règlements applicables, a examiné et approuvé la demande d'éthique du projet de recherche ci-nommé.

L'approbation est valide pour la durée indiquée plus haut et est sujette aux conditions énumérées dans la section intitulée "Conditions Spéciales ou Commentaires". Le formulaire « Renouvellement ou Fermeture de Projet » doit être complété quatre semaines avant la date d'échéance indiquée ci-haut afin de demander un renouvellement de cette approbation éthique ou afin de fermer le dossier.

Toutes modifications apportées au projet doivent être approuvées par le CÉR avant leur mise en place, sauf si le participant doit être retiré en raison d'un danger immédiat ou s'il s'agit d'un changement ayant trait à des éléments administratifs ou logistiques du projet. Les chercheurs doivent aviser le CÉR dans les plus brefs délais de tout changement pouvant augmenter le niveau de risque aux participants ou pouvant affecter considérablement le déroulement du projet, rapporter tout évènement imprévu ou indésirable et soumettre toute nouvelle information pouvant nuire à la conduite du projet ou à la sécurité des participants.

The University of Ottawa Research Ethics Board, which operates in accordance with the *Tri-Council Policy Statement* (2014) and other applicable laws and regulations, has examined and approved the ethics application for the above-named research project.

Ethics approval is valid for the period indicated above and is subject to the conditions listed in the section entitled "Special Conditions or Comments". The "Renewal/Project Closure" form must be completedfour weeks before the above-referenced expiry date to request a renewal of this ethics approval or closure of the file.

Any changes made to the project must be approved by the REB before being implemented, except when necessary to remove participants from immediate endangerment or when the modification(s) only pertain to administrative or logistical components of the project. Investigators must also promptly alert the REB of any changes that increase the risk to participant(s), any changes that considerably affect the conduct of the project, all unanticipated and harmful events that occur, and new information that may negatively affect the conduct of the project or the safety of the participant(s).

Kim THOMPSON (GESTIONNAIRE / MANAGER)
Directeur / Director
Pour/For **Daniel LAGAREC** Président(e) du/ Chair of the **Comité d'éthique de la recherche en sciences de la santé et sciences / Health Sciences and Sciences Research Ethics Board**

550, rue Cumberland, pièce 154 550 Cumberland Street, Room 154
Ottawa (Ontario) K1N 6N5 Canada Ottawa, Ontario K1N 6N5 Canada

613-562-5387 • 613-562-5338 • ethique@uOttawa.ca / ethics@uOttawa.ca
www.recherche.uottawa.ca/deontologie | www.recherche.uottawa.ca/ethics

Appendix F. Bilingual Consent Form

Université d'Ottawa | University of Ottawa

Faculté des sciences de la santé | Faculty of Health Sciences
École des sciences de l'activité physique | School of Human Kinetics

Research Consent Form

Research Project Title: **Evaluating Movement Quality in Women's Collegiate Soccer**

Principal Investigators: **Ryan Graham**

Supervisor: **Dr. Ryan Graham**
University of Ottawa
Faculty of Health Sciences
School of Human Kinetics
200 Lees Ave (E020)
Ottawa, ON
K1N6N5

There are two copies of the consent form, one of which is yours to keep.

Background and Purpose of the Study:
Movement quality assessment is important in sports and clinical settings to indicate an individual's injury risk and profile one's athletic performance capabilities. Some non-sport specific movements, viewed as screening movements, are frequently used to assess movement quality and injury risks. However, the subjective nature of these screening tests often requires a trained scorer or controlled environment, which makes the assessment biased and inconvenient. The ability of injury prediction of these methods is limited. Objective data-driven and convenient method are needed for movement quality assessment.
The purpose of this study is to explore the relationships between movement quality and risk of injury by assessing the movement quality and performance of the bilateral body-weight squat and some functional movement tests using markerless motion capture (Theia 3D, Theia Markerless Inc., CA) and force plates; and to develop and validate of a monocular markerless motion capture system for movement quality assessment.

Description of Study Procedures:
This study is divided into three components, in-lab testing, in-field testing and injury reports sharing. Note that consent to participate the in-lab sessions, share the data collected in the field and injury reports at the end of the season will be obtained at the beginning of the season during the first lab session, but the actual data from coaches will only be shared with the research team at the end of the season. This ensures that throughout the season, coaches remain unaware of who is participating or not. The researcher will seek your consent once more to share the injury reports, even if you had previously consented at the beginning of the study. At that time, you can choose to agree or decline without affecting the data already collected both in the lab and in the field. The decision by you to provide or withhold your injury report will be kept confidential.
1. For the in-lab testing, you are invited to participate in a multi-session (pre-, mid- and post-season) motion analysis procedure for approximately 30 minutes per session at the University of Ottawa Spine and Movement Biomechanics Laboratory (200 Lees Avenue, E020).
Once you have provided your informed consent, you will fill out a questionnaire about your injury history. You will then be asked to change into comfortable clothing, which is suitable for performing whole-body exercise movements. Then you will familiarize yourself with all test movements. Once you are comfortable with all the movements, you will perform a 5-second static calibration trial, one

Université d'Ottawa | University of Ottawa
Faculté des sciences de la santé | Faculty of Health Sciences
École des sciences de l'activité physique | School of Human Kinetics

trial of T-balance (eyes open and closed) and Y-balance bilaterally, one trial of L-hop bilaterally, 3 repetitions of single-leg and bilateral countermovement jump, 3 trials of broad jump, and two reaction time tests in a random order. After at least 5-minute break, you will perform 35 repetitions of bodyweight squatting exercise at 40 beats/minute to a metronome.
Note: if you cannot complete some of the tests, the results of the remaining tests will be utilized.
2. For the in-field testing, the results from your training sessions—including sprinting, Veo Cam 3 analytics, and Catapult data—will be shared with the researchers by your coaches for research purposes.
3. Your future injuries will be communicated between the medical team and the research team with the use of ID codes to help maintain privacy.

Possible Risks and Discomforts:
There are no significant risks associated with participating in this study. You may experience pain and fatigue due to the nature of the exercises. However, sufficient rest will be given to reduce these effects. Should you experience any major discomfort, please tell us immediately and seek primary care from a medical professional on campus (100 Marie Curie, Ottawa, Tel.: 613-564-3950) or a medical professional of your choosing.

Possible Benefits:
You will receive feedback with respect to your performance of squat and functional movements, which will identify your strengths and areas that could use improvement. Furthermore, the results of this study will greatly add to our knowledge of how to assess movement quality during squatting in a novel way and how functional movements and reaction time are related to injury risks.

Voluntary Participation:
You are not obligated to participate in this study; participation in this study is voluntary. You may also withdraw from the study at any time with no penalty or coercion, but your data collected in the lab before you withdraw will still be used for research purposes. If you want to remove your permission to access your field data, you can contact the research team. If you choose to withdraw from the study entirely, your data will be destroyed and not used in the study.

Confidentiality:
All personal information and injury history is kept confidential. Information gained from this study will be stored electronically and will need a password to access. Paper study records are stored in a locked cabinet and will be destroyed after 25 years; electronic records will be deleted, and paper records will be shredded. You will not be identified by name in any reports of the completed study. Your anonymity will be strictly maintained – you will not be identified by your name but will be determined by an independent study number. Dr. Ryan Graham, Dr. Janie Cournoyer and Xiong Zhao will be the only ones who have access to the study data.

Questions about the Study:
You are free to ask questions at any time; you can contact the principal investigators by email: Dr. Ryan Graham (rgraham@uottawa.ca). The ethical components of the project have been approved by the University of Ottawa research ethics board. If I have any questions regarding the ethical conduct of this study, I may contact the Protocol Officer for Ethics in Research, University of Ottawa, Tabaret

uOttawa
Université d'Ottawa | University of Ottawa
Faculté des sciences de la santé | Faculty of Health Sciences
École des sciences de l'activité physique | School of Human Kinetics
Hall, 550 Cumberland Street, Room 154, Ottawa ON, K1N 6N5. Tel.: (613) 562-5387 Email: ethics@uottawa.ca

Research Project Title: Evaluating Movement Quality in Women's Collegiate Soccer

☐ **Consent To Participate the In-Lab Data Collection Sessions:**
I have read this consent form, and I agree to participate in the procedures of this study.

☐ **Consent to Access Data from Coaches (Testing/Training within Team):**
I consent to the researchers accessing data from my testing and training sessions conducted within the team structure. This data may be used for research purposes as described in the project introduction.

☐ **Consent to Access Injury Reports:**
I consent to the researchers accessing my injury reports provided by the Athletic Trainers (ATs). The information will be used for research purposes as described in the project introduction. I understand that this is voluntary, and I can withdraw my consent at any time without my coaches being informed.

☐ **Informed Consent to have videos or pictures Taken:**
I consent to have video or pictures taken of myself completing the experiment and understand that none will be taken at any point without me knowing. I also understand that if any of these videos or pictures are used in a subsequent presentation or publication, that my face and any other identifiers will be blurred. You can still participate in the research study without consenting to have pictures taken.

☐ **Secondary Use of Data for Research:**
I consent to the secondary use of my data for research purposes. The data collected may be used beyond this study for additional research.

_____
Printed Name of Participant

_____ _____
Signature of Participant Date

_____
Witness Name

☐ **Future Participation:**
I am interested in being contacted to participate in future research performed by this laboratory (your email information will be saved in a password protected file).

Investigator Statement (or Person Explaining the Consent):
I have carefully explained to the research participant the nature of the above research study. To the best of my knowledge, the research participant signing this consent form understands the nature, demands, risks and benefits involved in participating in this study. I acknowledge my responsibility for the care and well-being of the above research participant, to respect the rights and wishes of the

uOttawa
Université d'Ottawa | University of Ottawa
Faculté des sciences de la santé | Faculty of Health Sciences
École des sciences de l'activité physique | School of Human Kinetics

research participant, and to conduct the study according to applicable Good Clinical Practice guidelines and regulations.

_____
Name of Investigator/Delegate (printed)

_____ _____
Signature of Investigator/Delegate Date

Université d'Ottawa | University of Ottawa

Faculté des sciences de la santé | Faculty of Health Sciences
École des sciences de l'activité physique | School of Human Kinetics

Formulaire de consentement à la recherche

Titre du projet de recherche : Évaluation de la qualité des mouvements dans le soccer féminin collégial

Chercheurs principaux : Ryan Graham

Superviseur : Dr. Ryan Graham
Université d'Ottawa
Faculté des sciences de la santé
École des sciences de l'activité physique
200, avenue Lees (E020)
Ottawa (Ont.)
K1N6N5

Il y a deux copies du formulaire de consentement, dont l'une est la vôtre.

Contexte et objet de l'étude :
L'évaluation de la qualité des mouvements est importante dans les milieux sportifs et cliniques pour indiquer le risque de blessure d'une personne et établir le profil de ses capacités de performance athlétique. Certains mouvements non-spécifiques au sport, considérés comme des mouvements de dépistage, sont fréquemment utilisés pour évaluer la qualité des mouvements et les risques de blessures. Cependant, la nature subjective de ces tests de dépistage nécessite souvent un évaluateur formé ou un environnement contrôlé, ce qui rend l'évaluation biaisée et peu pratique. La capacité de prédiction des blessures de ces méthodes est limitée. Une méthode objective et pratique, axée sur les données, est nécessaire pour l'évaluation de la qualité des mouvements.
Le but de cette étude est d'explorer les relations entre la qualité du mouvement et le risque de blessure en évaluant la qualité du mouvement et la performance au squat et de certains tests de mouvement fonctionnels en utilisant la capture de mouvement sans marqueur (Theia 3D, Theia Markerless Inc., CA) et plaques de force; ainsi que de développer et de valider un système monoculaire de capture de mouvement sans marqueur pour l'évaluation de la qualité du mouvement.

Description des procédures d'étude :
Cette étude est divisée en trois composants : les tests en laboratoire les tests sur le terrain et le partage des rapports de blessures. Veuillez noter que le consentement pour participer aux sessions en laboratoire, partager les données collectées sur le terrain et les rapports de blessures à la fin de la saison sera obtenu au début de la saison lors de la première session en laboratoire, mais les données réelles des entraîneurs ne seront partagées avec l'équipe de recherche qu'à la fin de la saison. Cela garantit qu'au cours de la saison, les entraîneurs ne sauront pas qui participe ou non. Le chercheur sollicitera à nouveau votre consentement pour partager les rapports de blessures, même si vous aviez donné votre consentement au début de l'étude. À ce moment-là, vous pourrez choisir d'accepter ou de refuser sans que cela n'affecte les données déjà collectées en laboratoire et sur le terrain. Votre décision de fournir ou de refuser votre rapport de blessure restera confidentielle.
1. Pour les tests en laboratoire, vous êtes invités à participer à une procédure d'analyse des mouvements multi-sessions (pré-saison, mi-saison et post-saison) d'environ 30 minutes par session au Laboratoire de biomécanique de la colonne vertébrale et du mouvement de l'Université d'Ottawa

uOttawa
Université d'Ottawa | University of Ottawa
Faculté des sciences de la santé | Faculty of Health Sciences
École des sciences de l'activité physique | School of Human Kinetics

(200, avenue Lees, E020). Une fois que vous aurez donné votre consentement éclairé, vous remplirez un questionnaire sur vos antécédents de blessures.
On vous demandera ensuite de vous changer dans des vêtements confortables, qui conviennent à l'exécution de mouvements d'exercice du corps entier. Ensuite, vous vous familiariserez avec tous les mouvements de test. Une fois que vous êtes à l'aise avec tous les mouvements, vous effectuerez un essai d'étalonnage statique de 5 secondes, un essai de l'équilibre T (yeux ouverts et fermés) et de l'équilibre Y bilatéralement, un essai de L-hop bilatéralement, 3 répétitions de saut unijambiste et de saut bilatéral avec contre-mouvement, 3 essais de saut en longueur et deux tests de temps de réaction dans un ordre aléatoire. Après une pause d'au moins 5 minutes, vous effectuerez 35 répétitions de squats sans charge à 40 battements/minute en suivant un métronome.
Remarque : Si vous ne pouvez pas terminer certains des tests, les résultats des tests restants seront utilisés.
2.Pour les tests sur le terrain, les résultats de vos sessions d'entraînement, y compris le sprint, les analyses de Veo Cam 3 et les données de Catapult, seront partagés avec les chercheurs par vos entraîneurs à des fins de recherche.
3. Vos blessures futures seront communiquées entre l'équipe médicale et l'équipe de recherche à l'aide de codes d'identification pour aider à maintenir la confidentialité.

Risques et inconforts possibles :
Il n'y a pas de risques importants associés à la participation à cette étude. Vous pouvez ressentir de la douleur et de la fatigue en raison de la nature des exercices. Cependant, suffisamment de repos sera accordé pour réduire ces effets. Si vous éprouvez un inconfort majeur, veuillez nous en informer immédiatement et demander des soins primaires à un professionnel de la santé sur le campus (100 Marie Curie, Ottawa, Tél. : 613-564-3950) ou à un professionnel de la santé de votre choix.

Avantages possibles :
Vous recevrez des commentaires concernant votre performance de squat et de mouvements fonctionnels, ce qui identifiera vos forces et les éléments qui pourraient être améliorés. En outre, les résultats de cette étude ajouteront grandement à nos connaissances sur la façon d'évaluer la qualité du mouvement pendant le squat et comment les mouvements fonctionnels et le temps de réaction sont liés aux risques de blessures.

Participation volontaire :
Votre participation à cette étude est entièrement volontaire et vous n'êtes pas obligé d'y participer. Vous pouvez également vous retirer de l'étude à tout moment sans pénalité ni contrainte, mais les données collectées en laboratoire avant votre retrait seront toujours utilisées à des fins de recherche. Si vous souhaitez retirer votre permission d'accès à vos données de terrain, vous pouvez contacter l'équipe de recherche. Si vous choisissez de vous retirer complètement de l'étude, vos données seront détruites et ne seront pas utilisées dans l'étude.

Confidentialité :
Tous les renseignements personnels et les antécédents de blessures demeurent confidentiels. Les renseignements tirés de cette étude seront stockés électroniquement et auront besoin d'un mot de passe pour y accéder. Les dossiers d'étude papier sont entreposés dans une armoire verrouillée et seront détruits après 25 ans; les documents électroniques seront supprimés et les documents papier

Université d'Ottawa | University of Ottawa
Faculté des sciences de la santé | Faculty of Health Sciences
École des sciences de l'activité physique | School of Human Kinetics

seront déchiquetés. Vous ne serez identifié par votre nom dans aucun rapport de l'étude finale. Votre anonymat sera strictement maintenu - vous ne serez pas identifié par votre nom mais sera déterminé par un numéro d'étude indépendant. Le Dr Ryan Graham, la Dre Janie Cournoyer et Xiong Zhao seront les seuls à avoir accès aux données de l'étude.

Questions au sujet de l'étude :
Vous êtes libre de poser des questions à tout moment; vous pouvez communiquer avec les chercheurs principaux par courriel : Dr Ryan Graham (rgraham@uottawa.ca). Les volets éthiques du projet ont été approuvés par le comité d'éthique de la recherche de l'Université d'Ottawa. Si j'ai des questions concernant la conduite éthique de cette étude, je peux communiquer avec l'agent du protocole pour l'éthique de la recherche, Université d'Ottawa, Pavillon Tabaret, 550, rue Cumberland, pièce 154, Ottawa (Ontario) K1N 6N5. Tél. : (613) 562-5387 Courriel : ethics@uottawa.ca

☐ **Consentement à Participer aux Sessions de Collecte de Données en Laboratoire :**
J'ai lu ce formulaire de consentement et j'accepte de participer aux procédures de cette étude.

☐ **Consentement pour l'accès aux données des entraîneurs (tests/entraînements au sein de l'équipe) :**
Je consens à ce que les chercheurs accèdent aux données de mes séances de tests et d'entraînements réalisées dans le cadre de l'équipe. Ces données peuvent être utilisées à des fins de recherche comme décrit dans l'introduction du projet.

☐ **Consentement pour l'accès aux rapports de blessures :**
Je consens à ce que les chercheurs accèdent à mes rapports de blessures fournis par les entraîneurs sportifs (ATs). Les informations seront utilisées à des fins de recherche comme décrit dans l'introduction du projet. Je comprends que cela est volontaire et que je peux retirer mon consentement à tout moment sans que mes entraîneurs en soient informés.

☐ **Consentement éclairé pour que des vidéos ou des photos soient prises :**
Je consens à ce que des vidéos ou des photos soient prises de moi-même en train de terminer l'expérience et je comprends qu'aucune image ne sera prise à tout moment à mon insu. Je comprends également que si l'une de ces vidéos ou images est utilisée dans une présentation ou une publication ultérieure, mon visage et tout autre identifiant sera flou. Vous pouvez toujours participer à l'étude de recherche sans consentir à ce que des photos soient prises.

☐ **Utilisation secondaire des données à des fins de recherche:**
Je consens à l'utilisation secondaire de mes données à des fins de recherche. Les données collectées peuvent être utilisées au-delà de cette étude pour des recherches supplémentaires.

_____ _____
Nom Date

_____
Signature du participant

uOttawa
Université d'Ottawa | University of Ottawa
Faculté des sciences de la santé | Faculty of Health Sciences
École des sciences de l'activité physique | School of Human Kinetics

☐ **Participation future :**
Je suis intéressé à être contacté pour participer à de futures recherches effectuées par ce laboratoire (vos informations de messagerie seront enregistrées dans un fichier protégé par mot de passe).

☐ **Déclaration de l'enquêteur (ou personne expliquant le consentement) :**
J'ai soigneusement expliqué au participant la nature de l'étude de recherche ci-dessus. À ma connaissance, le participant qui signe ce formulaire de consentement comprend la nature, les exigences, les risques et les avantages de la participation à cette étude. Je reconnais ma responsabilité à l'égard des soins et du bien-être du participant à la recherche ci-dessus, de respecter les droits et les souhaits du participant à la recherche et de mener l'étude conformément aux lignes directrices et aux règlements applicables en matière de bonnes pratiques cliniques.

_____
Nom de l'Investigateur/Délégué (en lettres moulées)

_____ _____
Signature de l'Investigateur/Délégué Date